

**EFFECT OF CASSAVA PULP ON PHYSICAL
PROPERTIES OF POLY (LACTIC ACID) AND
POLY (BUTYLENE SUCCINATE) BLENDS**

Parina Kangwanwatthanasiri



A Thesis Submitted in Partial Fulfillment of the Requirements for the

Degree of Master of Engineering in Polymer Engineering

Suranaree University of Technology

Academic Year 2014

ผลของกากมันสำปะหลังต่อสมบัติทางกายภาพของพอลิเมอร์ผสมระหว่าง
พอลิแลคติกแอซิดกับพอลิบิวทิลีนซัคซิเนต

นางสาวปรีญา กังวาลวัฒน์ศิริ



วิทยานิพนธ์นี้เป็นส่วนหนึ่งของการศึกษาตามหลักสูตรปริญญาวิศวกรรมศาสตรมหาบัณฑิต
สาขาวิชาวิศวกรรมพอลิเมอร์
มหาวิทยาลัยเทคโนโลยีสุรนารี
ปีการศึกษา 2557

**EFFECT OF CASSAVA PULP ON PHYSICAL PROPERTIES OF
POLY (LACTIC ACID) AND POLY (BUTYLENE SUCCINATE)
BLENDS**

Suranaree University of Technology has approved this thesis submitted in partial fulfillments of the requirements for a Master's Degree.

Thesis Examining Committee

(Asst. Prof. Dr. Wimonlak Sutapun)

Chairperson

(Assoc. Prof. Dr. Yupaporn Ruksakulpiwat)

Member (Thesis Advisor)

(Asst. Prof. Dr. Nitinat Suppakarn)

Member

(Asst. Prof. Dr. Kasama Jarukumjorn)

Member

(Asst. Prof. Dr. Pranee Chumsamrong)

Member

(Prof. Dr. Sukit Limpijumnong)

Vice Rector for Academic Affairs
and Innovation

(Assoc. Prof. Flt. Lt. Dr. Kontorn Chamniprasart)

Dean of Institute of Engineering

ปารีณา กังวาลวัฒนศิริ : ผลของกากมันสำปะหลังต่อสมบัติทางกายภาพของพอลิเมอร์ผสมระหว่างพอลิแลคติกแอซิดกับพอลิบิวทิลีนซัคซิเนต (EFFECT OF CASSAVA PULP ON PHYSICAL PROPERTIES OF POLY (LACTIC ACID) AND POLY (BUTYLENE SUCCINATE) BLENDS) อาจารย์ที่ปรึกษา : รองศาสตราจารย์ ดร.ยุพาพร รักสกุลพิวัฒน์ , 133 หน้า.

วิทยานิพนธ์นี้เป็นการศึกษาผลของปริมาณพอลิบิวทิลีนซัคซิเนตต่อสมบัติทางกายภาพของพอลิเมอร์ผสมระหว่างพอลิแลคติกแอซิดกับพอลิบิวทิลีนซัคซิเนต ปริมาณพอลิบิวทิลีนซัคซิเนตที่ใช้คือ 0 - 40 เปอร์เซ็นต์โดยน้ำหนัก เมื่อเพิ่มปริมาณพอลิบิวทิลีนซัคซิเนตของพอลิเมอร์ผสมพบว่าค่าความต้านทานต่อการกระแทกและค่าความยืดสูงสุด ณ จุดขาดของพอลิเมอร์ผสมมีค่าเพิ่มขึ้น อย่างไรก็ตาม ค่าความยืดสูงสุด ณ จุดขาดของพอลิเมอร์ผสมที่มีปริมาณพอลิบิวทิลีนซัคซิเนตมากกว่า 20 เปอร์เซ็นต์โดยน้ำหนักมีค่าลดลง อย่างไรก็ตาม ค่ามอดูลัสของยังค์และค่าความต้านทานการดึงยืดของพอลิเมอร์ผสมระหว่างพอลิแลคติกแอซิดกับพอลิบิวทิลีนซัคซิเนตมีค่าลดลงเมื่อปริมาณพอลิบิวทิลีนซัคซิเนตเพิ่มขึ้น ภาพถ่ายของชิ้นงานที่ได้จากเทคนิคกล้องจุลทรรศน์อิเล็กตรอนแบบส่องกราดพบการรวมตัวของพอลิบิวทิลีนซัคซิเนตบนพื้นผิวพอลิแลคติกแอซิดเพิ่มขึ้นเมื่อเพิ่มปริมาณพอลิบิวทิลีนซัคซิเนต

ไกลซิดิลเมทาคริเลทและมาเลอิกแอนไฮไดรด์กราฟท์ลงบนพอลิแลคติกแอซิด พอลิแลคติกแอซิดดัดแปรด้วยไกลซิดิลเมทาคริเลทและพอลิแลคติกแอซิดดัดแปรด้วยมาเลอิกแอนไฮไดรด์เตรียมโดยใช้เครื่องผสมภายใน การเกิดปฏิกิริยาระหว่างพอลิแลคติกแอซิดกับมอนอเมอร์ (ไกลซิดิลเมทาคริเลท และ มาเลอิกแอนไฮไดรด์) ตรวจสอบโดยใช้เครื่องมือที่ใช้พิสูจน์เอกลักษณ์โมเลกุลของสาร โดยการดูดกลืนรังสีอินฟราเรด การไตเตรทนำมาใช้เพื่อตรวจสอบหาปริมาณของมอนอเมอร์ที่กราฟท์บนโมเลกุลของพอลิแลคติกแอซิด พอลิแลคติกแอซิดดัดแปรด้วยไกลซิดิลเมทาคริเลทใช้เป็นตัวเชื่อมประสานในพอลิเมอร์ผสมระหว่างพอลิแลคติกแอซิดและพอลิบิวทิลีนซัคซิเนต ค่าความต้านทานการดึงยืดและค่าความยืดสูงสุด ณ จุดขาดของพอลิเมอร์ผสมมีค่าเพิ่มขึ้นเมื่อเติมพอลิแลคติกแอซิดดัดแปรด้วยไกลซิดิลเมทาคริเลท

กากมันสำปะหลังใช้เตรียมเป็นเทอร์โมพลาสติกสตาร์ชเพื่อใช้เป็นสารตัวเติมสำหรับพอลิเมอร์คอมพอสิตระหว่างเทอร์โมพลาสติกสตาร์ชจากกากมันสำปะหลัง พอลิแลคติกแอซิดและพอลิบิวทิลีนซัคซิเนต ค่าความต้านทานการดึงยืด ค่ามอดูลัสของยังค์ ค่าความยืดสูงสุด ณ จุดขาดและค่าความต้านทานต่อการกระแทกของพอลิเมอร์คอมพอสิตมีค่าลดลงเมื่อเพิ่มปริมาณเทอร์โมพลาสติกสตาร์ชจากกากมันสำปะหลัง พอลิแลคติกแอซิดดัดแปรด้วยไกลซิดิลเมทาคริเลทและพอลิแลคติก

แอสิตัดแปรด้วยมาเลอิกแอนไฮดรายด์ใช้เป็นตัวเชื่อมประสานในพอลิเมอร์คอมพอสิต พบว่า
ตัวเชื่อมประสานสามารถปรับปรุงสมบัติทางกลของพอลิเมอร์คอมพอสิตได้



สาขาวิชา วิศวกรรมพอลิเมอร์
ปีการศึกษา 2557

ลายมือชื่อนักศึกษา _____
ลายมือชื่ออาจารย์ที่ปรึกษา _____
ลายมือชื่ออาจารย์ที่ปรึกษาร่วม _____

PARINA KANGWANWATTHANASIRI : EFFECT OF CASSAVA PULP
ON PHYSICAL PROPERTIES OF POLY (LACTIC ACID) AND POLY
(BUTYLENE SUCCINATE) BLENDS. THESIS ADVISOR : ASSOC.
PROF. YUPAPORN RUKSAKULPIWAT, Ph.D., 133 PP.

POLY (LACTIC ACID)/POLY (BUTYLENE SUCCINATE)/ THERMOPLASTIC
STARCH/ CASSAVA PULP/ BIOCOMPOSITES

In this study, effect of PBS contents on physical properties of poly (lactic acid) (PLA) and poly (butylene succinate) (PBS) blends was investigated. The content of PBS was varied from 0 – 40 wt%. With increasing PBS contents, impact strength and elongation at break of PLA/PBS blends were increased. Nevertheless, elongation at break of blends was decreased for the blend with PBS content more than 20 wt%. However, Young's modulus and tensile strength of the PLA/PBS blends were decreased with increasing PBS contents. From SEM micrographs of PLA/PBS blends, the size of coalescence was increased with increasing PBS content in PLA matrix.

Glycidyl methacrylate (GMA) and maleic anhydride (MA) were grafted onto PLA. PLA grafted with glycidyl methacrylate (PLA-g-GMA) and PLA grafted with maleic anhydride (PLA-g-MA) were prepared by using an internal mixer. The interaction between PLA and monomer (GMA or MA) was characterized by using FTIR. A titration method was used to determine the content of monomer grafted onto PLA molecule. PLA-g-GMA was used as a compatibilizer in PLA/PBS blends. PLA-g-GMA improved compatibility between PLA and PBS. Tensile strength and elongation at break of PLA/PBS blends were increased with addition of PLA-g-GMA.

Cassava pulp was used to prepare thermoplastic starch. Thermoplastic starch from cassava pulp (CP) was used as a filler for CP/PLA/PBS composites. Effect of CP content on physical properties of CP/PLA/PBS composites was studied. Tensile strength, Young's modulus, elongation at break and impact strength of CP/PLA/PBS composites were decreased with increasing CP content. PLA-g-GMA and PLA-g-MA were used as compatibilizers in CP/PLA/PBS composites. Mechanical properties of CP/PLA/PBS composites can be improved by using compatibilizer.



School of Polymer Engineering

Academic Year 2014

Student's Signature _____

Advisor's Signature _____

Co-Advisor's Signature _____

ACKNOWLEDGEMENTS

The author wishes to acknowledge Suranaree University of Technology and the Center of Excellence on Petrochemical and Materials Technology for financial support.

The grateful thanks and appreciation are given to my thesis advisor, Assoc. Prof. Dr. Yupaporn Ruksakulpiwat, for her supervision, advice and support throughout the period of the study. Moreover, I would like to thank my thesis co-advisor, Asst. Prof. Dr. Nitinat Suppakarn, for her valuable suggestion. I am also grateful to Asst. Prof. Dr. Wimonlok Sutapun, Asst. Prof. Dr. Kasama Jarukumjorn and Asst. Prof. Dr. Pranee Chumsamrong for their valuable suggestion and guidance given as committee members.

The author is also grateful to all faculty members, staff and friends from the School of Polymer Engineering and the Center for Scientific and Technological Equipment of Suranaree University of Technology.

Finally, I would like to express my special appreciation to my parents, my sister and my brother for their support and encouraging me throughout the course of this study at Suranaree University of Technology.

Parina Kangwanwatthanasiri

TABLE OF CONTENTS

	Page
ABSTRACT (THAI).....	I
ABSTRACT (ENGLISH).....	III
ACKNOWLEDGMENTS.....	V
TABLE OF CONTENTS.....	VI
LIST OF TABLES.....	XI
LIST OF FIGURES.....	XIII
SYMBOLS AND ABBREVIATIONS.....	XVII
CHAPTER	
I INTRODUCTION.....	1
1.1 General Background.....	1
1.2 Research objectives.....	4
1.3 Scope and limitations of the study.....	5
1.4 References.....	6
II LITERATURE REVIEW.....	11
2.1 Poly (lactic acid) (PLA).....	11
2.1.1 PLA blend.....	12
2.1.2 Miscibility of PLA blend.....	13
2.1.3 Compatibilizer for PLA blend.....	14

TABLE OF CONTENTS (Continued)

	Page
2.2 Poly (butylene succinate) (PBS).....	19
2.2.1 PBS blend.....	20
2.3 Thermoplastic starch (TPS).....	24
2.3.1 Thermoplastic starch blend.....	24
2.4 Cassava pulp.....	27
2.4.1 Cassava pulp blend.....	28
2.5 References.....	29
III EXPERIMENTAL.....	34
3.1 Materials.....	34
3.2 Experimental.....	34
3.2.1 Preparation of raw cassava pulp (RCP) _i	34
3.2.2 Preparation of thermoplastic starch from cassava pulp (CP).....	36
3.2.3 Preparation of poly (lactic acid) grafted with glycidyl methacrylate (PLA-g-GMA).....	36
3.2.4 Preparation of poly (lactic acid) grafted with maleic anhydride (PLA-g-MA).....	37
3.2.5 Characterization of PLA-g-GMA and PLA-g-MA.....	38
3.2.5.1 Determination of GMA and MA content.....	38

TABLE OF CONTENTS (Continued)

	Page
3.2.5.2 Fourier Transform Infrared Spectroscopy.....	39
3.2.6 Preparation of PLA/PBS blends.....	39
3.2.7 Preparation of CP/PLA/PBS composites.....	40
3.2.8 Characterization of PLA/PBS blends and CP/PLA/PBS composites.....	42
3.2.8.1 Mechanical properties.....	42
3.2.8.2 Morphological properties.....	43
3.2.8.3 Thermal properties.....	43
3.2.8.4 X-ray diffraction (XRD).....	45
3.3 References.....	46
IV RESULTS AND DISCUSSION.....	48
4.1 Characterization of PLA-g-GMA and PLA-g-MA.....	48
4.1.1 PLA-g-GMA.....	48
4.1.2 PLA-g-MA.....	50
4.2 Effect of PBS content on physical properties of PLA/PBS blends.....	52
4.2.1 Mechanical properties of PLA/PBS blends.....	52
4.2.2 Morphological properties of PLA/PBS blends.....	57
4.2.3 Thermal properties of PLA, PBS and PLA/PBS blends.....	59

TABLE OF CONTENTS (Continued)

	Page
4.3 Effect of PLA-g-GMA on physical properties of PLA/PBS blends.....	65
4.3.1 The stress-strain curves of PLA, PBS, PLA-g-GMA and PLA/PBS blends with and without PLA-g-GMA..	65
4.3.2 Mechanical properties of PLA/PBS blends with and without PLA-g-GMA.....	66
4.3.3 Morphological properties of PLA/PBS blends with and without PLA-g-GMA.....	70
4.3.4 Thermal properties of PLA/PBS blends with and without PLA-g-GMA.....	72
4.3.5 X-ray diffraction analysis.....	77
4.4 Effect of glycerol content on physical properties of CP.....	81
4.4.1 Mechanical properties of CP.....	81
4.4.2 Comparison mechanical properties of composites from CP and RCP _t	84
4.5 Effect of CP contents on physical properties of CP/PLA/PBS composites.....	86
4.5.1 Mechanical properties of CP/PLA/PBS composites.....	86

TABLE OF CONTENTS (Continued)

	Page
4.5.2 Morphological properties of CP/PLA/PBS composites.....	90
4.5.3 Thermal properties of CP/PLA/PBS composites.....	92
4.6 Effect of compatibilizer on physical properties of CP/PLA/PBS composites.....	97
4.6.1 Mechanical properties of CP/PLA/PBS composites with and without compatibilizer.....	97
4.6.2 Morphological properties of CP/PLA/PBS composites with and without compatibilizer.....	101
4.6.3 Thermal properties of CP/PLA/PBS composites with and without compatibilizer.....	102
4.6 References.....	107
V CONCLUSIONS.....	113
APPENDICES	
APPENDIX A. COST CALCULATION FOR PLA/PBS BLENDS AND CP/PLA/PBS COMPOSITES.....	116
APPENDIX B. PUBLICATIONS.....	122
BIOGRAPHY.....	132

LIST OF TABLES

Table	Page
2.1 Physical properties of PBS (Mitsubishi Chemical Corporation, 2011).....	20
3.1 Component of RCP (starch and fiber).....	35
3.2 Amount of cellulose, hemicellulose and lignin of RCP.....	35
3.3 Formulation of the preparation of GMA grafted PLA.....	37
3.4 Formulation of the preparation of MA grafted PLA.....	37
3.5 Blends composition.....	40
3.6 Composites composition.....	42
4.1 Graft content of PLA-g-GMA and PLA-g-MA.....	52
4.2 Tensile strength, elongation at break, young's modulus and impact strength of PLA/PBS blends.....	56
4.3 TGA analysis of PLA, PBS and PLA/PBS blends.....	61
4.4 Thermal properties of PLA, PBS and PLA/PBS blends.....	64
4.5 ΔH_m , ΔH_{cc} , ΔH_c , %X of PLA, PBS and PLA/PBS blends.....	64
4.6 Tensile strength, elongation at break, Young's modulus and impact strength of PLA, PBS, PLA-g-GMA and PLA/PBS blends with and without PLA-g- GMA.....	69
4.7 TGA analysis of PLA, PBS and PLA/PBS blends with and without PLA-g- GMA.....	73

LIST OF TABLES (Continued)

Table	Page
4.8 Thermal properties of PLA, PBS and PLA/PBS blends.....	76
4.9 ΔH_m , ΔH_{cc} , ΔH_c , %X of PLA, PBS and PLA/PBS blends.....	77
4.10 X-ray diffraction analysis of PLA and stressed PLA.....	79
4.11 X-ray diffraction analysis of PLA-g-GMA and stressed PLA-g-GMA.....	80
4.12 Tensile strength, elongation at break and Young's modulus of CP.....	82
4.13 Tensile strength, elongation at break and Young's modulus of CP/PLA/PBS composite and RCP _t /PLA/PBS composite.....	84
4.14 Tensile strength, elongation at break, Young's modulus and impact strength of CP/PLA/PBS composites.....	87
4.15 TGA analysis of CP/PLA/PBS composites.....	93
4.16 Thermal properties of CP/PLA/PBS composites.....	96
4.17 ΔH_m , ΔH_{cc} , ΔH_c and %X of CP/PLA/PBS composites.....	97
4.18 Tensile strength, elongation at break, Young's modulus and impact strength of CP/PLA/PBS composites with and without compatibilizer.....	98
4.19 TGA analysis of CP/PLA/PBS composites with and without compatibilizer..	103
4.20 Thermal properties of CP/PLA/PBS composites with and without compatibilizer.....	107
4.21 ΔH_m , ΔH_{cc} , ΔH_c and %X of CP/PLA/PBS composites with and without compatibilizer.....	107

LIST OF FIGURES

Figure	Page
2.1 Chemical structure of poly (lactic acid) (PLA).....	12
2.2 Chemical structure of Poly (butylene succinate) (PBS).....	19
3.1 Diagram for preparation of RCP _t	36
3.2 Diagram for preparation of CP.....	36
3.3 ASTM D638 Type V specimens for tensile testing.....	43
3.4 The standard specimen size for impact testing.....	43
3.5 Diagram of thermal programming for DSC.....	45
3.6 Position of sample for XRD testing.....	46
4.1 FTIR spectra of PLA and PLA-g-GMA.....	49
4.2 Mechanism of the grafting of GMA onto the PLA chain (Xu, et al., 2012).....	49
4.3 FTIR spectra of PLA and PLA-g-MA.....	51
4.4 FTIR spectra of MA.....	51
4.5 Proposed grafting reaction pathway for the reaction of MA on PLA (Mani, Bhattacharya, and Tang, 1999).....	52
4.6 Tensile strength of PLA/PBS blends at various PBS contents.....	54
4.7 Young's modulus of PLA/PBS blends at various PBS contents.....	55
4.8 Elongation at break of PLA/PBS blends at various PBS contents.....	55
4.9 Impact strength of PLA/PBS blends at various PBS contents.....	56

LIST OF FIGURES (Continued)

Figure	Page
4.10 SEM micrographs (100x) of tensile fractured surface of PLA (a), PBS (b), PBS10 (c), PBS20 (d), PBS30 (e) and PBS40 (f).....	58
4.11 TGA curves of PLA, PBS and PLA/PBS blends.....	60
4.12 DTG curves of PLA, PBS and PLA/PBS blends.....	60
4.13 DSC curves from the cooling scan of PLA/PBS blends.....	63
4.14 DSC curves from the second heating scan of PLA/PBS blends.....	63
4.15 Tensile stress-strain curve of PLA, PBS, PLA-g-GMA and PLA/PBS blends..	66
4.16 Tensile strength of PLA, PBS, PBS20, PBS20-G10 and PLA-g-GMA.....	67
4.17 Young's modulus of PLA, PBS, PBS20, PBS20-G10 and PLA-g-GMA.....	68
4.18 Elongation at break of PLA, PBS, PBS20, PBS20-G10 and PLA-g-GMA.....	68
4.19 Impact strength of PLA, PBS, PBS20, PBS20-G10 and PLA-g-GMA.....	69
4.20 SEM micrographs of tensile fractured surface of PLA (a), PBS (b), PBS10 (c), PBS20 (d), PBS30 (e) and PBS40 (f).....	71
4.21 TGA curves of PLA/PBS blend with and without compatibilizer.....	73
4.22 DTG curves of PLA/PBS blend with and without compatibilizer.....	74
4.23 DSC curves from the cooling scan of PLA/PBS blend with and without compatibilizer.....	75
4.24 DSC curves from the second heating scan of PBS20, PLA-g-GMA and PBS20-G10.....	76
4.25 XRD patterns of neat PLA.....	78

LIST OF FIGURES (Continued)

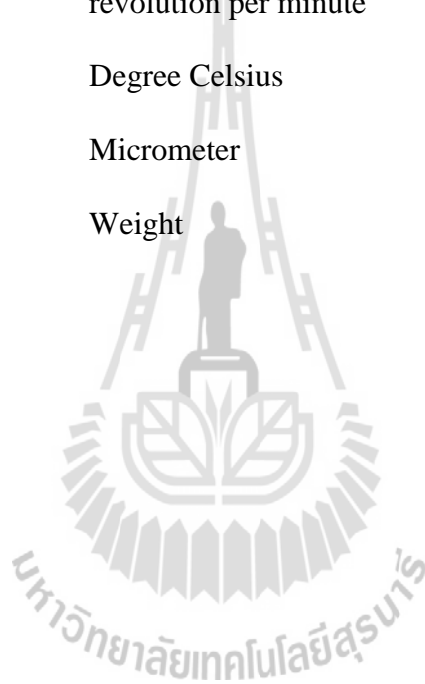
Figure	Page
4.26 XRD patterns of PLA-g-GMA.....	78
4.27 Tensile strength of CP with various glycerol contents.....	82
4.28 Young's modulus of CP with various glycerol contents.....	83
4.29 Elongation at break of CP with various glycerol contents.....	83
4.30 Tensile strength of CP/PLA/PBS composites and RCP _t /PLA/PBS composite..	85
4.31 Young's modulus of CP/PLA/PBS composites and RCP _t /PLA/PBS composite.....	85
4.32 Elongation at break of CP/PLA/PBS composites and RCP _t /PLA/PBS composite.....	86
4.33 Tensile strength of CP/PLA/PBS composites with various CP contents.....	88
4.34 Young's modulus of CP/PLA/PBS composites with various CP contents.....	88
4.35 Elongation at break of CP/PLA/PBS composites with various CP contents.....	89
4.36 Impact strength of CP/PLA/PBS composites with various CP contents.....	89
4.37 SEM micrographs of tensile fractured surface of PBS20 (a), PBS20-C10 (b), PBS20-C20 (c), PBS20-C30 (d) and PBS20-C40 (e).....	91
4.38 TGA curves of CP/PLA/PBS composites.....	93
4.39 DTG curves of CP/PLA/PBS composites.....	94
4.40 DSC curves from the cooling scan of CP/PLA/PBS composites.....	95
4.41 DSC curves from the second heating scan CP/PLA/PBS composites.....	96

LIST OF FIGURES (Continued)

Figure	Page
4.42 Tensile strength of CP/PLA/PBS composites with and without compatibilizer.....	99
4.43 Young's modulus of CP/PLA/PBS composites with and without compatibilizer.....	99
4.44 Elongation at break of CP/PLA/PBS composites with and without compatibilizer.....	100
4.45 Impact strength of CP/PLA/PBS composites with and without compatibilizer.....	100
4.46 SEM micrographs (1000x) of tensile fractured surface of PBS20-C20 (a), PBS20-G10-C20 (b) and PBS20-M10-C20 (c).....	102
4.47 TGA curves of CP/PLA/PBS composites with and without compatibilizer...	104
4.48 DTG curves of CP/PLA/PBS composites with and without compatibilizer...	104
4.49 DSC curves from the cooling scan of CP/PLA/PBS composites with and without compatibilizer.....	106
4.50 DSC curves from the second heating scan of CP/PLA/PBS composites with and without compatibilizer.....	106

SYMBOLS AND ABBREVIATIONS

ΔH	=	Heat of fusion
mg	=	Milligram
min	=	Minute
rpm	=	revolution per minute
$^{\circ}\text{C}$	=	Degree Celsius
μm	=	Micrometer
wt	=	Weight



CHAPTER I

INTRODUCTION

1.1 General Background

In recent years, the environmental pollution caused by the plastic wastes is an emerging problem. To overcome it, the development of new polymeric materials, which are easily degradable to replace the petroleum-based plastics is proposed. Biopolymers are polymers that are biodegradable. The input materials for the production of these polymers may be either renewable (based on agricultural plant or animal products) or synthetic. There are four main types of biopolymer based respectively on: starch, sugar, cellulose and synthetic materials. Poly (lactic acid) (PLA) degrades biologically into lactic acid, a product of the carbohydrate metabolism, and its importance as a substitute for the non-degradable thermoplastics is an attractive feature. It exhibits good physical properties including high strength, thermoplasticity, processability and excellent biodegradability. PLA can be used in mostly biomedical applications such as sutures and controlled drug delivery systems. However, PLA is quite brittle (low strain at break and high modulus) at room temperature, its applicability has been somewhat limited (Van Cong et al., 2012).

The flexibility and toughness of PLA can be improved by some approaches, such as copolymerization (Ouchi et al., 2004), blending (Gu et al., 2008), and addition of plasticizers (Baiardo et al., 2003). Generally, blending is a relatively simple and easy way compared to other approaches. Flexible polymers such as polycaprolactone

(PCL) (Broze et al., 2003), poly (butylene succinate) (PBS) (Shibata et al., 2006), poly (butylene succinate-co-adipate) (PBSA) and poly (butylene adipate-co-terephthalate) (PBAT) (Pivsa-Art et al, 2011.) were blended with PLA.

Poly (butylene succinate) (PBS) is a biodegradable aliphatic polyester produced by the polycondensation reaction of 1, 4-butanediol with succinic acid (Bhari et al. and Doi et al., 1998 and 1996). It has high flexibility, excellent impact strength, and thermal and chemical resistance (Doi et al., 1994). It can be processed easily and is one of the choices to blend with PLA. However, PLA/PBS blends produced by conventional melt-processing usually exhibit poor impact strength, mainly due to the poor miscibility between PLA and PBS. Moreover, PLA/PBS blends still suffer from poor tensile strength. (Bhatia A. et al., 2007)

Generally, the tensile strength of PLA is greatly improved when reinforced with fibers. Many studies have investigated the addition of natural fibers such as flax fibres (Oksman et al., 2003), kenaf fibers (Ochi, 2008), hemp fiber (Islam et al. and Sawpan et al., 2010 and 2011) and cassava bagasse (Teixeira et al., 2012) as reinforcing fillers in PLA. Raw cassava pulp (RCP) is one of attractive natural reinforcement that can be used to improve tensile strength of PLA. It is a tropical plant. RCP is a byproduct of starch production. RCP contains 50–60% residual starch. It may be dried in the sun and used as filler in cattle feed (Panichnumsin et al., 2010). It has also been tested as a feedstock for ethanol production and other fermentation processes (Iyer et al., 2010). However, most of the RCP are simply discarded as a wasted resource (Panichnumsin et al., 2010). RCP is composed of starch and fiber. Therefore, it is expected that the addition of thermoplastic starch from cassava pulp

(CP) in PLA/PBS blends can improve tensile strength and an inexpensive price can be obtained.

The drawbacks in bio-filler especially its high moisture absorption lead to their low mechanical properties and poor adhesion in composites. Hence bio-filler need to be treated to change their structural and surface properties by physical and chemical methods, and thereby improve the mechanical properties in their applications. Heat treatment is considered to enhance the fiber strength. Bio-filler after heat treatment is expected to improve mechanical properties of composites. Heat treatment is the useful way to modify the natural fibers in the traditional method. Bamboo fibers were treated by heat treatment. Effect of heat treatment on the tensile strength of bamboo fibers was investigated. The tensile strength of bamboo fiber was decreases at high temperatures of heat treatment. Temperatures of heat treatment should be treated below 140 °C in order to prevent strength reduction due to thermal degradation (Ochi, 2012). Kenaf fibers were treated by heat treatments. Compared with the untreated fiber, the tensile strength increased at heat temperature 140 °C. With heat treatment temperature was more than 140 °C, the color of the fibers became brown and black gradually by the observation of naked eye. Moreover the fibers became easily brittle and broken due to low tensile strength (Cao et al., 2007).

Mostly of PLA blend are highly immiscible blend, which can lead to poor mechanical properties. Many researchers try to improve their compatibility by using compatibilizer. Maleic anhydride (MA) is widely used as compatibilizer to improve the compatibility of PLA blend and composites. Corn starch and maleic anhydride were synthesized to obtain a maleic anhydride esterified starch (ES). It was blended

with PLA (Zuo et al., 2014). Compatibility between PLA and starch was improved by addition of ES. The improvement in the inter-face compatibility led to increase in the tensile strength, flexural strength and elongation at break of the starch/PLA composites. Maleic anhydride-grafted PLA (PLA-g-MA) was used to improve the mechanical properties of PLA and *Ganoderma lucidum* fibre (GLF) composites, compared with that of PLA/GLF composites. The PLA-g-MA/GLF composites exhibited superior mechanical properties, attributed to the greater compatibility between the polymer and GLF (Wu, 2014). Glycidyl methacrylate (GMA) grafted polymers are often used as reactive compatibilizers in polyester blends. Glycidyl methacrylate grafted poly (ethylene octane) (GPOE) was used as compatibilizer of PLA/TPS blends. The elongation at break and impact strength of the PLA/TPS blends were greatly increased with addition of GPOE, compared to non-GPOE blends (Shi et al. 2011). GMA was added as reactive compatibilizer to improve the interfacial adhesion between immiscible phases of PLA and PCL. Elongation at break and impact strength of PLA/PCL blends was improved with the addition of GMA 3 wt%, compared to pure PLA/PCL blends (Chee et al., 2013). MA and GMA expect to improve the compatibility of PLA blend and composites.

1.2 Research objectives

The main objectives of this research can be classified as follows:

- (i) To study the effect of PBS content on properties of PLA/PBS blends.
- (ii) To study the effect of PLA grafted glycidyl methacrylate (PLA-g-GMA) on properties of PLA/PBS blends.

- (iii) To study the effect of thermoplastic starch content from cassava pulp (CP) on properties of CP/PLA/PBS composites.
- (iv) To study the effect of compatibilizer, PLA grafted glycidyl methacrylate (PLA-g-GMA) and PLA grafted maleic anhydride (PLA-g-MA) on properties of CP/PLA/PBS composites.

1.3 Scope and limitations of the study

The PLA/PBS blends were melt blended using an internal mixer. The effect of PBS content on mechanical, morphological and thermal properties of PLA/PBS blends was studied. PLA-g-GMA and PLA-g-MA were prepared using an internal mixer. Dicumyl peroxide (DCP) was used as an initiator in the system. The structures of PLA-g-GMA and PLA-g-MA were characterized by Fourier Transform Infrared Spectroscopy (FTIR). The effect of compatibilizer, PLA-g-GMA, on properties of PLA/PBS blends was studied. Heat treatment method was made to obtain heat treated RCP_t. RCP_t was mixed with glycerol in an internal mixer to obtain CP. CP was used as filler at various contents from 0 to 40 wt% in CP/PLA/PBS composites. The CP/PLA/PBS composites were prepared using an internal mixer. The effects of CP content on mechanical, morphological and thermal properties of CP/PLA/PBS composites were investigated. PLA-g-GMA and PLA-g-MA were used as compatibilizer in composites. The effect of PLA-g-GMA and PLA-g-MA on properties of PLA/PBS blends and CP/PLA/PBS composites were investigated. The interaction between PLA and monomer (GMA or MA) was characterized by using FTIR. A titration method was used to determine the content of monomer grafted onto the PLA molecule. The morphology of the blends and composites were observed by

scanning electron microscopy (SEM). Thermal properties of PLA/PBS blends and CP/PLA/PBS composites were studied by differential scanning calorimetry (DSC) and thermo gravimetric analysis (TGA). The mechanical properties of all blends and composites were investigated.

1.4 References

- Baiardo, M., Frisoni, G., Scandola, M., Rimelen, M., Lips, D., Ruffieux, K. and Wintermantel, E. (2003). "Thermal and mechanical properties of plasticized poly(L-lactic acid)" **J. Polym. Sci.** 90: 1731–1738.
- Bhari, K., Mitomo, H., Enjoji, T., Yoshii, F. and Makuuchi, K. (1998). Radiation crosslinked poly (butylene succinate) foam and its biodegradation. **Polym. Degrad. Stab.** 62: 551-557.
- Bhatia, A., Gupta, R. K., Bhattacharya, S. N. and Choi, H. J. (2007).compatibility of biodegradable poly (lactic acid) (PLA) and poly (butylene succinate) (PBS) blends for packaging application. **J. Rheol.** 19: 125-131.
- Broz, M. E., VanderHart, D. L., and Washburn N. R. (2003). Structure and mechanical properties of poly (d,l-lactic acid)/poly(ϵ -caprolactone) blends. **Biomaterials.** 24: 4181–4190.
- Cao, Y., Sakamoto, S. and Goda, K. (2007). Effects of heat and alkali treatments on mechanical properties of kenaf fibers. **16TH INTERNATIONAL CONFERENCE ON COMPOSITE MATERIALS.**

- Carmona, V. B., Corre[^]a, A. C., Marconcini, J. M. and Mattoso, L. H. C. (2014). Properties of a Biodegradable Ternary Blend of Thermoplastic Starch (TPS), Poly(ϵ -Caprolactone) (PCL) and Poly(Lactic Acid) (PLA). **J. Polym. Environ.**
- Chee, W. K., Ibrahim, N. A., Zainuddin, N., Rahman, M. F. A., and Chieng, B. W. (2013). Impact Toughness and Ductility Enhancement of Biodegradable Poly(lactic acid)/Poly(ϵ -caprolactone) Blends via Addition of Glycidyl Methacrylate. **Adv. Mat. Sci. Eng.**
- Cunha, D. C., Deffieux, A. and Fontanille, M. (1993). Synthesis and polymerization of lignin-based macromonomers. III. Radical copolymerization of lignin-based macromonomers with methyl methacrylate. **J Appl Polym Sci.** 48(5): 819-831.
- Doi, Y. and Fukuda, K. (1994). **Biodegradable plastics and polymer.** Studies in Polymer Science 12. Elsevier: 627.
- Doi, Y., Kasuya, K., Abe, H., Koyama, N., Ishiwatara, S., Takagi, K. and Yoshida, Y. (1996). Evaluation of biodegradabilities of biosynthetic and chemosynthetic polyesters in river water. **Polym. Degrad. Stab.** 51: 281-286.
- Gu, S. Y., Zhang, K., Ren, J., and Zhan, H. (2008). Melt rheology of polylactide/poly(butylene adipate-co-terephthalate) blends. **Carbohydr. Polymer.** 74: 79–85.

- Islam, M. S., Pickering, K. L. and Foreman, N. J. (2010). Influence of alkali treatment on the interfacial and physico-mechanical properties of industrial hemp fibre reinforced polylactic acid composites. **Compos.** 41: 596–603.
- Iyer, S., Mattinson, D. and Fellman, J. (2010). Study of the early events leading to cassava root postharvest deterioration. **Tropical Plant Biology.** 3: 151–165.
- Ochi, S. (2008). Mechanical properties of kenaf fibers and kenaf/PLA composites. **Mech. Mater.** 40: 446-452.
- Ochi, S. (2012). Tensile Properties of Bamboo Fiber Reinforced Biodegradable Plastics. **Int. J. Compos. Mater.** 2(1): 1-4.
- Oksman, K., Skrifvars, M. and Selin, J. F. (2003). Natural fibres as reinforcement in polylactic acid (PLA) composites. **Compos. Sci. Technol.** 63: 1317–1324.
- Ouchi, T. and Ohya, Y. (2004). Design of lactide copolymers as biomaterials. **J. Polym. Sci.: Part A.** 42: 453–462.
- Oyama, H.T. (2009). Super-tough poly (lactic acid) materials: Reactive blending with ethylene copolymer. **Polymer.** 50: 747–75.
- Panichnumsin, P., Nopharatana, A., Ahring, B. and Chaiprasert, P. (2010). Production of methane by co-digestion of cassava pulp with various concentrations of pig manure. **Biomass Bioenergy.** 34: 1117–1124.
- Pivsa-Art, W., Pavasupree, S., O-Charoen, N., Insuan, U., Jailak, P. and Pivsa-Art, S. (2011). Preparation of Polymer Blends between Poly (L-lactic acid), Poly

(butylene succinate-co-adipate) and Poly (butylenesadipate-co-terephthalate) for Blow Film Industrial Application. **Energy Procedia**. 9: 581 – 588.

Sawpan, M. A., Pickering, K. L. and Fernyhough, A. (2011). Improvement of mechanical performance of industrial hemp fibre reinforced polylactide biocomposites. **Compos**. 42: 310–319.

Shi, Q., Chen, C., Gao, L., Jiao, L., Xu, H. and Guo, W. (2011). Physical and degradation properties of binary or ternary blends composed of poly(lactic acid), thermoplastic starch and GMA grafted POE. **Polym. Degrad. Stab**. 96: 175–182.

Shibata, M., Inoue, Y., and Miyoshi, M. (2006). Mechanical properties, morphology, and crystallization behavior of blends of poly (L-lactide) with poly (butylene succinate-co-L-lactate) and poly (butylene succinate). **Polymer**. 47: 3557–3564.

Teixeira, E. M., Curvelo, A. A. S., Corrêa, A. C., Marconcini, J. M., Glenn, G. M., Mattoso, L. H. C. (2012). Properties of thermoplastic starch from cassava bagasse and cassava starch and their blends with poly (lactic acid). **Industrial Crops and Products**. 37: 61– 68.

Van Cong, D., Hoang, T., Nguyen Vu Giang, Nguyen Thu, H., Tran Dai, L. and Sumita, M. (2012). A novel enzymatic biodegradable route for PLA/EVA blends under agricultural soil of Vietnam. **Mater. Sci. Eng.: Part C**. 32: 558–563.

Wu, C-S (2014). Preparation, characterisation, and biocompatibility of Ganoderma lucidum fibre-based composites with polylactic acid. **Compos. Sci. Tech.** 102: 1–9.

Zuo, Y., Gu, J., Yang, L., Qiao, Z., Tan, H. and Zhang, Y. (2014). Preparation and characterization of dry method esterified starch/polylactic acid composite materials. **Int. J. Biol. Macromolec.** 64: 174–180.



CHAPTER II

LITERATURE REVIEW

2.1 Poly (lactic acid) (PLA)

PLA is one of the widely used aliphatic polyesters, due to its environmentally friendly properties. Figure 2.1 shows the chemical structure of PLA. Lactic acid is derived from agricultural products, such as corn starch, or other starch-rich substances such as maize, sugar or wheat. The lactic acid catalytically cyclized to make a cyclic dilactate ester, lactide, ring opening polymerized to the wanted poly (lactic acid) (Lunt, 1998). In addition, PLA is proven as a biocompatible material with appreciable mechanical properties comparable to other commodity plastics. PLA has high mechanical properties and biocompatibility. It has been proposed as a renewable and degradable plastic for uses in service ware, grocery, loose-fill packaging, compost bags, food packaging, and disposable tableware. The products made from PLA are bio-degradable and reverts in less than 60 days in ideal conditions; namely, in commercial composting installations. Although PLA has several advantages, PLA is still more expensive than many petroleum-derived commodity plastics and some of other properties such as impact strength are frequently insufficient for various end-use applications (Rudnik, 2008).

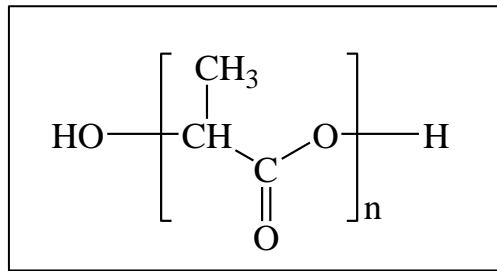


Figure 2.1 Chemical structure of poly (lactic acid) (PLA)

2.1.1 PLA blend

PLA has high modulus and tensile strength but low impact strength and elongation at break. Blending of PLA with other more flexible polymers are the interesting technique. The expectation of this operation is the increase of impact strength and elongation at break while blending of PLA maintains high modulus and tensile strength of PLA blend.

PLA has many good physical properties including tensile strength, thermal plasticity, processing ability and biocompatibility compared to many petroleum-based plastics (Martin and Averous 2001). However, PLA is very brittle under tensile and bending loads leading to serious physical aging during application (Lunt, 1998).Improvement of drawback of PLA, Generally, blending was a relatively simple and easy way compared to other approaches. Flexible polymers, such as PCL (Broze et al., 2003), PBS (Shibata et al., 2006), poly (butylene succinate-co-adipate) (PBSA) and poly (butylene adipate-co-terephthalate) (PBAT) (Pivsa-Art et al, 2011.), were blended with PLA. Those flexible polymers were expected that these polymers can improve mechanical properties of PLA. The experimental results showed that impact strength of the PLA blend was greatly increased. A significant increase in the

elongation at break and decrease in tensile strength can be observed. The stress-extension curve showed the material changed from brittle of PLA to ductile failure with the addition of flexible polymers. These works demonstrate that blending between PLA and other flexible polymers can improve weakness of PLA.

2.1.2 Miscibility of PLA blend

Gajria et al. (1996) studied poly (lactic acid) (PLA) and poly (vinyl acetate) (PVA). A single glass transition temperature showed for all PLA/PVA blend compositions, indicating that PLA and PVA form miscible blends. Results obtained from physical property testing indicated that the blends exhibit synergism in the range of 5 to 30% PVA, probably due to some interactions taking place in that region. The elongation is also seen to increase at 95% of PLA in PLA/PVA blend.

Then, reactive blending was work by Park et al. (2003). Poly (vinyl acetate-co-vinyl alcohol) copolymers [P(VAc-co-VA)] were prepared by acidic hydrolysis of poly(vinyl acetate) (PVAc) at various reaction time, and the degree of hydrolysis was analyzed by ^{13}C nuclear magnetic resonance spectroscopy (NMR). Blends of PLA and P(VAc-co-VA) were prepared by a solvent casting method using chloroform as a co-solvent. The PLA/PVAc blends exhibited a single glass transition over the entire composition range, indicating that the blends were miscible systems. On the contrary, for the blends with even 10% hydrolyzed PVAc copolymer, the phase separation and double glass transition were observed. With increasing neat PVAc contents, the heat of fusion decreased and the melting peaks shifted to lower temperature. The interaction parameter indicated negative values for up to 10% hydrolyzed samples, but positive values at more than 20% hydrolyzed one. Small

angle X-ray scattering analysis revealed that the long period and the amorphous layer thickness increased with PVAc composition, suggesting that a considerable amount of PVAc component located in the interlamellar region. Polarized optical microscopy showed that the texture of spherulites became rougher on increasing the PVAc content. In the case of P(VAc-co-VA) copolymer, the intensity of polarized light decreased significantly, indicating that P(VAc-co-VA) component seemed to be expelled out of the interfibrillar regions. Scanning electron microscopy analysis revealed that the significant phase separation occurred with increasing the degree of hydrolysis. In the case of P(VAc-co-VA) 30% with vinyl alcohol, the P(VAc-co-VA) copolymer formed the regular domains with a size of about 10 nm.

2.1.3 Compatibilizer for PLA blend

Most of PLA blends are highly immiscible blend, so immiscible blend can lead to poor mechanical properties. Accordingly, many researchers have done on improving miscibility while maintaining the biodegradability of polymer blend.

Firstly, Jun (2000) studied properties of PLA and starch blend. PLA and starch blend are important biodegradable polymers. Mechanical properties of blends of PLA and starch using conventional processes were very poor because of incompatibility. In Jun's study, PLA and starch were blended with a reactive agent during the extrusion process. The effects of the reactive blending were investigated and significant improvements were confirmed by measuring the tensile strength and elongation at break, IR spectra, and DSC. Very brittle PLA was blended with 25% and 50% of starch and addition of only 1% reactive agent resulted in very useful, wholly biodegradable polymeric material with 1000–1400 N/cm² of tensile strength

and about 40–80% elongation. Aliphatic diisocyanatohexane (DIH) was a very effective agent for the reactive blending of PLA/starch. The effect of plasticizer on the PLA/starch was also investigated. Depending on the processes of adding the reactive agents, different results were obtained. The two-step process, in which the reactive agent was added after all other ingredients were compounded, was more effective than the simple one-step process, in which all parts were compounded at the same time.

Then, Chen et al. (2006) also investigated PLLA/starch blends. They used poly (L-lactide)-g-starch copolymer (PLLA-g-St) as a compatibilizer. The results showed that the use of PLLA-g-St as a compatibilizer in PLLA/starch blends can improve the performances without changing their whole biodegradability. PLLA-g-St is a good compatibilizer for the blend of hydrophobic PLLA and hydrophilic granular corn starch. The PLLA-g-St effectively improved the interfacial adhesion and the mechanical properties of the composites. The PLLA-g-St compatibilized PLLA/Starch blends showed better mechanical properties and stronger medium-resistance in comparison with the simple starch/PLLA blend.

Huneault and Li (2007) investigated the properties and interfacial modification of blends of PLA and glycerol-plasticized TPS. A twin-screw extrusion process was used to gelatinize the starch, devolatilize the water to obtain a water-free TPS and then to blend into the PLA matrix. The investigated TPS concentration ranged from 27 to 60 wt%. In the absence of interfacial modification, the TPS/PLA blend morphology observed through SEM was very coarse with TPS particles sizes between 5 and 30 μm . Huneault and Li improved miscibility of these blends by free-

radical grafting of MA onto the PLA and then reacting the modified PLA with the starch macromolecules. Blends comprising MA-grafted PLA showed much finer dispersed phase size, in the 1- 3 μm range and exhibited a dramatic improvement in ductility. Elongation at break of modified blends was in the 100-200% range compared to 5-20% for non-modified control and for the pure PLA. Huneault and Li suggested that this improvement was due to a more homogeneous blend and smaller TPS particle sizes and possibly due to an improvement of interfacial adhesion between the TPS and PLA phases.

Shibata et al. (2006) studied mechanical properties, morphologies, and crystallization behavior of plasticized PLLA/poly (butylene succinate-co-L-lactate) (PBSL) blends. The blends of PLLA with PBSL containing the lactate unit of 3 mol% and Rikemal PL710 (RKM) which is a plasticizer mainly composed of diglycerine tetraacetate. The RKM content in PLLA/PBSL/RKM blends was 0-20 wt%, and the PLLA/PBSL weight ratio was 100/0 to 80/20. Although elongation at break in the tensile test did not increase by the addition of 10 wt% RKM to PLLA, the addition of a small amount of PBSL to the PLLA/RKM blend caused a considerable increase of the elongation. The SEM and DSC analyses revealed that all the PLLA/PBSL/RKM blends were immiscible blends where the PBSL particles were finely dispersed, and they suggested that there was some compatibility between PLLA-rich phase and PBSL-rich phase in the amorphous state when the RKM content is 20 wt%. As a result of investigation of the crystallization behavior by DSC and polarized optical microscopic measurements, it was revealed that the addition of RKM caused the acceleration of crystalline growth rate at a lower annealing temperature, and the addition of PBSL mainly enhanced the formation of PLLA crystal nucleus.

Ho et al. (2008) used a thermoplastic polyolefin elastomer-graft-poly lactide (TPO-PLA) as a compatibilizer for PLA/starch blends. TPO-PLA was prepared by grafting poly lactide onto maleic anhydride-functionalized TPO (TPO-MAH) in the presence of 4-dimethylaminopyridine (DMAP). A Molau test and the SEM images of cryo-fractured surface of PLA/TPO binary blends and PLA/TPO/TPO-PLA ternary blends, indicated that the particle size dispersed in PLA matrix substantially decreased as the concentration of the compatibilizers increased, until the content exceeded the critical micelle concentration. Compatibilizing the PLA/TPO (80/20) blend with TPO-PLA copolymer reduced the tensile strength and tensile modulus because of the natural elastic property with low strength and modulus. However, the enhanced interfacial adhesion strength markedly increased the elongation at break and tensile toughness. Moreover, the result indicated that a TPO-PLA copolymer is more efficient than TPO-MAH in compatibilizing the PLA/ TPO (80/20) blend; it is associated with the smaller particle size, narrower size distribution and higher elongation at break and greater tensile toughness.

Then, Li and Shimizu (2009) also improved the toughness of PLLA through reactive blending with acrylonitrile-butadiene-styrene copolymer (ABS). The results showed that uncompatibilized blends of PLLA and ABS have morphology with big phase size and weak interface. The blends exhibited poor mechanical properties with low elongation at break and low impact strength. Styrene/acrylonitrile/glycidyl methacrylate copolymer (SAN-GMA) was found to be an effective reactive compatibilizer for PLLA/ABS blend by the presence of ethyltriphenyl phosphonium bromide (ETPB) as a catalyst. The results showed significant improvement in the dispersion of rubber particles as well as the clearly

shifted glass transition temperature of both PLLA and ABS. Compatibilized PLLA/ABS blends exhibit an increase of impact strength and elongation at break with a slight loss in the modulus and tensile strength.

Another research on reactive blending was conducted by Oyama (2009) toughened PLA by reactive blending with poly (ethylene-glycidyl methacrylate) (EGMA). Oyama's study demonstrated a dramatic improvement in the mechanical characteristics of PLA by its reactive blending with EGMA. The results showed that very high performance of PLA blends was obtained by reactive blending of PLA and EGMA. The elongation at break of PLA blends showed 40 times higher than that of neat PLA. Annealed PLA/EGMA blends had impact strength over 50 times higher than that of the neat PLA. Here, it is considered that the epoxy group in EGMA reacts with both the carboxyl groups and the hydroxyl groups located at the PLA chain ends during melt-mixing leading to an improvement in miscibility and mechanical properties of PLA blend.

Leadprathom et al. (2010) studied reactive compatibilization of PLA and TPS. For all blend ratios, the tensile strengths of PLA/TPS reactive blends were higher than the physical blend of PLA/TPS. The reactive phase adhesion between PLA and TPS was improved by adding reactive compatibilizer. The addition of reactive compatibilizer into the PLA and TPS showed improvement in the mechanical properties and phase adhesion. The differential thermal analysis (DSC) indicated that the crystallization temperature of the reactive blend of PLA/TPS shifted to a lower temperature compared to the physical blend of PLA/TPS. This suggested that the compatibility between TPS and PLA was improved for the reactive blend system.

Most of PLA/TPS reactive blends showed the better water resistance compared to the physical blend of PLA/TPS.

2.2 Poly (butylene succinate) (PBS)

Poly (butylene succinate) (PBS) are aliphatic synthetic polyester. It is synthesized from dicarboxylic acids (e.g., succinic and adipic acid) (Tokiwa, Y. et al., 2009). It has high flexibility, excellent impact strength, and thermal and chemical resistance (Doi et al., 1994). It can be processed easily and is the one of the best choice to blend with PLA. Listed in Table 2.1 are some average physical properties of PBS.

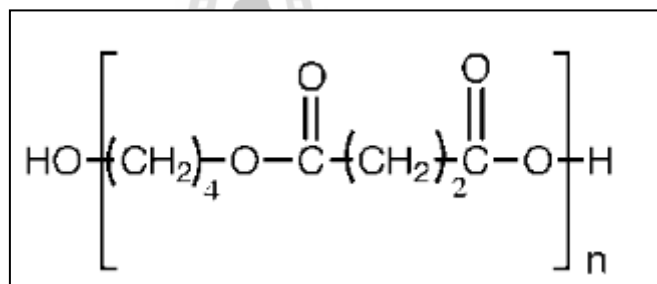


Figure 2.2 Chemical structure of Poly (Butylene Succinate) (PBS)

Table 2.1 Physical properties of PBS (Mitsubishi Chemical Corporation, 2011).

Physical property	Value	Units
Density	1.26	g/cm ³
Glass transition temperature	-22	°C
Melting temperature	115	°C
MFR(190°C/2.16 kg)	5	g/10 min
Flexural modulus	650	MPa
Flexural strength	40	MPa
Yield stress	39	MPa
Tensile Stress at Break	30	MPa
Elongation at Break	160	%
Izod impact strength (23 °C)	7.3	kJ/m ²
Heat Deflection Temperature (HDT) (0.45 MPa)	91	°C

2.2.1 PBS blend

Chen et al. (2005) studied effect of reactive organoclay on PLLA and PBS blends. The twice functionalized organoclay (TFC) was prepared by treating the organoclay, Cloisite[®] 25A (C25A) with (glycidoxypopyl) trimethoxy silane. The result showed that when a small amount of TFC was incorporated in a PLLA/PBS blend the clay layers were fully exfoliated and were located almost exclusively in the PLLA phase. The domain size of the dispersed PBS phase did not change considerably when the TFC content was 0.5 wt%. However, as the TFC content

increased, the clay layers were dispersed in both the PBS and PLLA phases, and the domain size of the dispersed PBS phase grew significantly smaller. The addition of TFC to the PLLA/PBS blend not only improved the tensile modulus but also improved the elongation at break.

Shibata, M. et al. (2006) studied the mechanical properties of blends of PLLA with PBSL and PBS. The tensile strength and modulus of the blends approximately followed the rule of mixtures over the whole composition range except those of 1% of PBS in PLLA/PBS blend which were exceptionally higher than those of pure PLLA. All the blends showed considerably higher elongation at break than pure PLLA, PBSL, and PBS. PBSL contents at 1 to 10% in PLLA/PBSL blends are promising material shaving better flexibility than pure PLLA. In addition, it is interesting that addition of 1% of PBS in PLLA/PBS blend has higher tensile strength and modulus than pure PLLA.

Another study of research to reactive blending was conducted by Bhatia et al. (2007) about blends of PLA and PBS. The morphological investigation by SEM revealed that both the polymers are immiscible beyond 20 wt% of PBS in PLA. Tensile strength and modulus of the blends decreased with PBS content but followed approximately the mixing rule for 90/10 and 80/20 (PLA/PBS) blends. It is concluded that percentage elongation at break remains almost constant for all the blends. Modulated DSC showed that the composition beyond 20 wt% PBS have two distinct melting peaks indicating immiscibility of the two polymers. However, compositions 90/10, 80/20 (PLA/PBS) seem to be miscible. Rheological study concluded that both the neat PBS and PLA polymers exhibited Newtonian behavior.

50/50 wt%(PLA/PBS) blend showed strong shear thinning behavior at low frequencies, while other blends showed similar behavior as that of neat polymers. The shear viscosity of the blend system exhibited shear thinning behavior similar to biodegradable polymers. Viscosities of blends increased as PBS content increased from 50 wt% while 10 wt% and 20 wt% PBS content had viscosities in between the neat polymers which indicate that below 20 wt% of PBS, blends were miscible and above that they become immiscible. Also, values of the blends below 20 wt% of PBS were quite near to the predicted values from the log-additivity rule for viscosity, thus could be considered as miscible. Blends of up to 20 wt% PBS content in PLA was also expected to overcome the deficiencies of PLA such as brittleness, flexural properties, heat distortion temperature and impact strength for applications in food packaging, compost bags, and other biodegradable disposable bags.

Tsi et al. (2009) studied the blend between poly (butylene succinate) and propylene-co-ethylene copolymer. Propylene-co-ethylene elastomer resin (PER) had been blended into biodegradable PBS by a melt-blending process to develop a novel semi-biodegradable thermoplastic elastomer. The PBS/PER blends displayed good compatibility in the range of weight ratio at 70/30 of PBS/PER blends was better than that of 30/70 of PBS/PER blends according to analyses by DSC, DMA and the Couchman method. Although the PBS/PER blends displayed compatibility, SEM analyses of most of the PBS/PER blends revealed two-phase structures including sea-island and irregular fiber-shaped morphologies, except for 70% of PBS in PBS/PER blends. At 50 to 60 % of PBS in PBS/PER blends displayed low tensile strength due to large sea-phase and irregular fiber shaped morphologies, even though they had good compatibility. At 70% PBS in PBS/PER blends apparently exhibited a single

phase by SEM and showed the best compatibility by DSC and DMA. Furthermore, the $\tan \delta$, elongation and initial moduli of the PBS/PER blends were seen to increase with increasing PER content, indicating that the toughness and shock resistance of PBS are improved by incorporating PER into the composition.

Wang et al. (2009) also studied toughening modification of PLLA/PBS Blends. Biodegradable polymer blends consisting of PLLA and PBS were prepared in the presence of dicumyl peroxide (DCP). The effects of DCP content on the mechanical properties, thermal and rheological behavior, phase morphology as well as the toughening mechanism of the blends were investigated. The notched Izod impact strength of 20% PBS in PLLA/PBS blend significantly increased after the addition of 0.05–0.2 phr DCP, but the strength and modulus monotonically decreased with increasing DCP content. PBS acted as a nucleating agent at the environmental temperature below its melting temperature and accelerated the crystallization rate of PLLA but had little effect on its final degree of crystallinity. The degree of crystallinity of PBS and the cold crystallization ability of PLLA gradually reduced with increasing DCP content. The addition of DCP induced an increase in viscosity of the blends at low frequencies as well as finer dispersion of PBS particles and better interfacial adhesion between PLLA and PBS, indicating the in situ compatibilization occurred between the two components. The optical clarity of PLLA/PBS blend was significantly improved after the addition of DCP, which was in accordance with the crystallization behavior and phase structure of the blends.

2.3 Thermoplastic starch (TPS)

Starch is an annually renewable resource. Starch is inherently biodegradable which is a low-cost material and readily available resource. It is often used as filler for the replacement of petroleum-derived synthetic polymers to decrease environmental pollution. However, starch has severe limitations because of its water solubility and poor water-resistance, making starch products very sensitive to the relative humidity at which they are stored and used (Lee et al., 2008).

The starch was first plasticized under heating to obtain thermoplastic starch, giving rise to a continuous phase in the form of a viscous melt which can be processed by conventional plastic processing technique. In general, plasticizers used include polyols such as glycerol, glycol, xylitol and sorbitol. Moreover amide groups such as urea, formaldehyde and acetamide or a mixture of plasticizers were also used as plasticizer.

2.3.1 Thermoplastic starch blend

Rodriguez-Gonzalez et al. (2003) studied LDPE/TPS blends. TPS was prepared by containing 36% glycerol. The elongation at break and modulus of PE/TPS blend with addition 45% TPS maintained 94 and 76% of polyethylene. At a composition 29 % of TPS in PE/TPS for the same glycerol content, the blend retained 96% of the elongation at break and 100% of the modulus of polyethylene. These excellent properties were achieved in the absence of any interfacial modifier and despite the high levels of immiscibility in the polar–nonpolar TPS–PE system. The 45% TPS of blend possessed a 100% continuous or fully interconnected TPS

morphology, as measured by hydrolytic extraction. This highly continuous TPS configuration within the blend should enhance its potential for environmental biodegradation. The elongation at break in the cross direction of these materials, although lower than the machine direction properties, also demonstrated ductility at high TPS concentrations. At a glycerol content of 36% in the TPS, the blends demonstrated only very low levels of sensitivity to moisture. A high degree of transparency was maintained over the entire concentration range due to the similar refractive indices of PE and TPS and the virtual absence of interfacial micro voiding. Effective control of the glycerol content, TPS concentration and processing conditions could result in a wide variety of morphological structures including spherical, fiber-like, highly continuous and co-continuous morphologies. These various blend morphologies were shown to be the determining parameters with respect to the observed mechanical properties.

Lee et al. (2008) investigated about tapioca starch and poly (lactic acid) nanocomposite foams. Tapioca starch (TS), PLA, and four different organoclays (Cloisite 10A, Cloisite 25A, Cloisite 93A and Cloisite 15A) were used to produce nanocomposite foams by melt-intercalation. The morphological study showed that the four nanocomposites had higher cell densities and exhibited smaller and more uniform cells with noticeably decreased cell size. From the DSC study, the TS/PLA/10A and TS/PLA/93A nanocomposite foams had the same T_g of 63.8 °C which was quite similar to the T_g of TS/PLA foam. The T_g of TS/PLA/25A and TS/PLA/15A nanocomposite foams were lower than the T_g of TS/PLA foam at 60.8 and 62.4 °C, respectively. From the DSC thermographs of the first heating scans, T_m of the TS/PLA/10A, TS/PLA/93A and TS/PLA/15A nanocomposite foams were

164.2, 157.4 and 169.1 °C, respectively, were lower than the T_m of the TS/PLA foam. TS/PLA/25A nanocomposite foam had the same T_m of the TS/PLA foam. From the second heating scans, T_m of all the nanocomposite foams was lower than the TS/PLA foam. The largest increase in young's modulus 96% was obtained from TS/PLA/10A nanocomposite foam as compared to the TS/PLA foam, followed by the TS/PLA/25A (14%) and TS/PLA/15A (6%) nanocomposite foams. TS/PLA/93A nanocomposite foam had a significantly lower young's modulus because of its softer texture.

Another research on starch blending was conducted by Chuayjuljit et al. (2009). Biodegradable cassava starch, montmorillonite (MMT) and low density polyethylene (LDPE) were blended in their research. MMT was first modified by sorbitol via a solid state method. Results from X-ray diffraction (XRD) indicated that sorbitol molecules were intercalated in between MMT layers along 001 direction. Cassava starch was plasticized with sorbitol and formamide on a two-roll mill to obtain thermoplastic starch (TPS). The TPS/modified-MMT nanocomposites were prepared by means of melt blending of TPS with various amounts of MMT (0, 2, 4, and 6 phr). XRD and transmission electron microscopy (TEM) results showed that the nanocomposites formed were all exfoliated. The prepared nanocomposites were subsequently blended with a mixture of 80% LDPE and 20% PE was blended and was waxed on a two-roll mill followed by a compression molding machine. The obtained polymer blends were examined for their impact and flexural strength, water absorption, morphology and biodegradability. The mechanical properties of LDPE were improved by incorporating 10 phr of TPS nanocomposite that contained MMT 2 phr and gained the highest impact and flexural strengths of 2900 J m⁻² and 17 N m⁻², respectively. The scanning electron micrographs displayed that the TPS

nanocomposites with a high loading of starch and MMT exhibited poor distribution in Beatrix. Water absorption and biodegradability of the nanocomposites were enhanced with the increasing amount of cassava starch. However, silicate layers with high aspect ratio could serve as a barrier and reduce the water-uptake ability of these materials.

2.4 Cassava pulp

Cassava (*Manihot esculenta Crantz*) is one of the main sources of industrial starch. Its consumption is high and is important in the preparation of many typical food dishes in Brazil as well as in other tropical countries. The bagasse or pulp resulting from the industrial process to obtain the starch is composed by fibrous materials and by remaining starch that was not extracted. The amount of pulp produced by the industry is significant, being roughly equal to 900 kg of pulp with 85% of moisture for each ton of processed root. The precise composition of dry pulp depends on the cassava origin as well as on the processing procedure, but starch 40-60% and fiber about 15-50% predominates followed by small quantities of proteins and lipids. In Brazil, cassava pulp is a problem for the starch industry due to its elevated percentage of water, which makes drying and transport expensive. Many companies, as a shortcut, deposit this waste in their neighborhoods. Usually it is carried away by animal owners to be used for feeding. The improper disposal of the material creates an environmental problem and waste of a raw product, which could be used for other purposes (Matsui et al., 2004).

2.4.1 Cassava pulp blend

Teixeira et al. (2009) studied cassava bagasse cellulose nanofibrils reinforced thermoplastic cassava starch. Their work showed that high added-value products can be obtained from an agricultural waste residue. All-cassava nanocomposite materials were processed. Cellulose nanofibrils with high length (360–1700 nm) and low diameter (2–11 nm) were directly extracted from cassava bagasse. The cellulose cassava bagasse nanofibrils (CBN) reinforced to cassava starch thermoplastic could be verified for all compositions. The addition of cellulose nanofibers in the thermoplastic starch matrix results in a decrease of its hydrophilic character and capacity of water uptake especially for glycerol plasticized samples.

Teixeira et al. (2012) also investigated cassava bagasse and cassava starch and blends with poly (lactic acid). It contains roughly 50% cassava starch along with mostly fiber and could be a valuable feedstock for various bioproducts. Cassava bagasse and cassava starch were used in this study to make fiber-reinforced thermoplastic starch (TPSB and TPSI, respectively). In addition, blends of poly (lactic acid) and TPSI (20%) and TPSB (5, 10, 15 and 20%) were prepared as a means of producing low cost composite materials with good performance. The TPS and PLA blends were prepared by extrusion and their morphological, mechanical, spectral, and thermal properties were evaluated. The results showed the feasibility of obtaining thermoplastic starches from cassava bagasse. The presence of fiber in the bagasse acted as reinforcement in the TPS matrix and increased the maximum tensile strength (0.60 MPa) and the tensile modulus (41.6 MPa) compared to cassava starch TPS (0.40 and 2.04 MPa, respectively). As expected, blending TPS with PLA reduced the tensile strength (55.4 MPa) and modulus (2.4 GPa) of neat PLA. At higher TPSB content

(20%) the maximum strength (19.9 MPa) and tensile modulus (1.7 GPa) were reduced about 64% and 32%, respectively, compared to the PLA matrix. In comparison, the tensile strength (16.7) and modulus (1.2 GPa) of PLA blends made with TPSI were reduced 70% and 51% respectively. The fiber from the cassava bagasse was considered a filler since no increase in tensile strength of PLA/TPS blends was observed. The TPSI (33.1%) had higher elongation to break compared to both TPSB (4.9%) and PLA (2.6%). The elongation to break increased from 2.6% to 14.5% by blending TPSI with PLA. In contrast, elongation to break decreased slightly by blending TPSB with PLA. Thermal analysis indicated there was some low level of interaction between PLA and TPS. In PLA/TPSB blends, the TPSB increased the crystallinity of the PLA component compared to neat PLA. The fiber component of TPSB appeared to have a nucleating effect favoring PLA crystallization.

Nevertheless, the reported previous studies of PLA blends, PLA blended with flexible polymer and adding reinforcement by cassava pulp in PLA blend, including by fiber and starch, were relatively unexplored. In my context, I will study about the improvement of PLA/flexible polymer blend and addition of cassava pulp for reinforcement in blend.

2.5 References

Bhatia, A., Gupta, R. K., Bhattacharya, S. N. and Choi, H. J. (2007).compatibility of biodegradable poly (lactic acid) (PLA) and poly (butylene succinate) (PBS) blends for packaging application. **J. Rheol.** 19: 125-131.

- Chen, G. X., Kim, H. S., Kim E. S. and Yoon J. S. (2005). Compatibilization-like effect of reactive organoclay on the poly(L-lactide)/poly(butylene succinate) blends. **Polymer**. 46: 11829–11836.
- Chen, L., Qiu, X., Xie, Z., Hong, Z., Sun, J., Chen, X. and Jing, X. (2006). Poly(L-lactide)/starch blends compatibilized with poly(L-lactide)-g-starch copolymer. **Carbohydr. Polym.** 65: 75–80.
- Chuayjuljit, S., Hosililak, S. and Athisart, A. (2009). Thermoplastic Cassava Starch/Sorbitol-Modified Montmorillonite Nanocomposites Blended with Low Density Polyethylene: Properties and Biodegradability Study. **J. Miner. Met. Mater.** 19: 59-65.
- Doi, Y. and Fukuda, K. (1994). **Biodegradable plastics and polymer**. Studies in Polymer Science 12. Elsevier: 627.
- Gajria, A. M., Dave, V., Gross, R. A. and McCarthy, S. P. (1996). Miscibility and biodegradability of blends of poly (lactic acid) and poly (vinyl acetate). **Polymer**. 37: 437-444.
- Ho, C.H., Wang, C.H., Lin, C.I. and Lee, Y.D. (2008). Synthesis and characterization of TPO–PLA copolymer and its behavior as compatibilizer for PLA/TPO blends. **Polymer**. 49: 3902–3910.
- Huneault, M. A. and Li, H. (2007). Morphology and properties of compatibilized. **Polymer**. 48: 270-280.

- Jun, C.L. (2000). Reactive Blending of Biodegradable Polymers: PLA and Starch. **J. Polym. Environ.** 8: 33-37.
- Leadprathom, J., Suttiruengwong, S., Threepopnatkul, P. and Seadan, M. (2010). Compatibilized Polylactic Acid/Thermoplastic Starch by Reactive Blend. **J. Miner. Met. Mater.** 20: 87-90.
- Lee, S. Y., Chen, H. and Hanna, M. A. (2008). Preparation and characterization of tapioca starch–poly (lactic acid) nanocomposite foams by melt intercalation based on clay type. **Industrial Crops and Products.** 28: 95–106.
- Lee, S. Y., Hanna, M. and Jones, D. D. (2008). **An Adaptive Neuro-Fuzzy Inference System for Modeling Mechanical Properties of Tapioca Starch-Poly (Lactic Acid) Nanocomposite Foams.** Biological Systems Engineering--Dissertations, Theses, and Student Research.
- Li, Y. and Shimizu, H. (2009). Improvement in toughness of poly (L-lactide) (PLLA) through reactive blending with acrylonitrile–butadiene–styrene copolymer (ABS): Morphology and properties. **J. Euro. Polym.** 45: 738–746.
- Lunt, J. (1998). Large-scale production, properties and commercial applications of polylactic acid polymers. **Polym. Degrad.** 59: 145-152.
- Martin, O. and Averous, L. (2001). Poly (lactic acid): plasticization and properties of biodegradable multiphase systems. **Polymer.** 42: 6209-6219.

- Matsui, K.N., Larotonda, F.D.S., Paes, S.S., Luiz, D.B., Pires, A.T.N. and Laurindo, J.B. (2004). Cassava bagasse-Kraft paper composites: analysis of influence of impregnation with starch acetate on tensile strength and water absorption properties. **Carbohyd. Polym.** 55: 237–243.
- Oyama, H.T. (2009). Super-tough poly (lactic acid) materials: Reactive blending with ethylene copolymer. **Polymer.** 50: 747–75.
- Park, J. W. and Im, S. S. (2003). Miscibility and morphology in blends of poly (L-lactic acid) and poly (vinyl acetate-co-vinyl alcohol). **Polymer.** 44: 4341–4354.
- Pivsa-Art, W., Pavasupree, S., O-Charoen, N., Insuan, U., Jailak, P. and Pivsa-Art, S. (2011). Preparation of Polymer Blends between Poly (L-lactic acid), Poly (butylene succinate-co-adipate) and Poly (butylenesadipate-co-terephthalate) for Blow Film Industrial Application. **Energy Procedia.** 9: 581 – 588.
- Rodriguez-Gonzalez, F. J., Ramsay, B. A. and Favis, B. D. (2003). High performance LDPE/thermoplastic starch blends: a sustainable alternative to pure polyethylene. **Polymer.** 44: 1517–1526.
- Rudnik, E. (2008). **Compostable polymer material.** Amsterdam: Elsevier.
- Shibata, M., Inoue, Y., and Miyoshi, M. (2006). Mechanical properties, morphology, and crystallization behavior of blends of poly (L-lactide) with poly (butylene succinate-co-L-lactate) and poly (butylene succinate). **Polymer.** 47: 3557–3564.

- Teixeira, E. M., Curvelo, A. A. S., Corrêa, A. C., Marconcini, J. M., Glenn, G. M., Mattoso, L. H. C. (2012). Properties of thermoplastic starch from cassava bagasse and cassava starch and their blends with poly (lactic acid). **Industrial Crops and Products**. 37: 61– 68.
- Teixeira, E. M., Pasquini, D., Curvelo, A. A. S., Corradini, E., Belgacem, M. N. and Dufresne, A. (2009). Cassava bagasse cellulose nanofibrils reinforced thermoplastic cassava starch. **Carbohydr. Polym.** 78: 422–431.
- Tokiwa, Y., Calabia, B. P., Ugwu, C. U. and Aiba, S. (2009). Biodegradability of Plastics. **Int. J. Mol. Sci.** 10: 3722-3742.
- Tsi, H. Y., Tsen, W. C., Shu, Y. C., Chuang, F. S. and Chen, C. C. (2009). Compatibility and characteristics of poly (butylene succinate) and propylene-co-ethylene copolymer blend. **Polym. Test.** 28: 875–885.
- Wang, R., Wang, S., Zhang, Y., Wan, C. and Ma, P. (2009). Toughening Modification of PLLA/PBS Blends via In Situ Compatibilization. **Polym. Eng. Sci.**: 26-33.

CHAPTER III

EXPERIMENTAL

3.1 Materials

A commercial grade of PLA (PLA 4043D) was purchased from Nature Works LLC. A commercial grade of PBS (PBS FZ91PD) was purchased from Mitsubishi Chemical Co., Ltd. Dicumyl peroxide (DCP, 99%), glycidyl methacrylate monomer (GMA, 99%), maleic anhydride monomer (MA, 99%) and glycerol were supplied from Sigma-Aldrich. GMA was purified to remove inhibitors by a basic alumina pack column before used. Raw cassava pulp (RCP) was purchased from Ratchasima Boonpa Co., Ltd.

3.2 Experimental

3.2.1 Preparation of raw cassava pulp (RCP_t)

Raw cassava pulp (RCP) was ground with a grinder. Then, it was separated by sieve with a wire rack. The size of the mesh is 150-250 μm . RCP was dried in an oven at 120°C for 24 hours for the removal of excess moisture. RCP was modified by heat treatment to obtain RCP_t at the temperature of 180°C for 1 hour before mixing. Figure 3.1 showed diagram for preparation of RCP. RCP was analyzed and measured content of crude fiber, starch and other components. Crude fiber of RCP was analyzed by using Association of Official Analytical Chemists Fiber (Crude) in Animal Feed and Pet Food 978.10 (AOAC 978.10) and starch was using

Anthrone method. Content of crude fiber, starch and other components were shown in Table 3.1. Crude fiber contained cellulose, hemicellulose and lignin. Amount of cellulose, hemicellulose and lignin of RCP were determined by Van Soest method fiber analysis (Fibretherm FT 12 machine). Cellulose, hemicellulose and lignin contents of RCP are shown in Table 3.2.

Table 3.1 Component of RCP (starch and fiber).

Component	Raw cassava pulp (RCP, dimension size 150-250 μm)
Starch (%)	43.14
Crude fiber (%)	30.02
Other components (%)	26.84

Table 3.2 Amount of cellulose, hemicellulose and lignin of RCP before and after heat treatment.

Name	Cellulose (%)	Hemicellulose (%)	Lignin (%)	Non Lignocellulose (%)
RCP before heat treatment (RCP)	20.89	5.14	3.99	69.96
RCP after heat treatment (RCP _t)	22.82	4.42	2.79	69.95

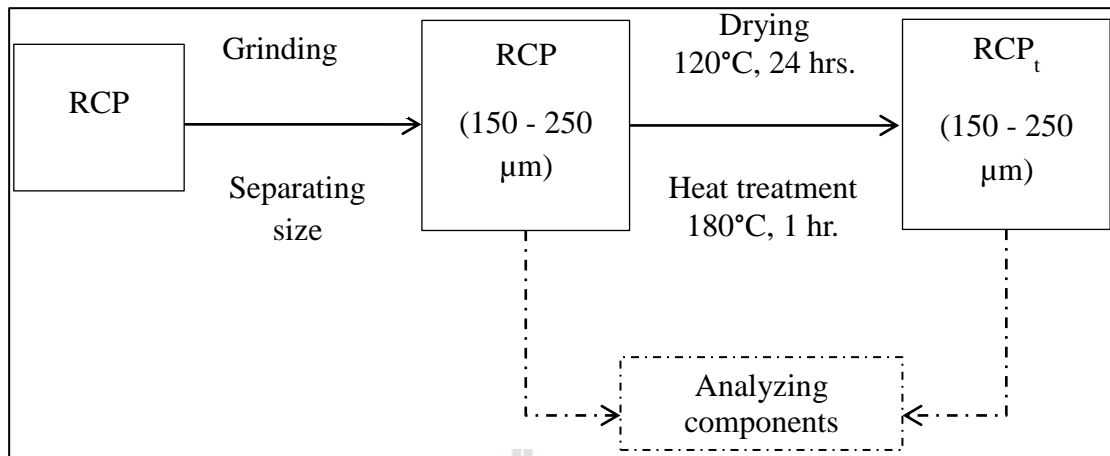


Figure 3.1 Diagram for preparation of RCP_t.

3.2.2 Preparation of thermoplastic starch from cassava pulp (CP)

RCP_t was mixed to obtain CP with 20 - 60 wt% of glycerol in an internal mixer (Hakke Rheomix, 3000p) at 120 °C and mixing speed was 60 rpm for 10 minutes. CP was used for filler in CP/PLA/PBS composites in this study. Figure 3.2 showed diagram for preparation of CP. The test specimens were prepared by a compression molding machine (LabTech, LP20-B). The compression condition was processed at the temperature of 120°C for 10 minutes and the pressure of 100 MPa.

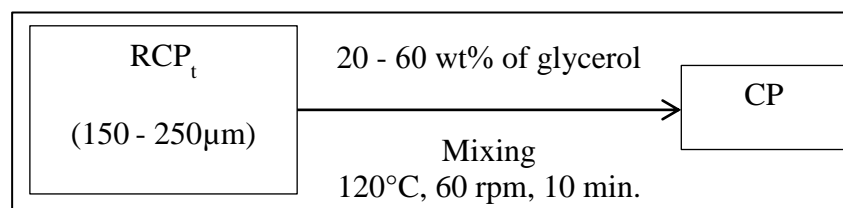


Figure 3.2 Diagram for preparation of CP.

3.2.3 Preparation of poly (lactic acid) grafted with glycidyl methacrylate (PLA-g-GMA)

PLA-g-GMA was prepared using an internal mixer (Hakke Rheomix, 3000p). PLA pellet was dried at 70°C for 4 hours before mixing. The mixing temperature was kept at 170°C. A rotor speed was 60 rpm and mixing time was 7 min. First, PLA and DCP were added in the internal mixer. After 2 minutes, GMA was added. The formulation which used to prepare PLA-g-GMA was shown in Table 3.3.

Table 3.3 Formulation of the preparation of GMA grafted PLA.

Ingredients	PLA (wt%)	GMA (phr)	DCP (phr)
PLA-g-GMA	100	10	0.2

3.2.4 Preparation of poly (lactic acid) grafted with maleic anhydride (PLA-g-MA)

PLA-g-MA was prepared using an internal mixer (Hakke Rheomix, 3000p). PLA pellet was dried at 70°C for 4 hours before mixing. The mixing temperature was kept at 170°C. A rotor speed was 60 rpm and mixing time was 7 min. First, PLA and DCP were added in the internal mixer. After 2 minutes, MA was added. The formulation which used to prepare PLA-g-MA was shown in Table 3.4.

Table 3.4 Formulation of the preparation of MA grafted PLA.

Ingredients	PLA (wt%)	MA (phr)	DCP (phr)
PLA-g-MA	100	10	0.2

3.2.5 Characterization of PLA-g-GMA and PLA-g-MA

3.2.5.1 Determination of glycidyl methacrylate and maleic anhydride content

The quantity of glycidyl methacrylate and maleic anhydride content on PLA was determined by titration method. The acid groups of PLA-g-GMA and PLA-g-MA derived from functions group by using phenolphthalein as an indicator. Samples were dissolved in chloroform. It was precipitated by methanol for removal of residual monomers (GMA and MA) and initiator (DCP). Then, PLA-g-MA was accurately weighed and completely dissolved in chloroform : methanol for ratio 80:20 %v/v and it was titrated with potassium hydroxide solution (KOH). The grafting degree of GMA was defined as the weight percentage of GMA in PLA-g-GMA. It was determined by means of acid-alkali titration. About 0.5 g of the purified sample was first dissolved in 70 ml refluxing chloroform for 1 h, in which a few drops of trichloroacetic acid/ chloroform solution were added. The hot solution was titrated immediately with 0.05 N NaOH methanol solution, after adding drops of 1% phenolphthalein in methanol as indicator. Titration was stopped when the coloration remained for 30 s (Su et al., 2009). The acid number and the graft content (%G) were calculated using Eq. 3.1, Eq. 3.2 for PLA-g-MA. %G was calculated using Eq. 3.3 for PLA-g-GMA. Pure PLA without GMA and MA was also titrated under the same condition to obtain blank values (Wu, 2003)

$$\text{Acid number (mg KOH/g)} = \frac{V_{\text{KOH}} (\text{ml}) \times N_{\text{KOH}} (\text{N})}{\text{sample (g)}} \times 56.1 \quad (3.1)$$

$$\%G \text{ of PLA-g-MA} = \frac{(\text{Acid number} - M_0)}{2 \times 561} \times 98.06 \quad (3.2)$$

$$\%G \text{ of PLA-g-GMA} = \frac{142.15 \times (V_0 - V) \times c}{1000 \times m} \times 100 \quad (3.3)$$

Where N is the normality (mol/L), V is the volume (ml); M_0 is the blank titration value of pure PLA; 98.06 is the molecular weight of MA.

Where V (ml) and V_0 (ml) represent the volume of KOH solution used for titration of grafted and blank samples, respectively; c (mol/L) is molar concentration of KOH solution; m (g) is the weight of grafted sample; 142.15 is the molecular weight of GMA (Su et al., 2009).

3.2.5.2 Fourier Transform Infrared Spectroscopy

The structural characterization of PLA-g-GMA and PLA-g-MA were conducted by Bruker Tensor 27 FTIR Fourier transform infrared spectroscopy using attenuated total reflectance (ATR) equipped with platinum diamond crystal (TYPE A225/QL). Spectra were obtained at 4 cm^{-1} resolution in the wave range from $4000 - 400 \text{ cm}^{-1}$. All samples were dried in oven at 70°C for 4 hours before testing.

3.2.6 Preparation of PLA/PBS blends

The blends of PLA and PBS at various PBS contents of 10, 20, 30 and 40 wt% were investigated. The blend which gave maximum elongation at break was selected to study the effect of PLA-g-GMA on the properties of the PLA/PBS blends. The compatibilizer, 10 phr of PLA-g-GMA was added in the blends. The

compositions of blends are shown in Table 3.5. Before blending, PLA and PBS were dried in an oven at 70°C for 4 hours. PLA/PBS blends were prepared using an internal mixer (Hakke Rheomix, 3000p). The mixing temperature was kept at 170°C. A rotor speed was 60 rpm and a mixing time was 10 min. The PLA/PBS blend was ground into small pellets with a grinder (Emod Motoren GmbH 36364). The test specimens were prepared by a compression molding machine (LabTech, LP20-B). The compression condition was processed at the temperature of 170°C for 10 minutes and the pressure of 100 MPa.

Table 3.5 Blends composition.

Name	PLA (wt%)	PBS (wt%)	PLA-g-GMA (phr)
PLA	100	-	-
PBS10	90	10	-
PBS20	80	20	-
PBS30	70	30	-
PBS40	60	40	-
PBS20-G10	80	20	10
PBS	-	100	-

3.2.7 Preparation of CP/PLA/PBS composites

In cases of CP/PLA/PBS composites, CP was added as a filler in PLA/PBS blends which gave maximum elongation at break. CP contents were 10, 20, 30 and 40 wt%. Effect of compatibilizer, PLA-g-GMA and PLA-g-MA, on the

properties of the CP/PLA/PBS composites was studied. The compatibilizer, 10 phr of PLA-g-GMA and 10 phr PLA-g-MA were added in the composites. The composition of composites is shown in Table 3.6. Before mixing, PLA, PBS and CP were dried in an oven at 70°C for 4 hours. CP/PLA/PBS composites were prepared using an internal mixer (Hakke Rheomix, 3000p). The mixing temperature was kept at 170°C. A rotor speed was 60 rpm and mixing time was 10 min. The CP/PLA/PBS composites were ground into small pellets with a grinder (Emod Motoren GmbH 36364). The test specimens were prepared by a compression molding machine (LabTech, LP20-B). The compression condition was processed at the temperature of 170°C for 10 minutes and the pressure of 100 MPa.

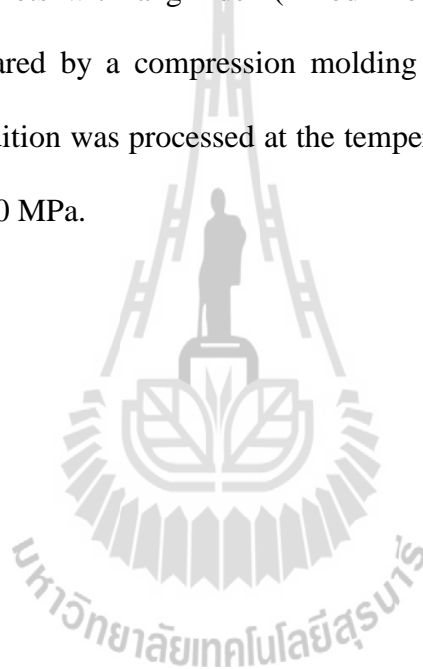


Table 3.6 Composite composition.

Name	PLA (wt%)	PBS (wt%)	CP (wt%)	RCP _t (wt%)	PLA-g-GMA (phr)	PLA-g-MA (phr)
PLA	100	-	-	-	-	-
PBS20	80	20	-	-	-	-
PBS20-C10	72	18	10	-	-	-
PBS20-C20	64	16	20	-	-	-
PBS20-C30	56	14	30	-	-	-
PBS20-C40	48	12	40	-	-	-
PBS20-RCP _t 20	64	16	-	20	-	-
PBS20-G10	80	20	-	-	10	-
PBS20-G10-C20	64	16	20	-	10	-
PBS20-M10-C20	64	16	20	-	-	10
PBS	-	100	-	-	-	-

3.2.8 Characterization of PLA/PBS blends and CP/PLA/PBS composites

3.2.8.1 Mechanical properties

Tensile properties of PLA, PBS, PLA/PBS blends and CP/PLA/PBS composites were performed using an Instron universal testing machine (UTM, model 5565) with a load cell of 5 kN and a crosshead speed of 1 mm/min. The specimens were obtained according to ASTM D638. Impact testing was using an Atlas testing machine (model BPI). Impact tests were performed according to unnotched Izod impact strength (ASTM D256). A pendulum of 2.7 J was selected.

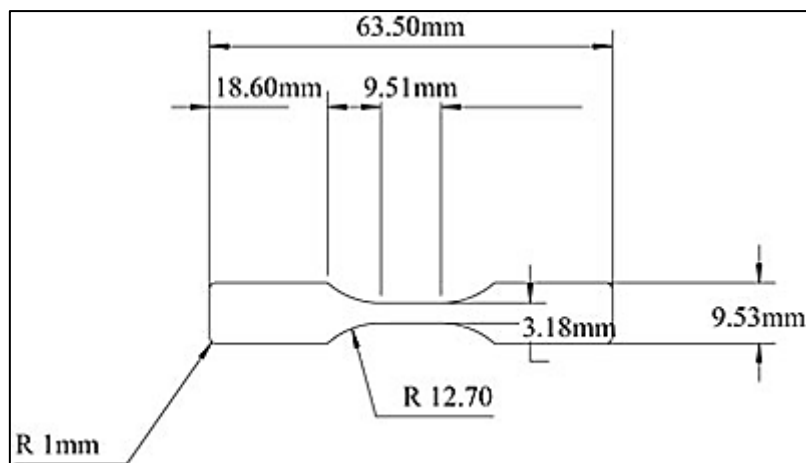


Figure 3.3 ASTM D638 Type V specimens for tensile testing.

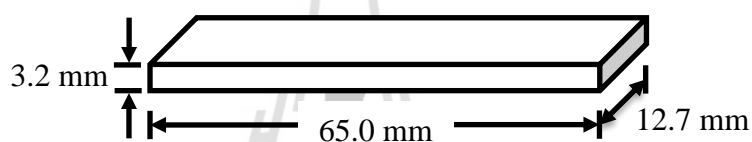


Figure 3.4 The standard specimen for impact testing.

3.2.8.2 Morphological properties

Tensile fracture surfaces of all blends and composites were investigated by a scanning electron microscope (SEM, model JEOL JSM6010LV). The specimens were coated with gold prior to the examination. Acceleration voltage of 10 kV was used to collect SEM images of the sample

3.2.8.3 Thermal properties

Thermogravimetric analysis (TGA) was performed using a Mettler Toledo STARE System (TGA/DSC1 Modulae) by heating sample under a nitrogen atmosphere. The sample with a weight between 5 to 10 mg was used for each

run. Each sample was heated from room temperature to 650 °C at a heating rate of 10 °C/min.

Thermal properties of samples were investigated using differential scanning calorimetry (DSC: DSC204F1 Phoenix). The degree of crystallinity of the sample was heated from 40°C to 200°C with a heating rate of 5°C/min (First heating scan) under a nitrogen atmosphere, and was held at 200°C for 5 min to remove thermal history. Then, the sample was cooled to 40°C with a cooling rate of 5°C/min (Cooling scan). After keeping the sample at 200°C for 5 min it was cooled to 40°C at 5°C/min. The sample was heated again from 40°C to 200°C with a heating rate of 5°C/min (second heating scan). Diagram of thermal programming for DSC was shown in Figure 3.3. The degree of crystallinity (%X) was determined using the following equation (Amash and Zugenmaier, 2000):

$$\% X = \frac{\Delta H_m}{\Delta H_{m_o} W} \times 100 \quad (3.4)$$

ΔH_m is the measured melting enthalpy, ΔH_{m_o} is the melting enthalpy of purely crystalline sample (93.0 J/g for PLA and 110.3 for PBS) and W is the weight fraction in the blends.

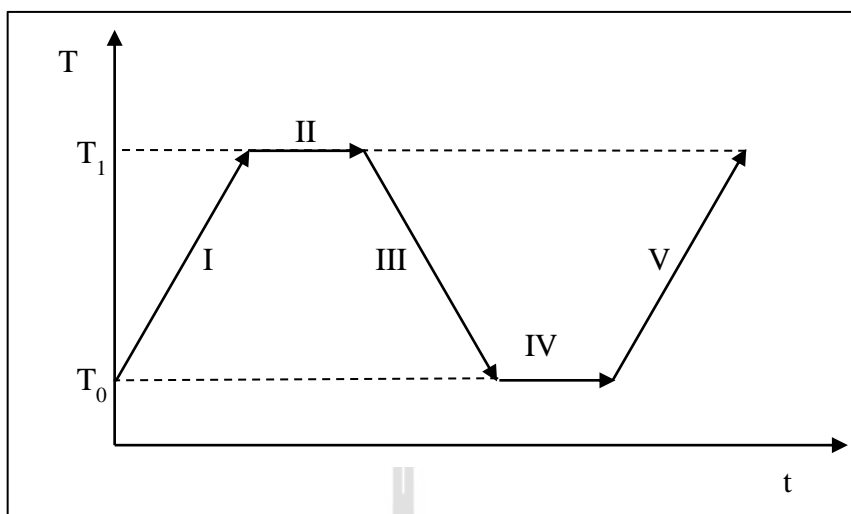


Figure 3.5 Diagram of thermal programming for DSC. ($T_0 = 40^\circ\text{C}$, $T_1 = 200^\circ\text{C}$)

Stage I : Heating from 40°C to 200°C with a heating rate of $5^\circ\text{C}/\text{min}$ under a nitrogen atmosphere. (First heating scan)

Stage II : Isothermal at 200°C for 5 min under a nitrogen atmosphere.

Stage III : Cooling from 200°C to 40°C with cooling rate of $5^\circ\text{C}/\text{min}$ under a nitrogen atmosphere. (Cooling scan)

Stage IV : Isothermal at 40°C for 5 min under a nitrogen atmosphere.

Stage V : Heating again from 40°C to 200°C with a heating rate of $5^\circ\text{C}/\text{min}$ under a nitrogen atmosphere. (Second heating scan)

3.2.8.4 X-ray diffraction (XRD)

The diffraction patterns were obtained using a diffractometer (AXS Nanostar-D8 Discover, Bruker) equipped with a $\text{CuK}\alpha$ generator ($\lambda = 1.5404$

Å) at 40 kV and 40 mA, in a 2θ range from 2.0° to 90.0° . Average crystallite size was calculated by Scherrer's Equation (Monshi, A. et al., 2012)

$$L = \frac{(K\lambda)}{(B\cos\theta)} \quad (3.5)$$

L is average crystal size, K is a constant related to crystal shape, normally taken as 0.9, λ is X-ray wavelength (CuK α radiation, wavelengths $\lambda = 0.154178$ nm, 1.54178 Å), B is Full width at half max ($\Delta 2\theta$ in radian) and θ is Bragg angle.

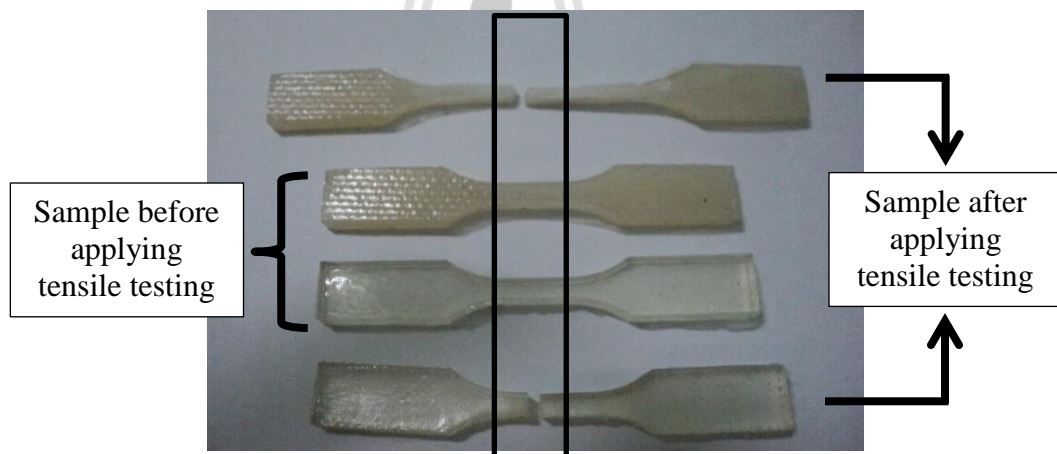


Figure 3.6 Position of sample for XRD testing.

3.3 References

Amash, A. and Zugenmaier, P. (2000). Morphology and properties of isotropic and oriented samples of cellulose fiber-polypropylene composites. **Polymer**. 41: 1589-1596.

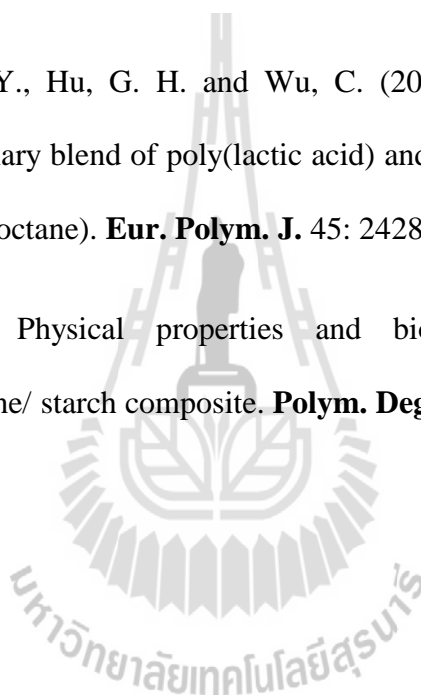
Juntuek, P. 2011. **Effect of glycidyl methacrylate grafted natural rubber on physical properties of PLA/NR blends and PLA/vetiver/NR composites.**

Doctoral Thesis, Suranaree University of Technology. 194.

Monshi, A., Foroughi, M. R. and Monshi, M. R. (2012). Modified Scherrer Equation to Estimate More Accurately-Nano-Crystallite Size Using XRD. **World Journal of Nano Science and Engineering**. 2: 154-160.

Su, Z., Li, Q., Liu, Y., Hu, G. H. and Wu, C. (2009). Compatibility and phase structure of binary blend of poly(lactic acid) and glycidyl methacrylate grafted poly (ethylene octane). **Eur. Polym. J.** 45: 2428-2433.

Wu, C.-S. (2003). Physical properties and biodegradability of maleated-polycaprolactone/ starch composite. **Polym. Degrad. Stab.** 80: 127-134.



CHAPTER IV

RESULTS AND DISCUSSION

4.1 Characterization of PLA-g-GMA and PLA-g-MA

Melt grafting of glycidyl methacrylate (GMA) and maleic anhydride (MA) onto PLA molecule chain were prepared by an internal mixer. Infrared spectrometry was used to identify the grafting reaction of PLA-g-GMA and PLA-g-MA. This analysis was performed with a Fourier transform infrared spectrophotometer (FTIR). The FTIR spectra of PLA, PLA-g-GMA and PLA-g-MA were scanned. The graft content was determined by a non-aqueous titration method.

4.1.1 PLA-g-GMA

FTIR spectra of neat PLA and PLA-g-GMA were given in Figure 4.1. Graft content (%) of PLA-g-GMA was shown in Table 4.1. FTIR spectrum of neat PLA showed CH₃ stretching at 3000–2940 cm⁻¹. The C=O cm⁻¹ stretching at 1761 cm⁻¹ and the O–C=O stretching at 1190–1090 cm⁻¹ were characteristics of ester peak (Orozco et al., 2009). Polyglycidyl methacrylate (PGMA) spectrum showed band at 907 cm⁻¹, 1716 cm⁻¹ and 1153 cm⁻¹ which were corresponded to the characteristic of epoxy group, carbonyl group (C=O) and ester group (C–O) (Juntuek, 2011). Compared with the spectrum of pure PLA, a new peak was appeared at 910 cm⁻¹ in the spectrum of PLA-g-GMA. This peak was associated with the asymmetric stretching of the epoxy group (Xu, et al., 2012). This showed that the GMA was

4.1.2 PLA-g-MA

FTIR spectra of PLA, PLA-g-MA and MA are shown in Figures 4.3 and 4.4. Graft content (%) of PLA-g-MA is shown in Table 4.1. FTIR spectrum of neat PLA showed CH₃ stretching at 3000–2940 cm⁻¹. The C=O cm⁻¹ stretching at 1761 cm⁻¹ and the O–C=O stretching at 1190–1090 cm⁻¹ were characteristics of ester bonds (Orozco et al., 2009). In comparison, PLA-g-MA exhibited a very similar spectrum to neat PLA. According to John et al., 1997 cyclic anhydrides should exhibit an intensive absorption band near 1780 cm⁻¹ due to the symmetric of C=O. The new peak of PLA-g-MA observed at 1850 cm⁻¹ was ascribed to the asymmetric C=O stretching of the succinic anhydride ring. These peaks indicated that MA monomers were grafted onto the PLA.

The organic peroxide was used as an initiator. Some free MA monomer could react directly with the PLA macroradicals. The grafted macroradicals could react with MA monomers with a hydrogen atom on its PLA chain to form a new macroradical. This process continued until grafting was terminated by recombination. The probable mechanism for grafting reaction was suggested in Figure 4.5.

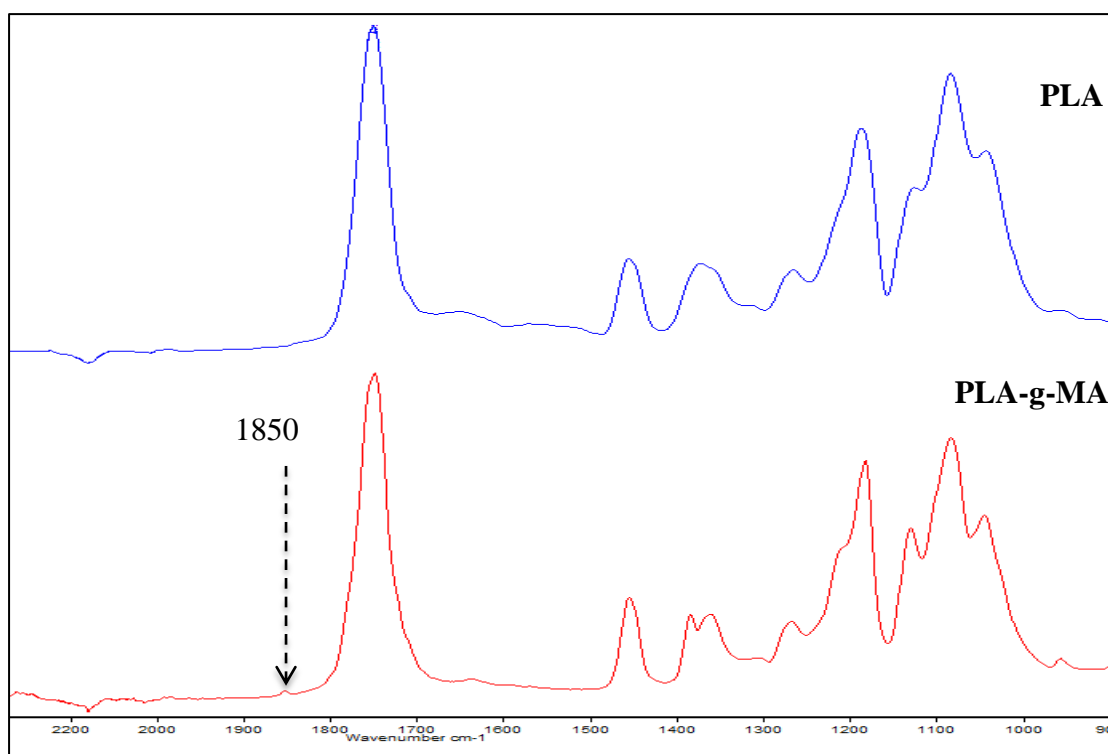


Figure 4.3 FTIR spectra of PLA and PLA-g-MA.

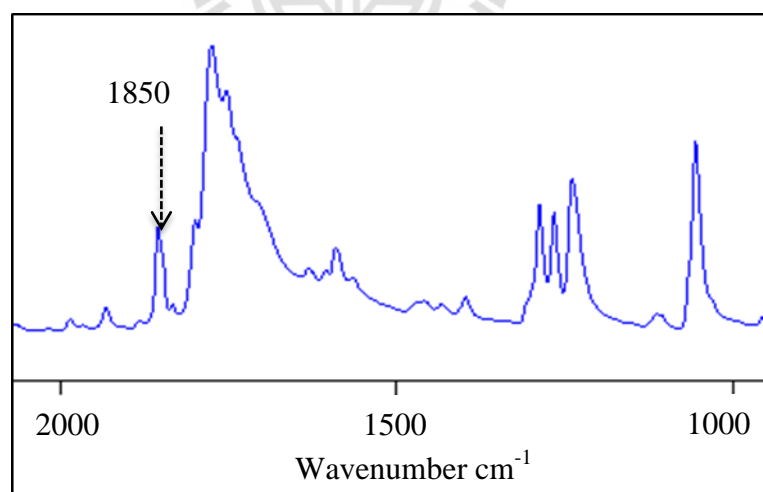


Figure 4.4 FTIR spectra of MA.

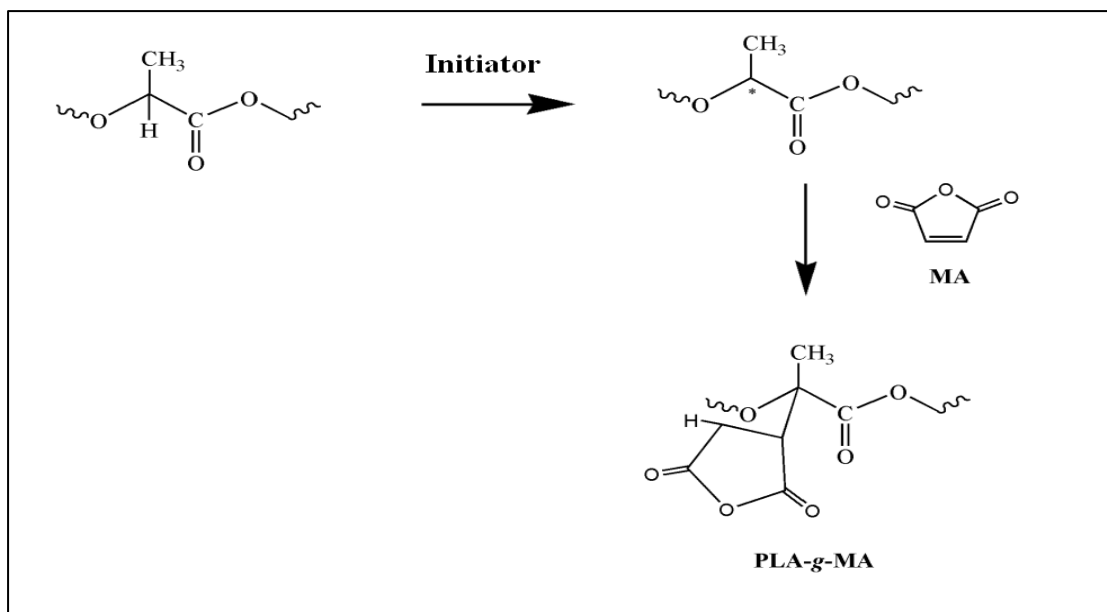


Figure 4.5 Possible reaction of MA on PLA (Mani, Bhattacharya, and Tang, 1999).

Table 4.1 Graft content of PLA-g-GMA and PLA-g-MA. (Graft content (%G) was calculated using Eq. 3.2 for PLA-g-MA and Eq. 3.3 for PLA-g-GMA, respectively).

Name	Graft content (%)
PLA-g-GMA	0.500
PLA-g-MA	1.814

4.2 Effect of PBS contents on physical properties of PLA/PBS blends

4.2.1 Mechanical properties of PLA/PBS blends

Figure 4.6 indicated tensile strength of PLA, PBS and their blends. The tensile strength of neat PLA was 61.44 MPa, which was higher than that of PBS (27.53 MPa). With increasing PBS contents from 10 to 40 wt%, tensile strength of PLA/PBS blends was decreased. Hassan et al. (2013) also studied PLA/PBS blends. The tensile strength of blends was decreased with increasing PBS content. Young's modulus of PLA, PBS and PLA/PBS blends at various PBS contents was shown in Figure 4.7. Young's modulus of PLA/PBS blends was decreased with increasing PBS content. The reduction in tensile strength and Young's modulus was due to the result of the flexible property of PBS. Figure 4.8 exhibited elongation at break of PLA/PBS blends with various contents of PBS. Elongation at break of blends was increased with increasing PBS content up to 20 wt%. Elongation at break was increased from 5.20% for neat PLA to 52.82% for PBS20. This may be attributed to more elastic characteristic of PBS. With increasing PBS content to 30 wt% and 40 wt%, elongation at break of PLA/PBS blends was decreased. The decrease of elongation at break of PLA/PBS blends at high PBS contents was due to the coalescence of PBS phase. Larger PBS phases may induce stress concentration. Stress concentration took place in the vicinity of the dispersed phase separations due to the difference of elastic modulus between the dispersed phases (PBS) and the matrix (PLA), and initiates localized micro-damages in this region. Therefore, tensile strength, Young's modulus and elongation at break were decreased at high PBS contents. This behavior was also found in Poly(L-lactide) (PLLA) and poly(ϵ -caprolactone) (PCL) blends (Todo et al., 2007). Impact strength of PLA/PBS blends was shown in Figure 4.9. The impact strength of PLA was 12.61 kJ/m². Impact strength of PLA/PBS blends was increased with increasing PBS content. When the PBS content reached 40 wt%, impact strength

of PLA/PBS blend was 25.91 kJ/m^2 , which was about 2 times higher than that of neat PLA. This suggested that the impact strength of PLA could be improved by addition of PBS. Impact strength of PLA/PBS blends was improved due to toughness of PBS, in comparison with PLA. Hassan et al. (2013) also observed this behavior in PLA/PBS blends. Impact strength of PLA/PBS blends was increased with increasing PBS contents. Impact strength of PLA/PBS blends was higher compared to impact strength of neat PLA. Tensile strength, Young's modulus, elongation at break and impact strength of PLA/PBS blends are summarized in Table 4.2.

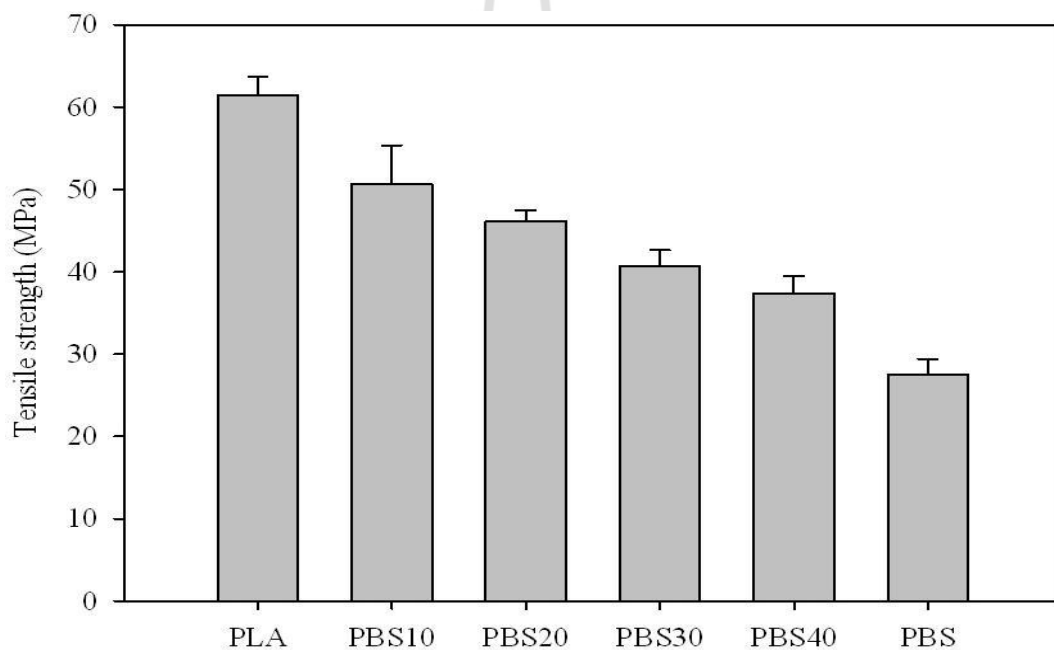


Figure 4.6 Tensile strength of PLA/PBS blends at various PBS contents.

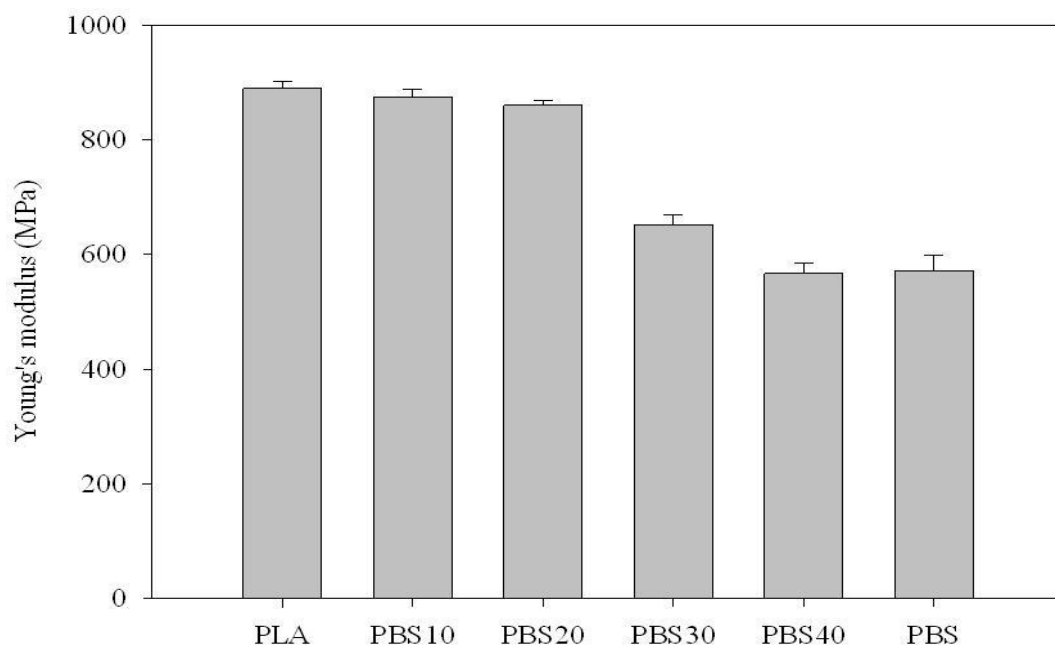


Figure 4.7 Young's modulus of PLA/PBS blends at various PBS contents.

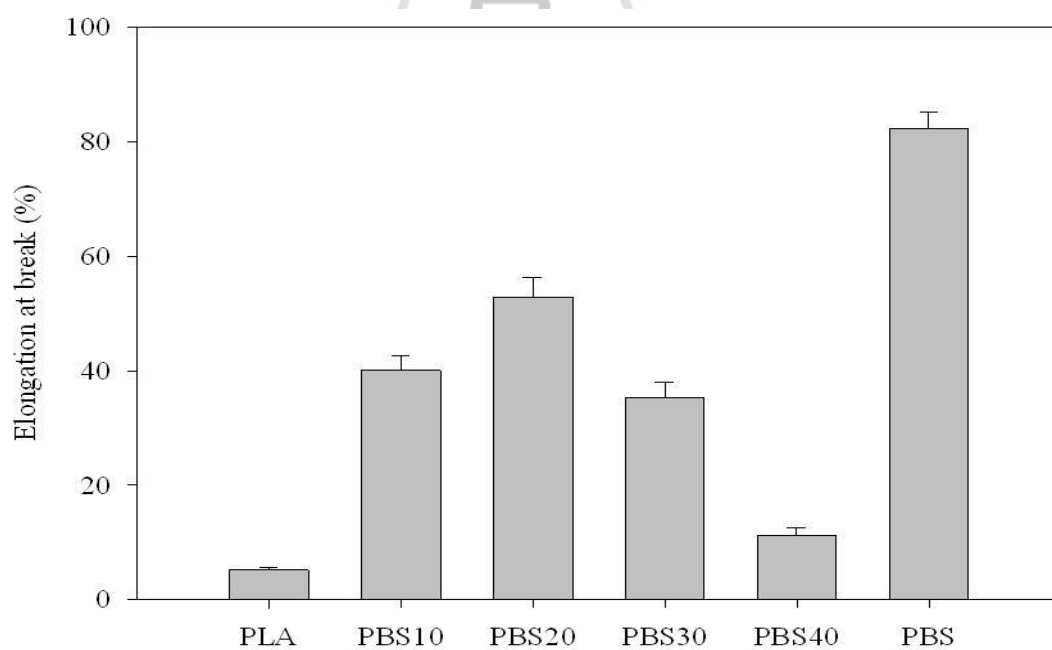


Figure 4.8 Elongation at break of PLA/PBS blends at various PBS contents.

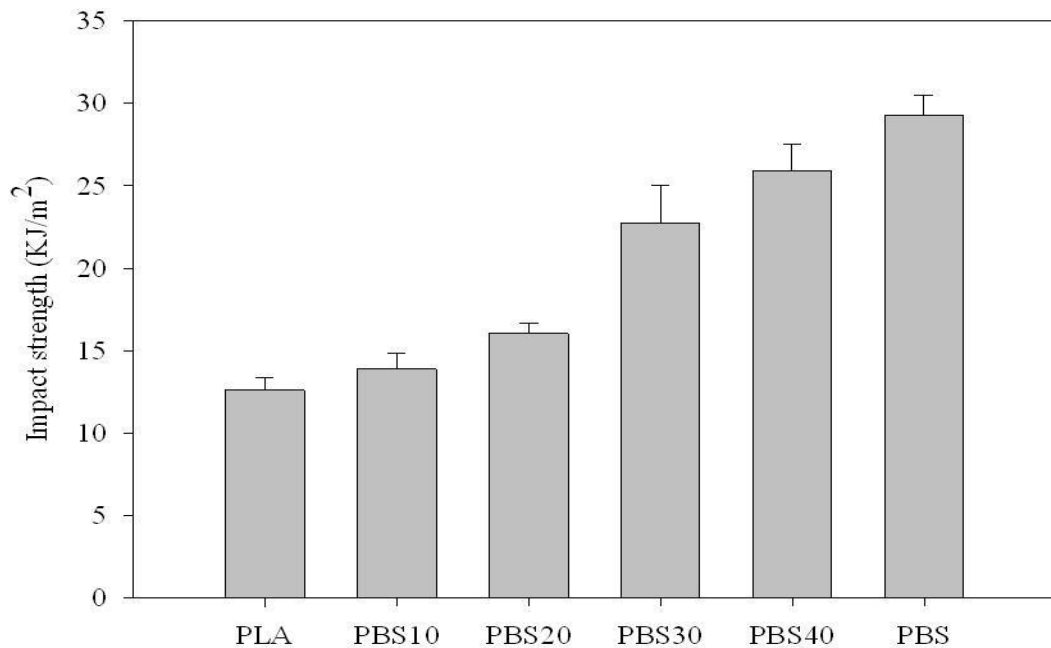


Figure 4.9 Impact strength of PLA/PBS blends at various PBS contents.

Table 4.2 Tensile strength, elongation at break, Young's modulus and impact strength of PLA/PBS blends.

Name	Tensile strength (MPa)	Young's modulus (MPa)	Elongation at break (%)	Impact strength (kJ/m ²)
PLA	61.44±2.29	890.20±12.64	5.20±0.39	12.61±0.75
PBS10	50.66±4.70	874.45±13.57	40.07±2.59	13.88±0.99
PBS20	46.10±1.37	860.90±8.74	52.82±3.43	16.03±0.61
PBS30	40.67±1.96	652.43±17.59	11.76±0.86	22.77±2.24
PBS40	37.36±2.08	567.06±17.48	11.29±1.27	25.91±1.64
PBS	27.53±1.90	571.96±27.72	82.28±2.82	29.26±1.22

4.2.2 Morphological properties of PLA/PBS blends

SEM micrographs of tensile fractured surface of PLA, PBS and PLA/PBS blends are shown in Figure 4.10. The particles represent the PBS phases distributed in the PLA matrix. The particle size of PBS was increased with increasing PBS content. Type of fracture surface of neat PLA in Figure 4.10(a) was brittle fracture. PLA/PBS blends with PBS content up to 20 wt% exhibited plastic deformation and higher elongation at break compared to that of neat PLA. PBS10 and PBS20 were shown in Figure 4.10(c – d). PLA/PBS blends with PBS 30 - 40 wt% was shown in Figure 4.10(e) and Figure 4.10(f), respectively. The poor distribution of PBS at high loading PBS was observed. These caused the decrease in elongation at break of PLA/PBS blend at 30 - 40 wt% of PBS. The space between the particles and the matrix indicating poor surface adhesion between those two polymers was observed. Moreover, the phase interface between PBS and PLA was clearly shown, which also indicates that they were immiscible blend. The behavior was also observed in the PLA/PBAT blends (Dong, W. et al., 2013)

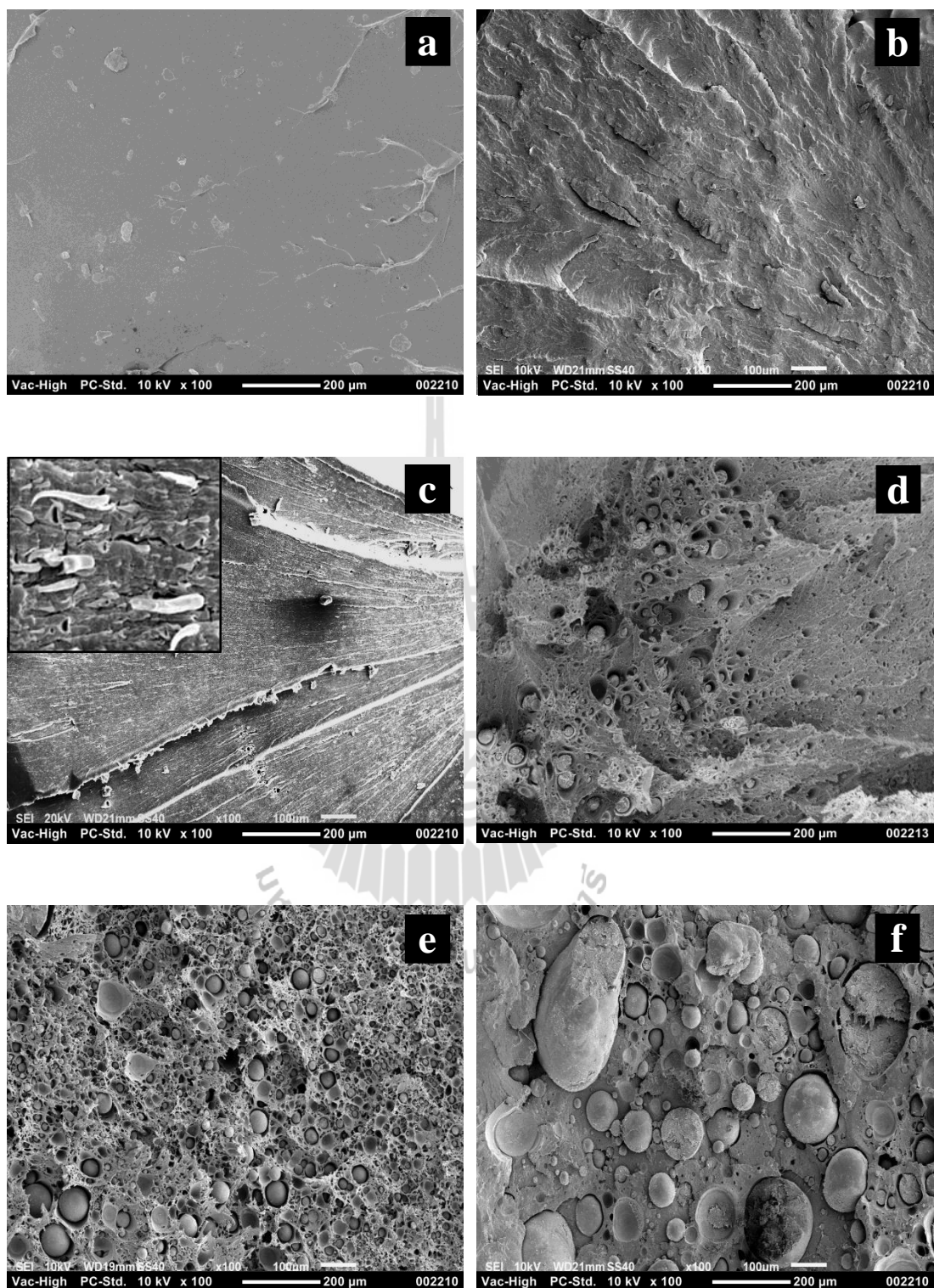


Figure 4.10 SEM micrographs (100x) of tensile fractured surface of PLA (a), PBS (b), PBS10 (c), PBS20 (d), PBS30 (e) and PBS40 (f).

4.2.3 Thermal properties of PLA, PBS and PLA/PBS blends

Thermogravimetric analysis (TGA) and derivative thermogravimetry (DTG) curves of PLA, PLA/PBS blends and PBS are shown in Figure 4.11 and 4.12, respectively. The degradation temperature (T_d) of PLA, PBS and PLA/PBS blends was listed in Table 4.3. T_{d1} of PLA and T_{d2} of PBS were 365.86 °C and 406.51 °C, respectively. This indicated the higher thermal stability of PBS compared to that of PLA. T_{d1} and T_{d2} of PBS10, PBS20, PBS30 and PBS40 are shown in Table 4.3. Moreover, all ratios of PLA/PBS blends were shown a two-step decomposition process due to the different thermal resistance of PLA and PBS. The first decomposition step was corresponded to the decomposition of PLA, while the second decomposition step was corresponded to the decomposition of PBS due to poor compatibility between PLA and PBS. Ojijo et. al. (2012) studied thermal properties of PLA and poly(butylene succinate adipate) (PBSA) blends. They found that thermal stability of the PLA was increased with increasing PBSA up to 30 wt%.

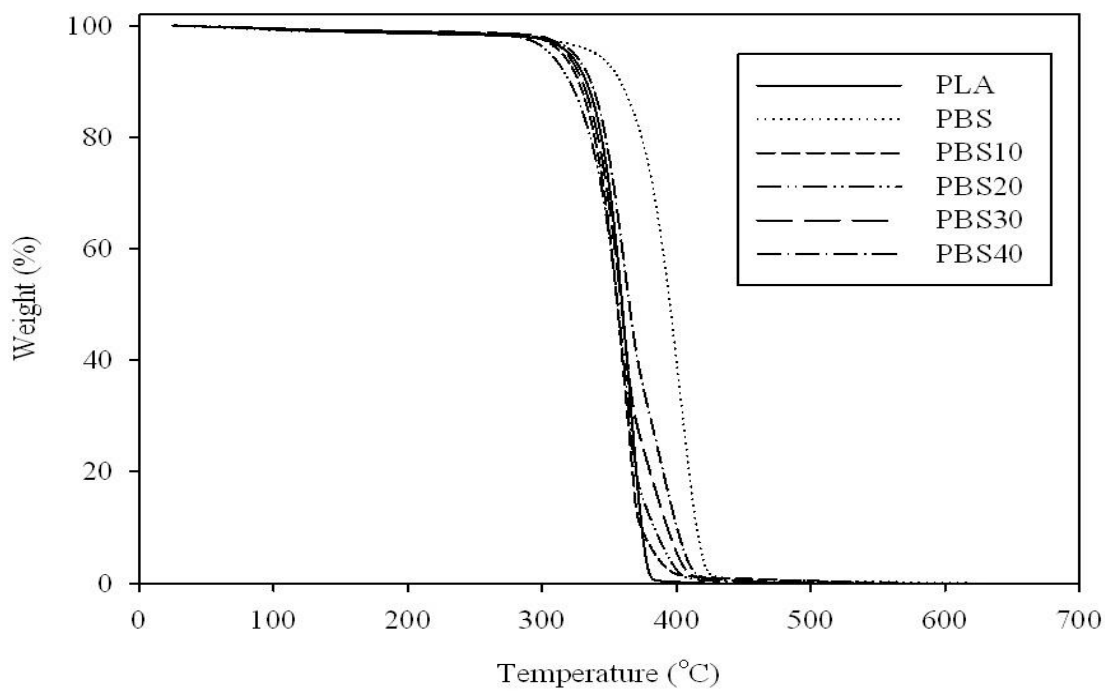


Figure 4.11 TGA curves of PLA, PBS and PLA/PBS blends.

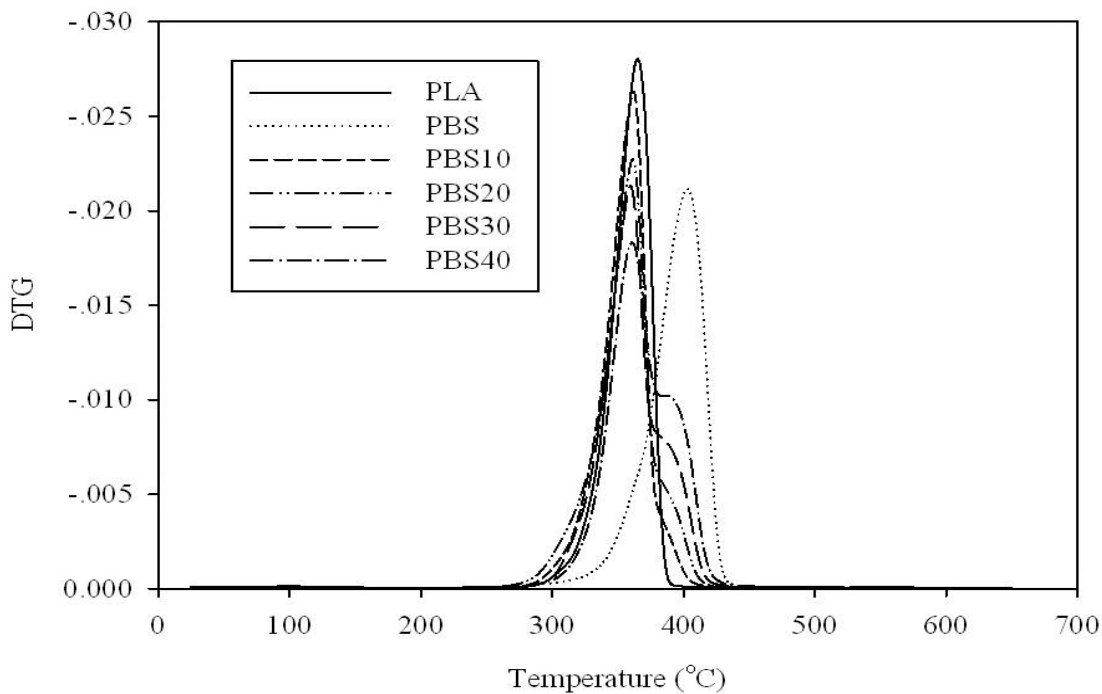


Figure 4.12 DTG curves of PLA, PBS and PLA/PBS blends.

Table 4.3 TGA analysis of PLA, PBS and PLA/PBS blends.

Name	T _{d1}	T _{d2}
	Peak(°C)	Peak(°C)
PLA	365.86	-
PBS10	364.69	404.43
PBS20	364.32	405.69
PBS30	363.26	405.10
PBS40	364.70	405.95
PBS	-	406.51

DSC thermograms recorded during cooling scan and second heating scan of PLA, PBS and PLA/PBS blends are reported in Figure 4.13 and Figure 4.14, respectively. The data derived from DSC analyses was reported in Table 4.4 and Table 4.5. Crystallization temperature on cooling scan (T_c) of neat PBS, PBS30 and PBS40 were 79.6°C, 51.3°C and 56.3°C, respectively. T_c of PLA/PBS blends shifted to higher temperature. This indicated that the crystallization of PBS was promoted in the blends (Zhang et al., 2012). PLA did not show T_c peak upon cooling as generally observed in other papers (Ji et al., 2014). T_c of PLA (76.3°C) in PBS40 was observed. This indicated that high loading PBS induced PLA crystallization on cooling scan. Yokohara and Yamaguchi (2008) also observed this result in PLA/PBS blends. T_c of PLA was clearly detected around at 90 °C, demonstrating that PBS droplets acted as nucleating entities for PLA. Glass transition temperature (T_g) of PLA and PBS were 52.5°C and -22.0°C, respectively. T_g of blends was decreased with addition of PBS.

This also indicates that PBS is partially miscible with PLA. Jun and Im (2002) also observed this behavior in PLA/PBS blends. Cold crystallization temperature on heating step (T_{cc}) of neat PLA was observed at 108.8°C. This indicated that crystallization of neat PLA occurred during heating. Tábi et al. (2010) also found T_{cc} of PLA at 107.7 °C (heating rate at 5 °C/min). T_{cc} of PBS10 and PBS20 shifted to a lower temperature when PBS content was not more than 20 wt%. T_{cc} of PBS30 and PBS40 shifted to higher temperature. This indicates that the addition of PBS up to 20 wt% enhanced the crystallization of PLA. Melting temperature (T_m) of PLA was 146°C and 155°C. T_m of PLA in PLA/PBS blends was decreased with increasing PBS contents. T_m of neat PBS was 106.0 °C and 113.5 °C. T_m of PBS in PLA/PBS blends was increased with increasing PBS contents. The degree of crystallinity of PLA ($\%X_{PLA}$) was increased with increasing PBS content. However, the degree of crystallinity of PBS ($\%X_{PBS}$) was decreased with increasing PLA contents. It means that crystallization of PLA was promoted by PBS but crystallization of PBS was restricted by PLA.

The double melting temperature of neat PLA and neat PBS also was explained by the melting and recrystallization. T_{m1} (low temperature melting) corresponded to the melting of the crystals formed during the nonisothermal melt crystallization, while T_{m2} (high temperature melting) corresponded to the melting of the crystals formed through melting and recrystallization during DSC heating scans. Zhang et al. (2013) found this behavior in PLA and Song and Qiu (2009) found that in PBS.

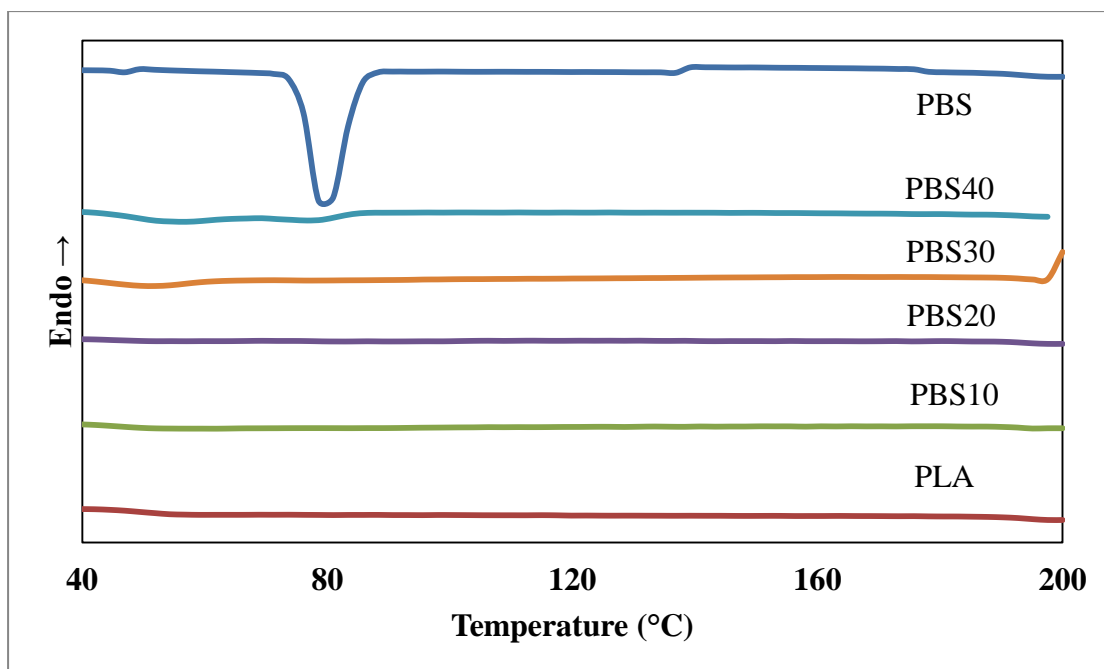


Figure 4.13 DSC curves from the cooling scan of PLA/PBS blends.

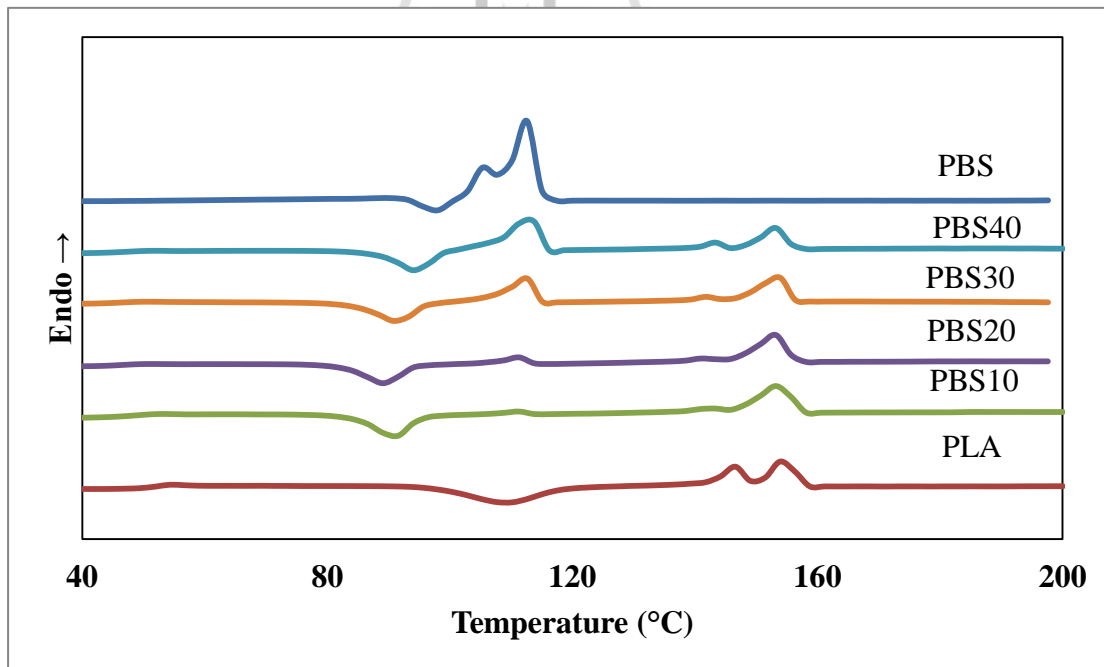


Figure 4.14 DSC curves from the second heating scan of PLA/PBS blends.

Table 4.4 Thermal properties of PLA, PBS and PLA/PBS blends.

Name	T _g (°C)	T _{m1PLA} (°C)	T _{m2PLA} (°C)	T _{m1PBS} (°C)	T _{m2PBS} (°C)	T _{cc} (°C)	T _c (°C)
PLA	52.5	146.6	155.0	-	-	108.8	-
PBS10	47.2	142.5	154.0	-	111.5	90.8	-
PBS20	46.4	142.1	153.6	-	111.9	89.3	-
PBS30	46.3	142.6	153.6	-	112.6	91.5	51.3
PBS40	47.4	143.4	153.7	-	113.0	94.5	56.3
PBS	-22.0	-	-	106.0	113.5	97.8	79.6

Table 4.5 ΔH_m , ΔH_{cc} , ΔH_c , %X of PLA, PBS and PLA/PBS blends.

Name	ΔH_{mPLA} (J/g)	ΔH_{mPBS} (J/g)	ΔH_{cc} (J/g)	ΔH_c (J/g)	%X _{mPLA} (%)	%X _{mPBS} (%)
PLA	39.28	-	37.28	-	42.23	-
PBS10	36.19	1.73	30.33	-	43.24	15.68
PBS20	34.13	5.97	25.88	-	45.87	27.06
PBS30	29.77	21.28	25.76	15.39	45.73	64.31
PBS40	24.82	31.99	25.27	27.56	44.48	72.51
PBS	-	84.07	9.548	86.27	-	76.22

4.3 Effect of PLA-g-GMA on physical properties of PLA/PBS blends

4.3.1 The stress-strain curves of PLA, PBS, PLA-g-GMA and PLA/PBS blends with and without PLA-g-GMA

Figure 4.15 shows the stress-strain curves of PLA, PBS, PLA-g-GMA and PLA/PBS blends with and without PLA-g-GMA. PLA exhibited brittle fracture. PLA/PBS blends showed higher elongation at break compared to that of neat PLA. PLA/PBS blends exhibited a relatively low ductility probably due to the weak interfacial adhesion between PLA and PBS phases. In contrast, PLA-g-GMA showed ductile fracture. Necking and cold drawing was occurred during tensile stress in a case of PLA-g-GMA. This indicates the ability of the molecular chain of PLA-g-GMA to reorganize and cold crystallization can take place under tensile stress. However, this cold crystallization under tensile stress was not shown in PLA indicating the difference in crystallization behavior between PLA and PLA-g-GMA. The elongation at break of PLA-g-GMA (263.93%) was significantly higher than that of PLA (5.20%). The elongation at break of the blends was dramatically increased up to 308.87% with adding 10 phr of PLA-g-GMA. The elongation at break of PBS20-G10 was higher than that of PLA and the tensile stress was not different with PLA. Moreover, strain induced crystallization was appeared on PBS20-G10. This indicated that PLA-g-GMA improved compatibility between PLA and PBS. Fracture behavior in the tensile test changed from the brittle fracture of neat PLA to the ductile fracture of PLA/PBS blends with and without PLA-g-GMA.

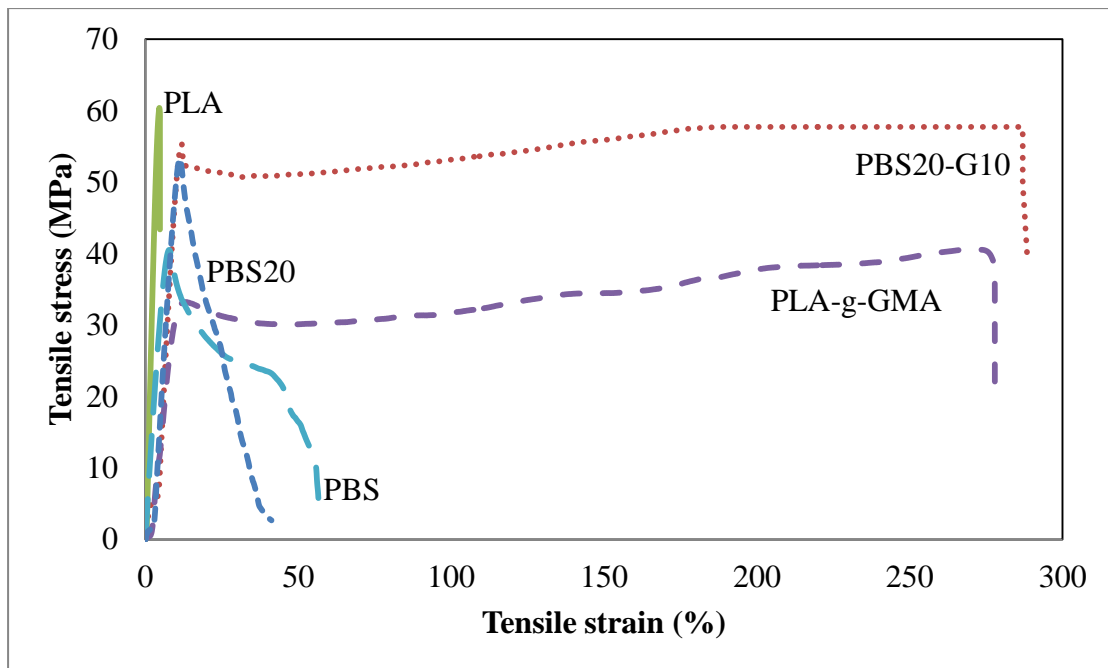


Figure 4.15 Tensile stress-strain curves of PLA, PBS, PLA-g-GMA and PLA/PBS blends.

4.3.2 Mechanical properties of PLA/PBS blends with and without PLA-g-GMA

Figure 4.16 shows tensile strength of PLA, PBS, PBS20 and PBS20-G10. The tensile strength of PLA/PBS blend increased with addition of PLA-g-GMA. Elongation at break of PLA, PBS, PBS20 and PBS20-G10 were shown in Figure 4.17. The elongation at break of PBS20-G10 was increased up to 308.87%. The ductility of this material was clearly much higher than that of neat PLA and PLA/PBS blend without PLA-g-GMA (PBS20). Figure 4.18 shows Young's modulus of PLA, PBS, PBS20 and PBS20-G10. Young's modulus of PLA/PBS blends was decreased with addition of PLA-g-GMA. The reduction in this Young's modulus was due to the result of the flexible property of PLA-g-GMA. Impact strength of PLA, PBS, PBS20

and PBS20-G10 were shown in Figure 4.19. The impact strength of PBS20 was increased with addition of PLA-g-GMA. The impact strength of PBS20-G10 was 22.54 kJ/m², which was about 2 times higher than that of neat PLA. In contrast, the impact strength of PBS20 was only about 1.5 times higher than that of neat PLA. This resulted from an improvement in compatibility between PLA and PBS. Tensile strength, Young's modulus, elongation at break and impact strength of PLA/PBS blends are summarized in Table 4.6.

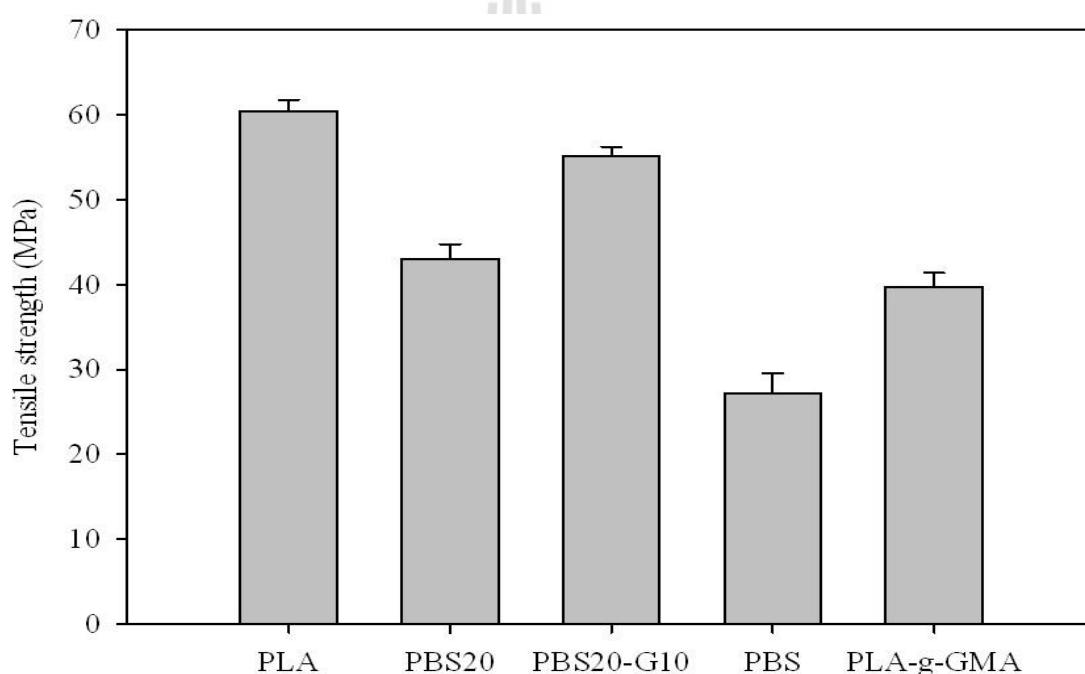


Figure 4.16 Tensile strength of PLA, PBS, PBS20, PBS20-G10 and PLA-g-GMA.

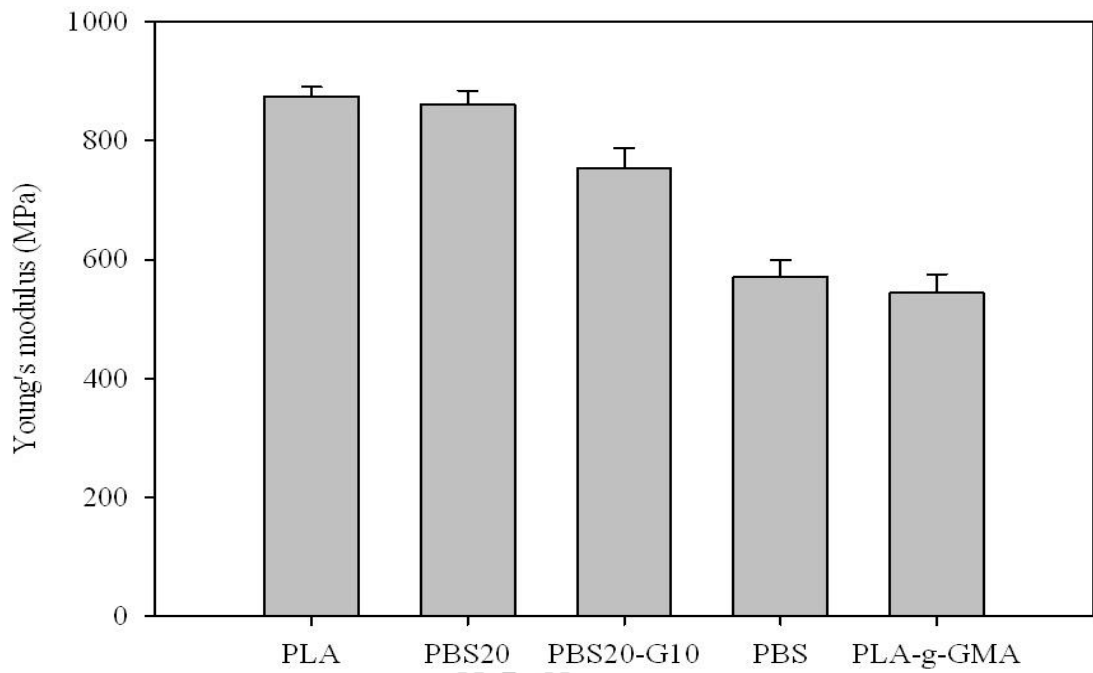


Figure 4.17 Young's modulus of PLA, PBS, PBS20, PBS20-G10 and PLA-g-GMA.

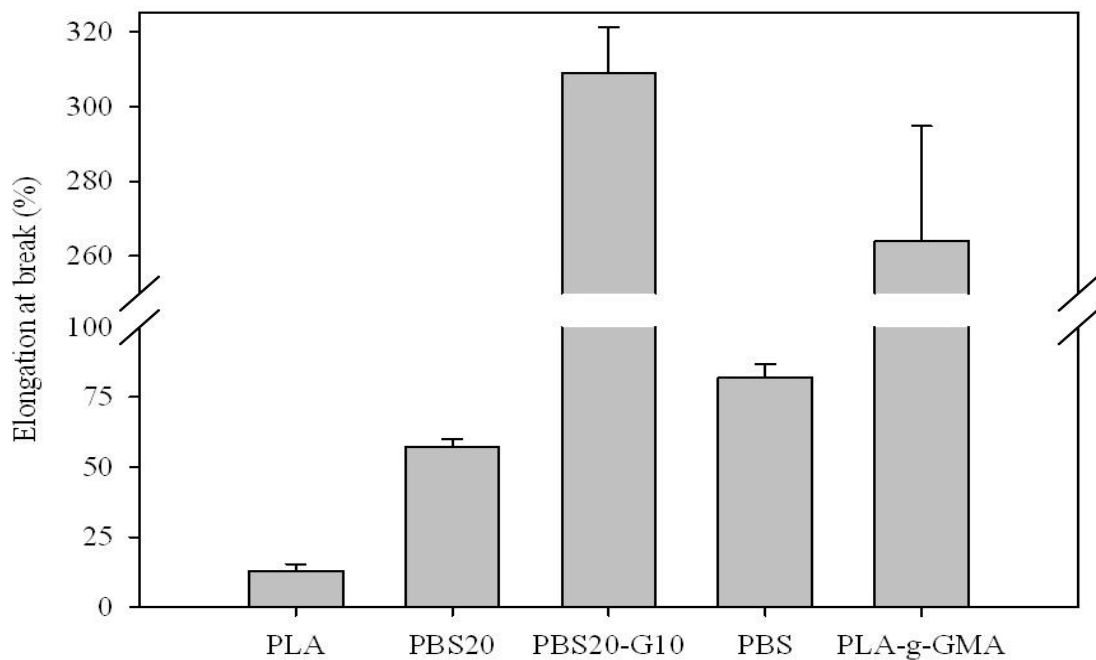


Figure 4.18 Elongation at break of PLA, PBS, PBS20, PBS20-G10 and PLA-g-GMA.

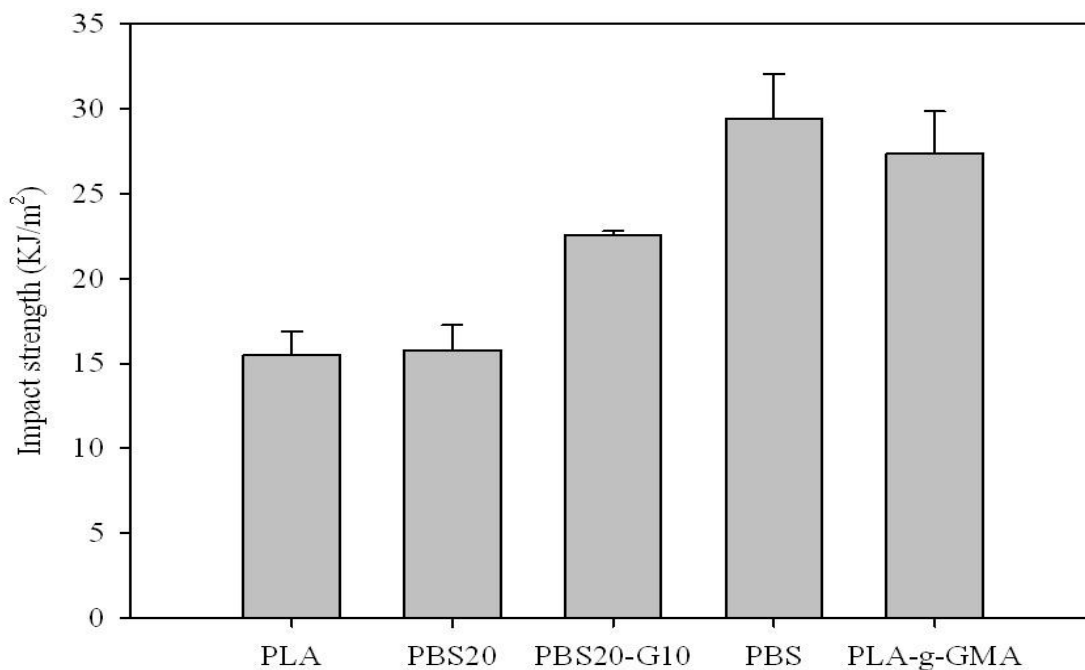


Figure 4.19 Impact strength of PLA, PBS, PBS20, PBS20-G10 and PLA-g-GMA.

Table 4.6 Tensile strength, elongation at break, Young's modulus and impact strength of PLA, PBS, PLA-g-GMA and PLA/PBS blends with and without PLA-g-GMA.

Name	Tensile strength (MPa)	Young's modulus (MPa)	Elongation at break (%)	Impact strength (kJ/m ²)
PLA	61.44±2.29	890.20±12.64	5.20±0.39	12.61±0.75
PBS20	46.10±1.37	860.90±8.74	52.82±3.43	16.03±0.61
PBS20-G10	55.15±1.09	676.33±21.71	308.87±12.45	22.57±0.23
PBS	27.53±1.90	571.96±27.72	82.28±2.82	29.26±1.22
PLA-g-GMA	39.76±1.62	544.43±31.35	263.93±30.91	27.38±2.48

4.3.3 Morphological properties of PLA/PBS blends with and without PLA-g-GMA

Figure 4.20 (a-d) shows SEM micrographs of tensile fractured surface of PLA, PBS, PBS20 and PBS20-G10. The blend without PLA-g-GMA showed large PBS dispersed phase size. PBS dispersed phase was pulled out from the PLA matrix indicating poor interfacial adhesions between PLA and PBS as show in Figure 4.20(c). The domain sizes of PBS of blend with PLA-g-GMA (Figure 4.20d) were much smaller than that of PBS20 (Figure 4.20c). This indicated that the compatibility between PLA and PBS was improved when PLA-g-GMA was used as a compatibilizer. The reaction most probably took place between the epoxy group of GMA and hydrolyzed carboxyl or hydroxyl groups of PLA. Reaction between PLA and GMA was also found by Brito et al. (2012) and Kumar et al. (2010). Meanwhile, PLA-g-GMA showed fractured rough surface (Figure 4.20 (f)) indicating ductile behavior as confirmed by the stress-strain curve in Figure 4.15.

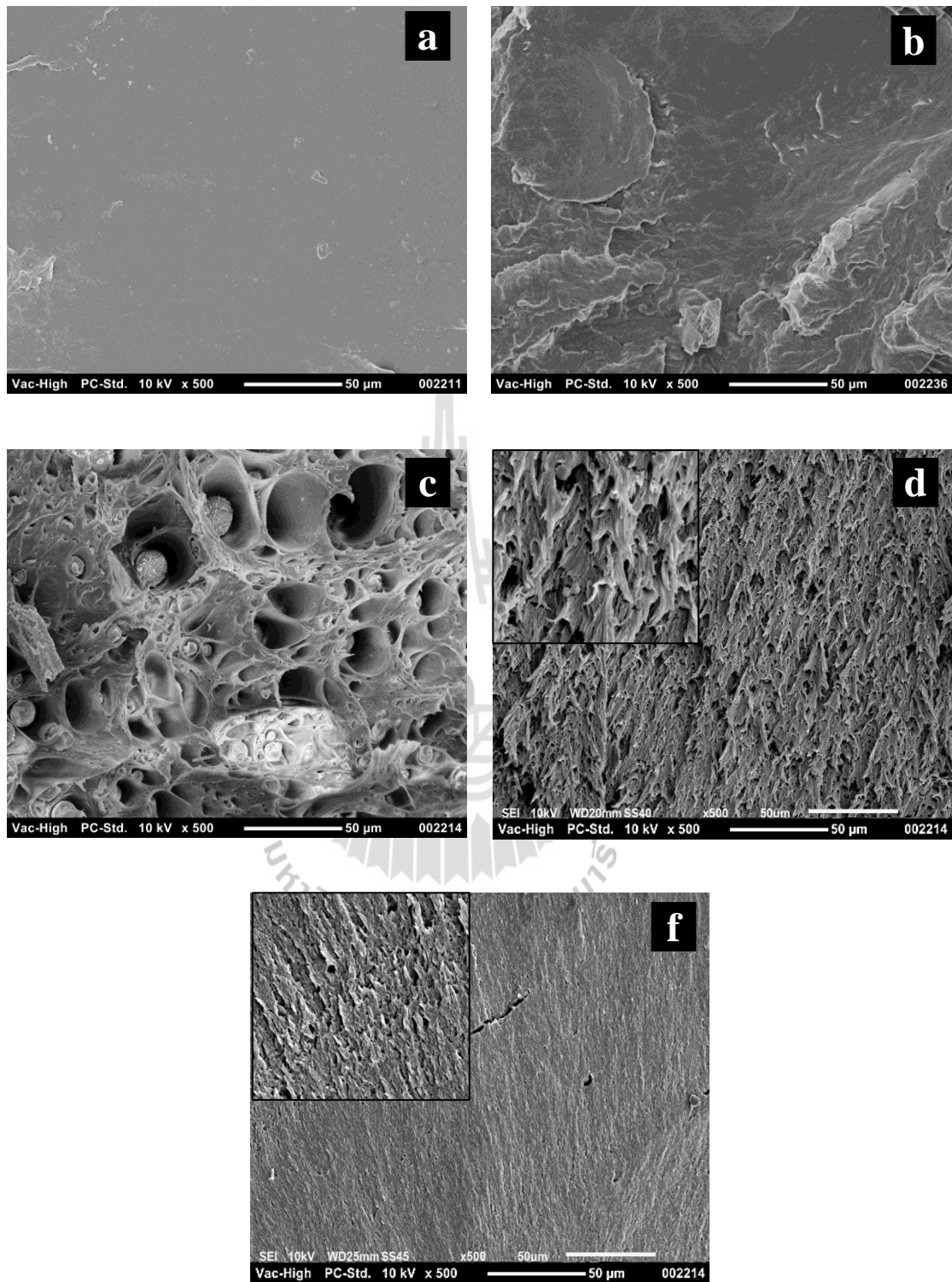


Figure 4.20 SEM micrographs (500x) of tensile fractured surface of PLA (a), PBS (b), PBS20 (c), PBS20-G10 (d) and PLA-g-GMA (f).

4.3.4 Thermal properties of PLA/PBS blends with and without PLA-g-GMA

TGA and DTG curves of PBS20 and PBS20-G10 are shown in Figure 4.21 and 4.22. PBS20-G10 showed higher T_d than that of PBS20 because PLA-g-GMA enhanced interfacial adhesion between PLA and PBS. The increasing thermal stability of PBS20-G10 may be attributed to the good compatibility between PLA and PBS. Moreover, PBS20 showed a two-step decomposition process due to the different thermal resistance of PLA and PBS. The two-step decomposition process of PBS20-G10 was unclear. Therefore, PLA-g-GMA improved compatibility between PLA and PBS. T_{d3} at 532.72°C of PBS20-G10 was observed. This result was probably due to reaction of PBS and GMA. High thermal stability of sample at T_{d3} may be due to structure of reaction between PBS and GMA. Glycidyl methacrylate-grafted poly(butylene succinate) (PBS-g-GMA) was studied by Wu et al. (2013). Composites of PBS-g-GMA and palm fibre (PBS-g-GMA/PF) exhibited excellent mechanical properties compared with those of PBS/PF composites. T_d of PBS20 and PBS20-G10 were summarized in Table 4.7.

Table 4.7 TGA analysis of PLA, PBS and PLA/PBS blends with and without PLA-g-GMA.

Name	T_{d1}	T_{d2}	T_{d3}
	Peak(°C)	Peak(°C)	Peak(°C)
PLA	365.86	-	-
PBS20	364.32	405.69	-
PBS20-G10	374.80	406.56	532.72
PBS	-	406.51	-

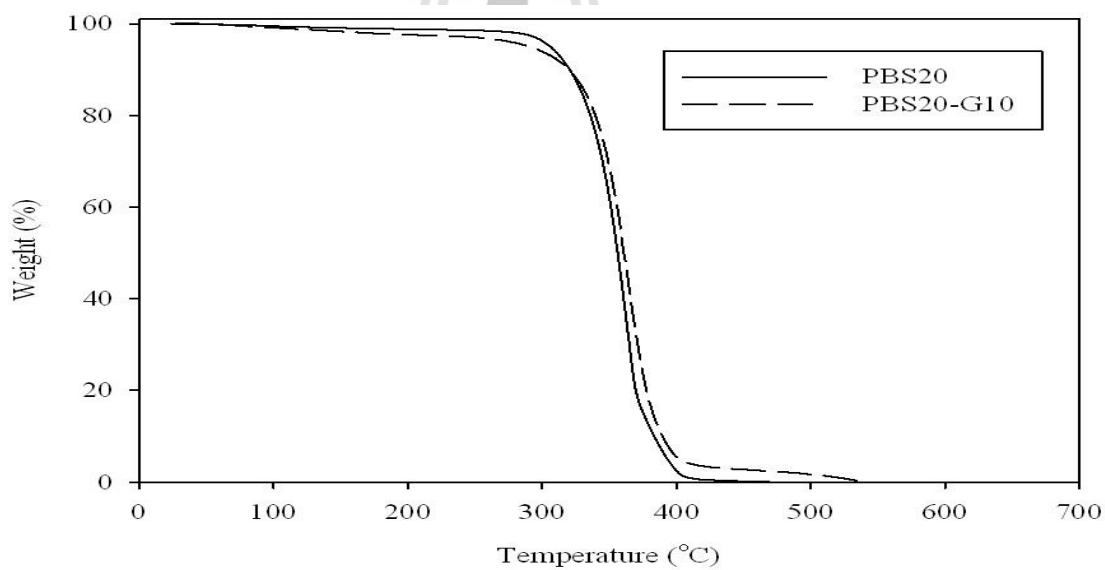


Figure 4.21 TGA curves of PLA/PBS blend with and without compatibilizer.

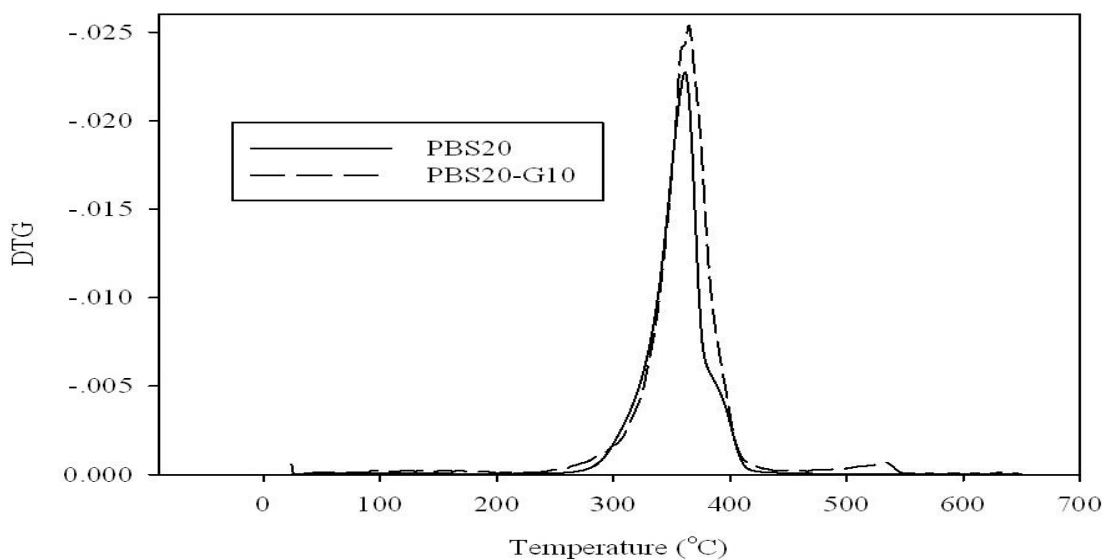


Figure 4.22 DTG curves of PLA/PBS blend with and without compatibilizer.

The DSC thermograms recorded during cooling scan and second heating scan of PBS20, PLA-g-GMA and PBS20-G10 were reported in Figure 4.23 and Figure 4.24, respectively. The data derived from DSC analyses was reported in Table 4.8 and Table 4.9. Crystallization temperature on cooling scan (T_c) of PLA-g-GMA shows melt crystallization upon cooling at 88.9°C. This may be due to the nucleation effect caused by GMA under cooling stage. Glass transition temperature (T_g) of PBS20-G10 was slightly lower than that of PBS20. This indicated that PLA-g-GMA improved compatibility between PLA and PBS. T_g of PLA-g-GMA (48.6°C) was lower than that of PLA (52.5°C) indicating more flexibility of PLA-g-GMA than that of PLA. Cold crystallization temperature on second heating (T_{cc}) of neat PLA appeared at 108.8°C. This indicated the recrystallization of neat PLA occurred during heating. T_{cc} of PLA-g-GMA shifted to lower temperature (75.0°C) than that of neat PLA. This indicated that the recrystallization of PLA-g-GMA can be initiated at lower crystallization temperature. However, T_{cc} of PBS20-G10 was higher than that of

PBS20 due to PLA-g-GMA hindered the crystallization in PBS20-G10. Melting temperatures (T_m) of PLA were 146°C and 155°C while PLA-g-GMA shows single peak of T_m at 142.8°C. This implied that PLA-g-GMA hindered the lamella formation and led to less perfect crystals of PLA-g-GMA. For PLA, T_{m1} (low temperature melting) corresponded to the melting of the crystals formed during the nonisothermal melt crystallization, while T_{m2} (high temperature melting) corresponded to the melting of the crystals formed through melting and recrystallization during DSC heating scans (Kumar et al., 2010 and Zhang et al., 2013). T_m of PBS20-G10 decreased approximately 1–2°C with the addition of PLA-g-GMA. This indicated that PLA-g-GMA could improve compatibility between PLA and PBS. The degree of crystallinity of PLA in PBS20-G10 ($\%X_{mPLA}$) was decreased with the addition of PLA-g-GMA. However, the degree of crystallinity of PBS ($\%X_{mPBS}$) was increased with addition of PLA-g-GMA. The degree of crystallinity of PLA was more than that of PLA-g-GMA.

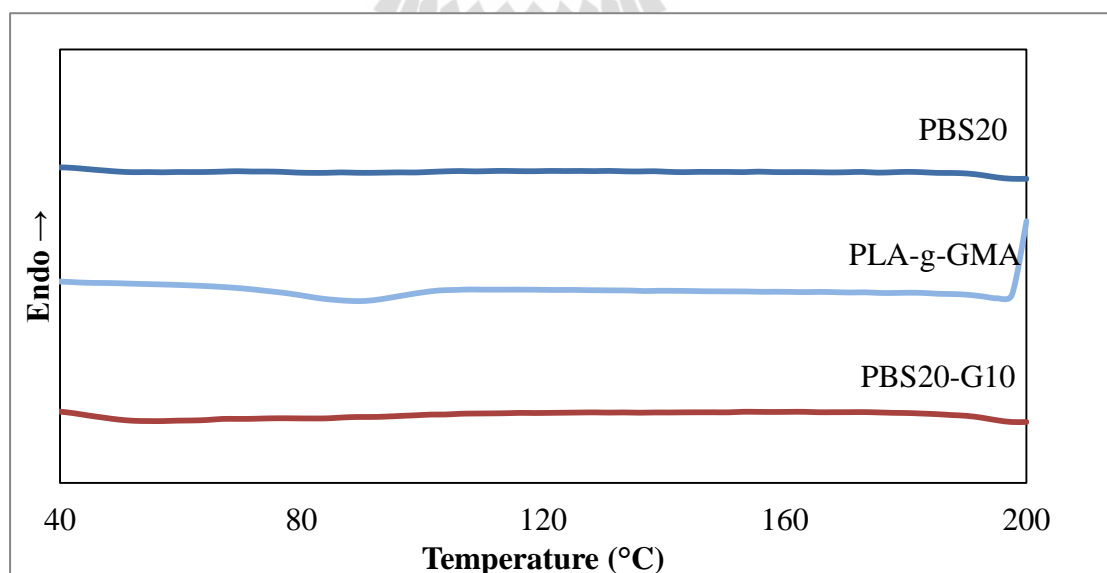


Figure 4.23 DSC curves from the cooling scan of PBS20, PLA-g-GMA and PBS20-G10.

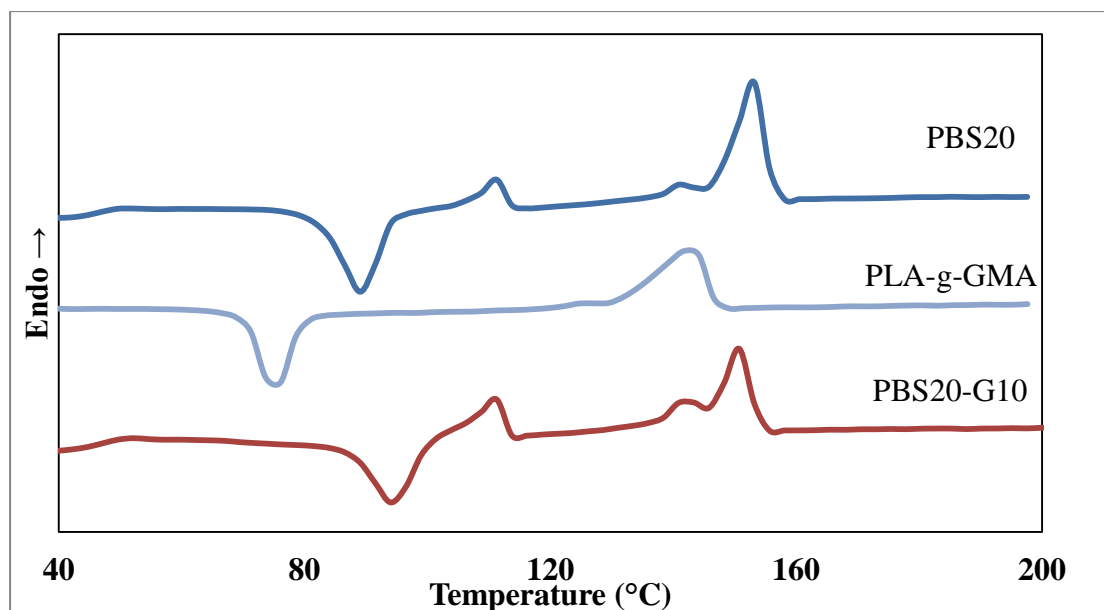


Figure 4.24 DSC curves from the second heating scan of PBS20, PLA-g-GMA and PBS20-G10.

Table 4.8 Thermal properties of PLA, PBS and PLA/PBS blends.

Name	T_g (°C)	T_{m1PLA} (°C)	T_{m2PLA} (°C)	T_{m1PBS} (°C)	T_{m2PBS} (°C)	T_{cc} (°C)	T_c (°C)
PLA	52.5	146.6	155.0	-	-	108.8	-
PBS20	46.4	142.1	153.6	-	111.9	89.3	-
PBS20-G10	46.1	142.1	151.1	-	111.1	94.5	-
PBS	-22.0	-	-	106.0	113.5	97.8	79.6
PLA-g-GMA	48.6	-	142.8	-	-	75.0	88.9

Table 4.9 ΔH_m , ΔH_{cc} , ΔH_c , %X of PLA, PBS and PLA/PBS blends.

Name	ΔH_{mPLA} (J/g)	ΔH_{mPBS} (J/g)	ΔH_{cc} (J/g)	ΔH_c (J/g)	% X_{mPLA} (%)	% X_{mPBS} (%)
PLA	39.28	-	37.28	-	42.23	-
PBS20	34.13	5.97	25.88	-	45.87	27.06
PBS20-G10	28.11	7.80	24.01	-	37.78	35.36
PBS	-	84.07	9.548	86.27	-	76.22
PLA-g-GMA	24.39	-	7.42	11.43	24.33	-

4.3.5 X-ray diffraction analysis

The XRD patterns of neat PLA and PLA-g-GMA are shown in Figure 4.25 and Figure 4.26. PLA-g-GMA before applying tensile stress, diffraction peak (2θ) at 9° , 14° , 16° , 19° and 22° were clearly observed. In contrast, these peaks were not observed in neat PLA indicating different crystallization behavior. The crystallization behavior of PLA-g-GMA in this study is similar to that found from the annealing process of PLA (Lai et al., 2013). After applying tensile stress to PLA and PLA-g-GMA, no significantly change in XRD patterns of PLA was observed (Figure 4.25). In case of PLA-g-GMA after tensile test, diffraction peak (2θ) of PLA-g-GMA was clearly changed as shown in Figure 4.26. Intensity of diffraction peak (2θ) at about 29° increased but intensity at 19° decreased. Such a result indicated that applying tensile force significantly influence the crystallization of PLA-g-GMA. Moreover, intensity of 2θ at about 35° , 38° , 42° , 56° , 60° , 65° , 72° , 76° and 83° were appeared in PLA-g-GMA after applying tensile force. This result indicated that applying tensile force significantly influences the crystallization of PLA-g-GMA.

Crystalline size was calculated by the Scherrer's equation. 2θ , crystalline size and intensity of PLA and PLA-g-GMA were shown in Table 4.10 and Table 4.11, respectively.

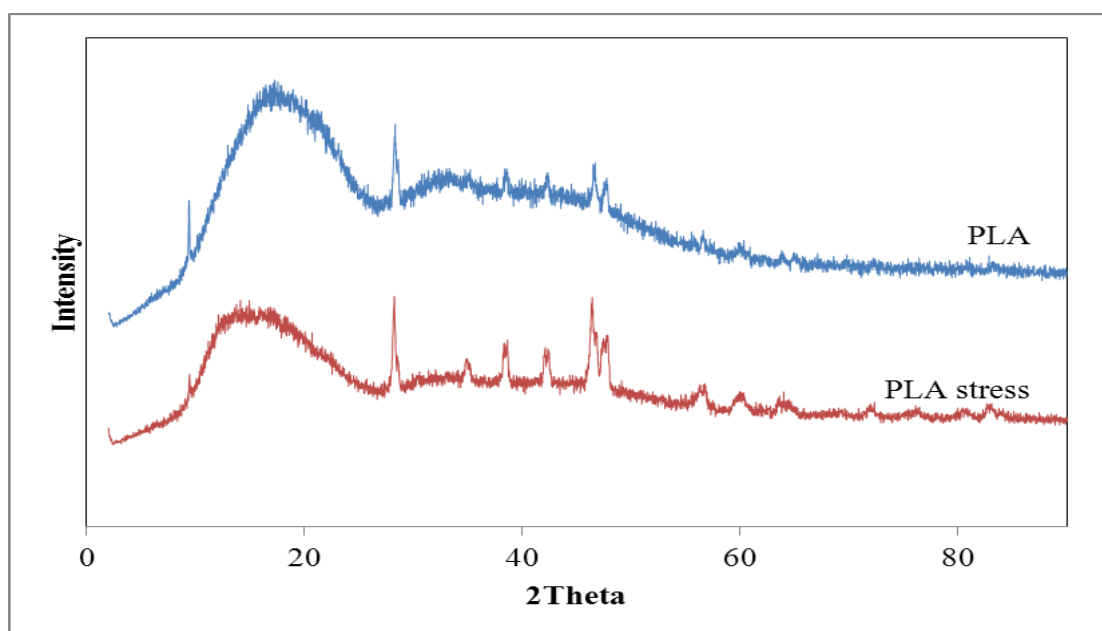


Figure 4.25 XRD patterns of neat PLA.

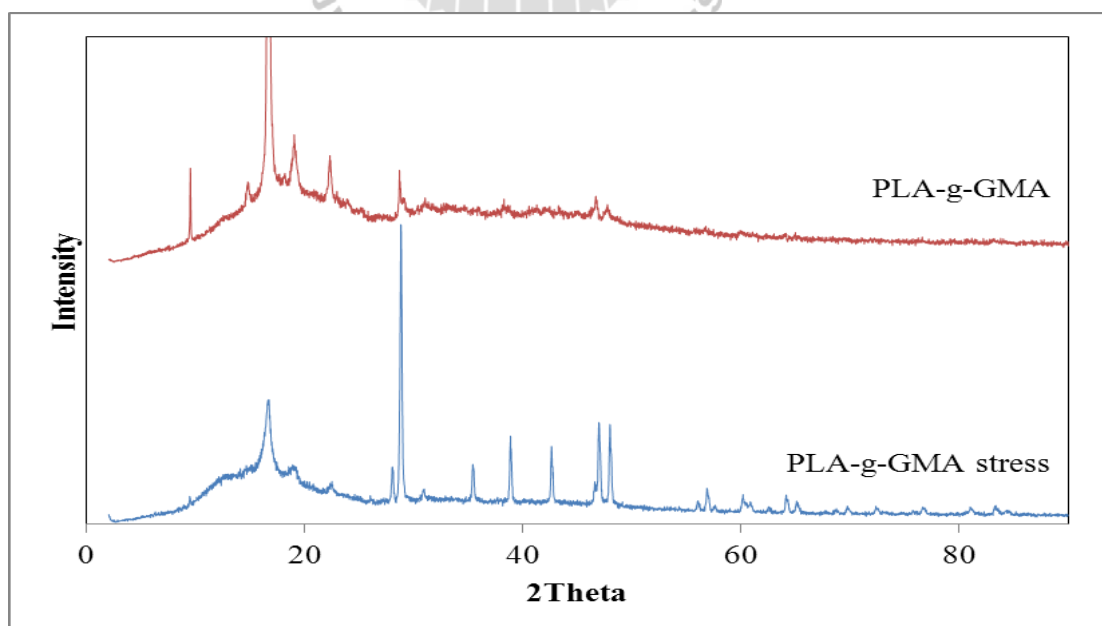


Figure 4.26 XRD patterns of PLA-g-GMA.

Table 4.10 X-ray diffraction analysis of PLA and stressed PLA.

PLA			PLA-stressed		
2Theta (degrees)	Crystalline size (Å)	Intensity	2Theta (degrees)	Crystalline size (Å)	Intensity
9.380	748.6	335	9.422	856.1	140
-	-	-	14.120	87.4	93
17.201	145.8	87	16.799	133.7	63
28.309	223.4	419	28.229	291.0	488
-	-	-	34.934	179.5	119
38.552	330.8	144	38.615	171.8	231
42.315	386.4	148	42.336	243.2	191
46.671	321.7	225	46.400	173.2	450
47.733	272.8	181	47.712	132.9	276
-	-	-	56.728	101.9	126
-	-	-	59.999	137.9	102
-	-	-	63.987	135.2	105
-	-	-	72.307	274.8	79
-	-	-	76.085	271.8	58
-	-	-	80.401	95.7	58
-	-	-	82.631	106.2	81

Table 4.11 X-ray diffraction analysis of PLA-g-GMA and stressed PLA-g-GMA.

PLA-g-GMA			PLA-g-GMA-stressed		
2Theta (degrees)	Crystalline size (Å)	Intensity	2Theta (degrees)	Crystalline size (Å)	Intensity
9.483	1085.1	854	9.392	785.0	69
14.727	269.7	205	14.017	198.2	61
16.652	337.8	7713	16.593	136.2	878
19.041	190.3	469	19.038	117.0	168
22.227	282.6	324	22.341	306.1	62
-	-	-	27.956	458.8	298
28.665	481.0	481.0	28.815	423.0	3344
-	-	-	30.929	422.5	141
-	-	-	35.356	400.3	399
-	-	-	38.857	433.8	718
-	-	-	42.623	418.2	659
46.585	1.948	454.4	46.984	365.4	956
47.714	1.904	321.5	47.975	364.4	976
-	-	-	56.035	405.4	125
-	-	-	56.893	344.9	270
-	-	-	60.924	197.1	167
-	-	-	64.161	337.8	165
-	-	-	65.152	305.8	102
-	-	-	69.776	394.8	71

Table 4.11 X-ray diffraction analysis of PLA-g-GMA and stressed PLA-g-GMA.

PLA-g-GMA			PLA-g-GMA-stressed		
2Theta (degrees)	2Theta (degrees)	2Theta (degrees)	2Theta (degrees)	2Theta (degrees)	2Theta (degrees)
-	-	-	72.419	361.8	73
-	-	-	76.713	273.0	69
-	-	-	81.008	429.1	88
-	-	-	83.320	339.1	75

4.4 Effect of glycerol content on physical properties of CP

4.4.1 Mechanical properties of CP

Tensile strength, Young's modulus and elongation at break of CP with various glycerol contents are shown in Fig 4.27 - 4.29. CP with different glycerol loadings from 20–60 wt% was prepared. Elongation at break of CP was increased with increasing glycerol contents. However, with increasing glycerol contents, tensile strength and Young's modulus of CP were decreased. These results indicate that the ductility of material increases and, as expected, a plasticization effect was obtained by glycerol. Glycerol reduced direct interaction between starch chains, thus facilitating movement of starch chains under tensile forces (Saiah, R. et al., 2012). During the thermoplastic processing of starch in the presence of a plasticizer a semicrystalline granule of starch is transformed into a homogeneous material with hydrogen bond cleavage between starch molecules. This process called gelatinization (Mekonnen et al., 2013). At 20 wt% of glycerol could not be form to TPS. 30 wt% of glycerol was

enough for the gelatinization of CP. CP with 30 wt% of glycerol was chosen to study effect of CP content on physical properties of CP/PLA/PBS composites. Tensile strength, elongation at break and Young's modulus of CP was summarized in Table 4.12.

Table 4.12 Tensile strength, elongation at break and Young's modulus of CP.

Glycerol content (%)	Tensile strength (MPa)	Young's modulus (MPa)	Elongation at break (%)
30	4.09±0.21	207.42±17.45	7.18±0.78
40	2.73±0.13	89.24±6.34	10.22±0.80
50	1.62±0.21	46.20±9.33	12.04±1.45
60	1.00±0.02	26.37±4.61	18.18±2.93

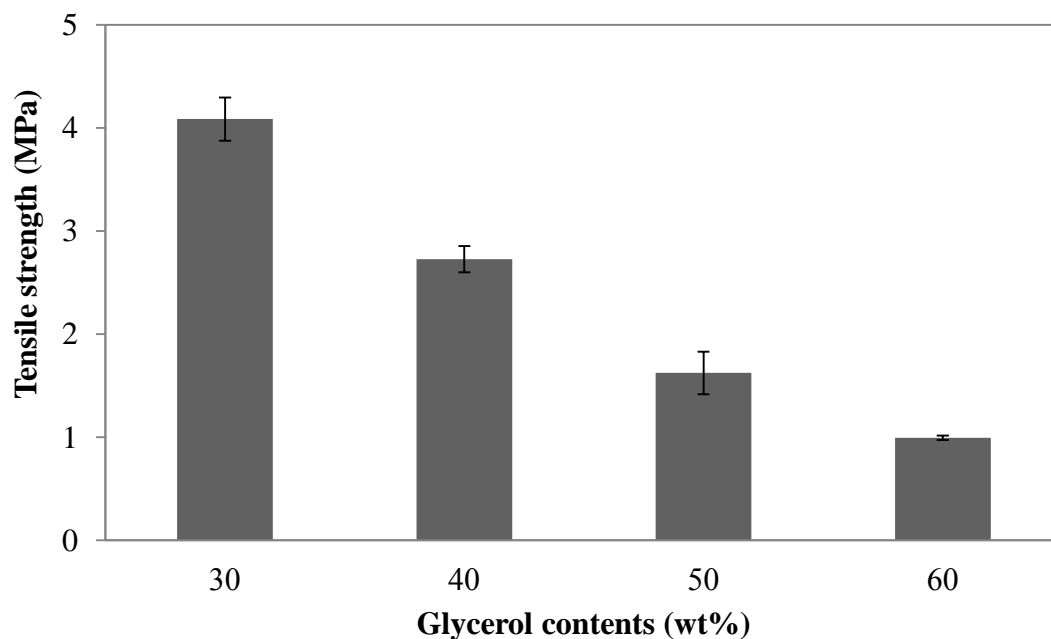


Figure 4.27 Tensile strength of CP with various glycerol contents.

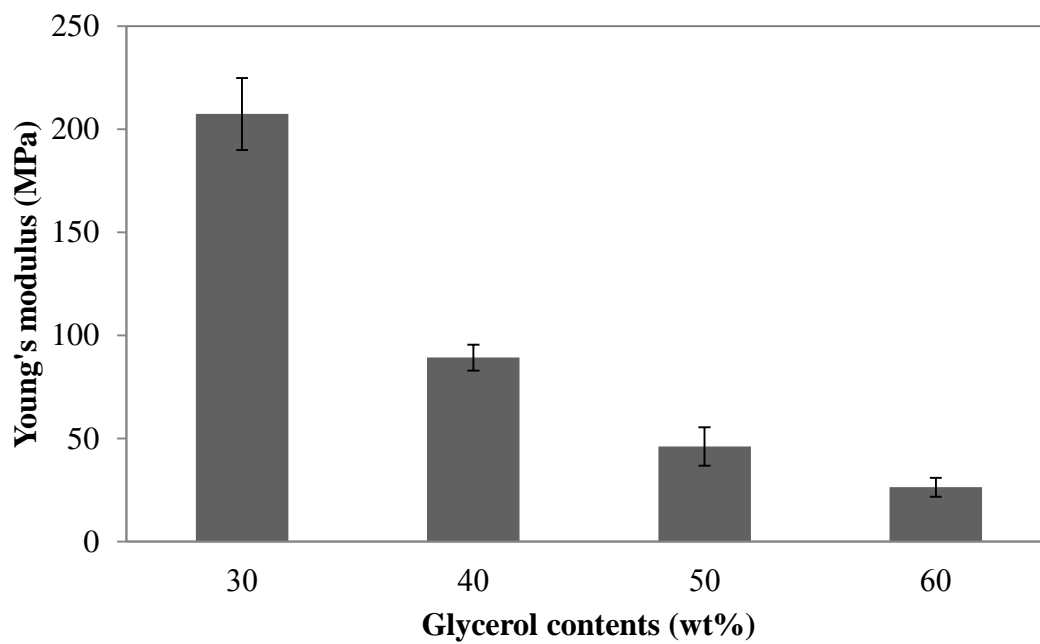


Figure 4.28 Young's modulus of CP with various glycerol contents.

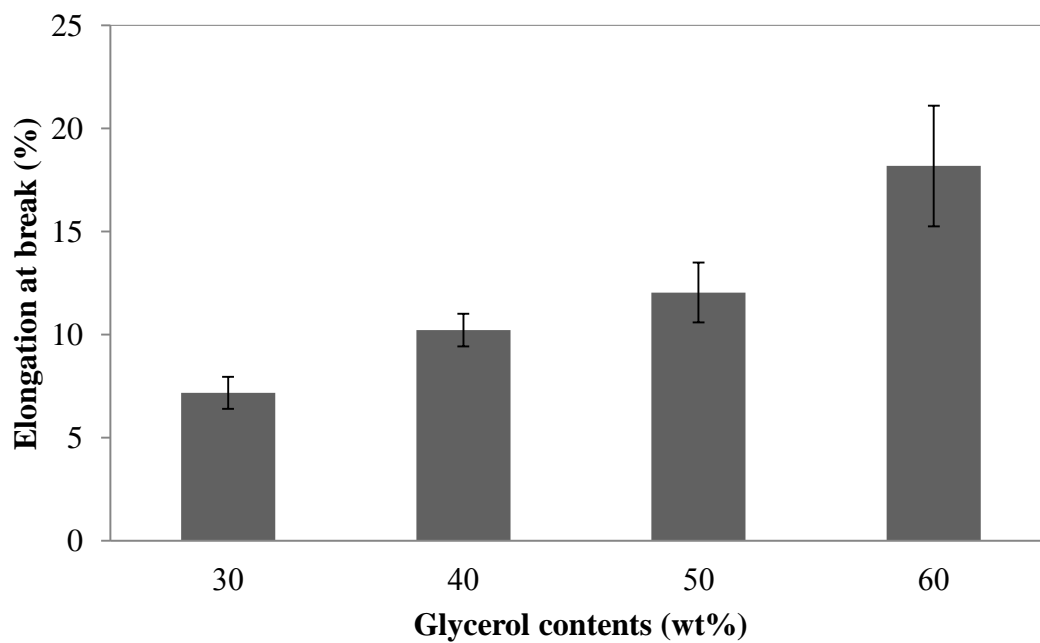


Figure 4.29 Elongation at break of CP with various glycerol contents.

4.4.2 Comparison mechanical properties of composites from CP and RCP_t

Figure 4.30 – 4.32 show tensile strength, Young's modulus and elongation at break of CP/PLA/PBS composite and RCP_t/PLA/PBS composite. Tensile strength and elongation at break of composite were improved by using CP. These indicated that addition of glycerol in the starch – polymer blend aided the distribution of starch in CP. Starch granules were stabilized by a cross linking effect of glycerol inside the granule (Van Soest et al., 1995). Tensile strength, elongation at break and Young's modulus of CP/PLA/PBS composite and RCP_t/PLA/PBS composite were summarized in Table 4.13.

Table 4.13 Tensile strength, elongation at break and Young's modulus of CP/PLA/PBS composite and RCP_t/PLA/PBS composite

Name	Tensile strength (MPa)	Young's Modulus (MPa)	Elongation at break (%)
PBS20-C20	24.03±1.14	673.00±31.86	6.22±0.33
PBS20-RCP _t 20	18.68±1.15	638.49±61.74	2.08±0.22

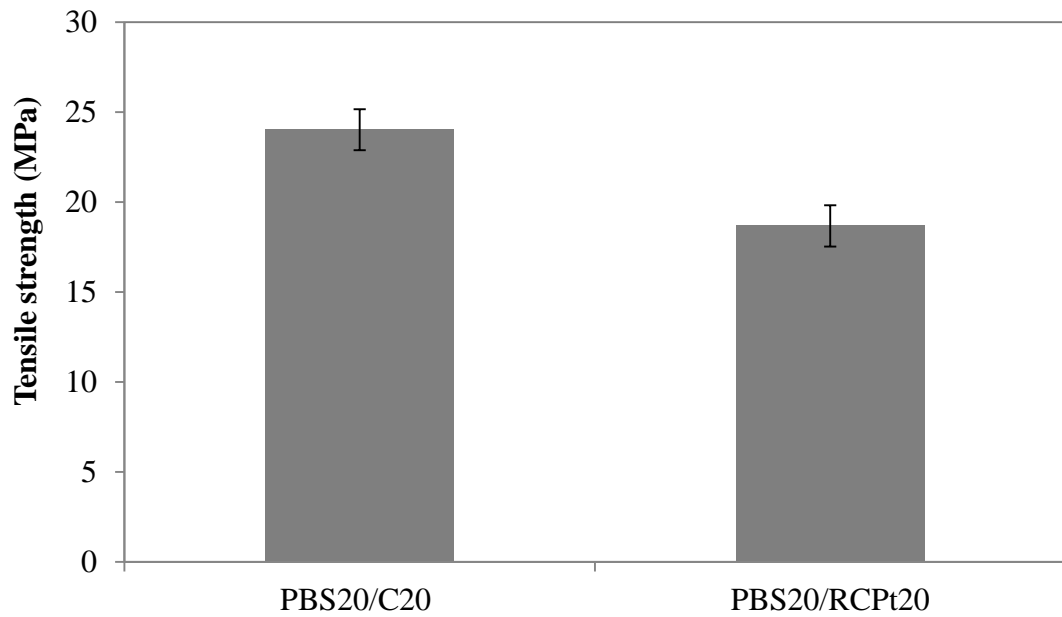


Figure 4.30 Tensile strength of CP/PLA/PBS composites and RCP_t/PLA/PBS composite.

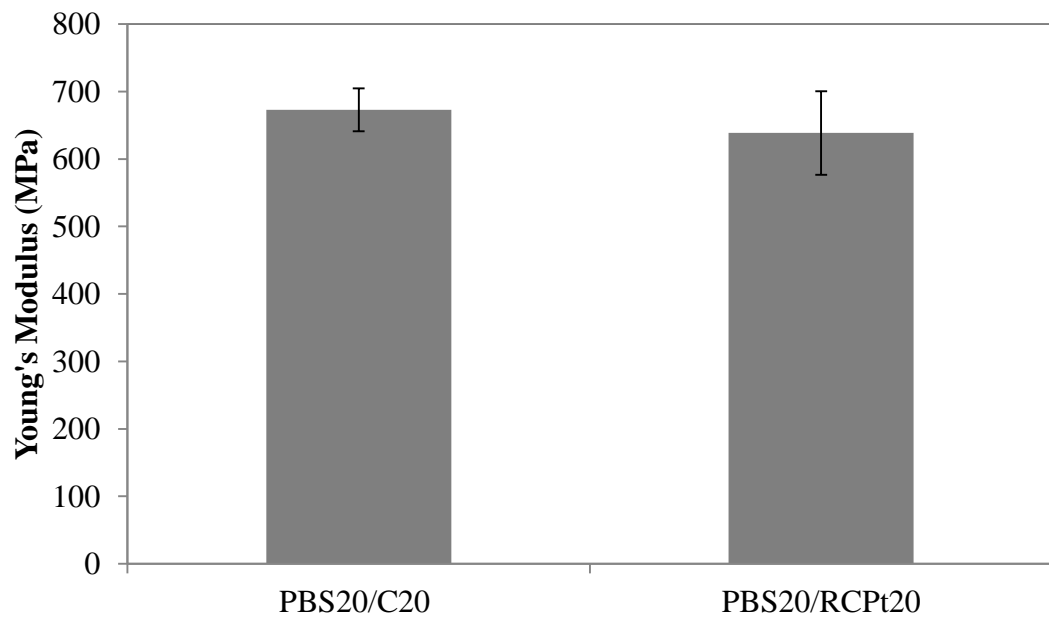


Figure 4.31 Young's modulus of CP/PLA/PBS composites and RCP_t/PLA/PBS composite.

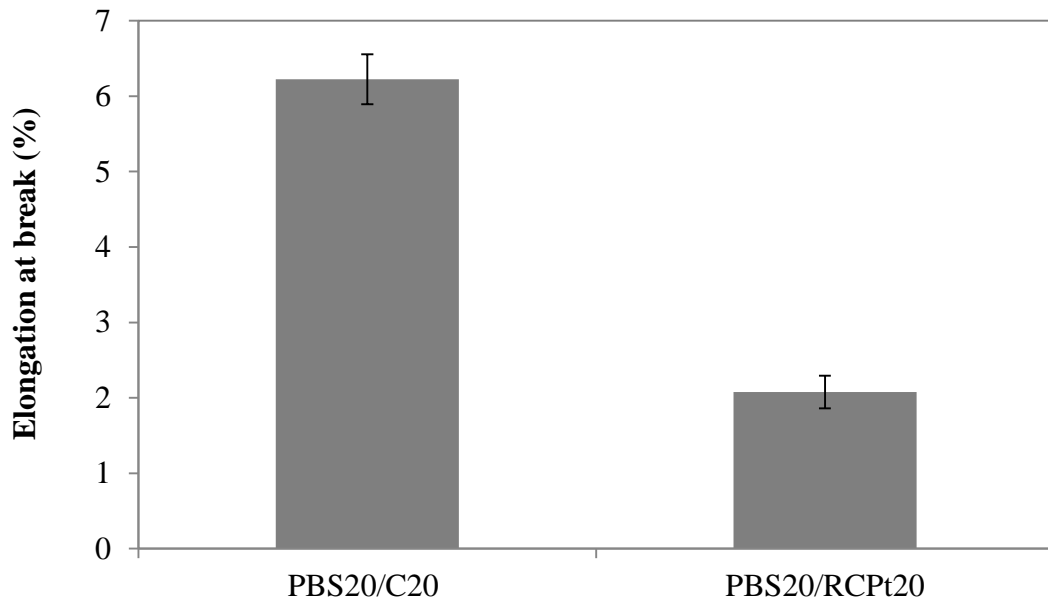


Figure 4.32 Elongation at break of CP/PLA/PBS composites and RCP_t/PLA/PBS composite.

4.5 Effect of CP contents on physical properties of CP/PLA/PBS composites

4.5.1 Mechanical properties of CP/PLA/PBS composites

Figure 4.33 shows tensile strength of PBS20 and its composites. Tensile strength of PBS20 without CP was 46.10 MPa. Tensile strength of CP/PLA/PBS composites was decreased with increasing CP content. The reduction of tensile strength might be attributed to the coalescence of CP, especially at high loading of CP. This may be attributed to poor interfacial interaction between the matrix and CP. The coalescence of CP caused stress concentrations in the composites and led to the decrease of tensile strength. These results were corresponding to SEM micrographs. Young's modulus, elongation at break and impact strength of

CP/PLA/PBS composites (Figure 4.34, Figure 4.35 and Figure 4.36) were decreased with increasing CP content. This may be due to that an increasing CP contents was possibly increased coalescence of CP in CP/PLA/PBS composites. Another reason was the present of poor interfacial adhesion between matrix and natural filler. PLA and PBS had hydrophobic surface (Peltzer et al., 2014 and Kim et al., 2005), but natural filler, CP had hydrophilic surface (Kim et al., 2010). This led to poor compatibility on the CP/PLA/PBS composites. Chen et al. (2014) studied ternary composites of PLA/PBS/calcium sulfate whiskers (CSW). The tensile strength of ternary blends was decreased with addition of CSW. Kim et al. (2010) also found this reason in PLA and PBS composite with bamboo flour (BF) and wood flour (WF). Tensile strength, elongation at break, Young's modulus and impact strength of CP/PLA/PBS composites are summarized in Table 4.14.

Table 4.14 Tensile strength, elongation at break, Young's modulus and impact strength of CP/PLA/PBS composites.

Name	Tensile strength (MPa)	Young's modulus (Mpa)	Elongation at break (%)	Impact strength (KJ/m ²)
PBS20	46.10±1.37	860.90±8.74	52.82±3.43	16.03±0.61
PBS20-C10	23.61±0.56	659.83±10.54	7.28±0.28	5.20±0.75
PBS20-C20	22.34±0.81	633.71±9.53	6.03±0.42	4.91±0.80
PBS20-C30	11.87±0.43	489.13±13.28	5.18±0.55	3.28±0.86
PBS20-C40	10.20±0.97	310.31±11.55	5.69±0.19	2.32±0.67

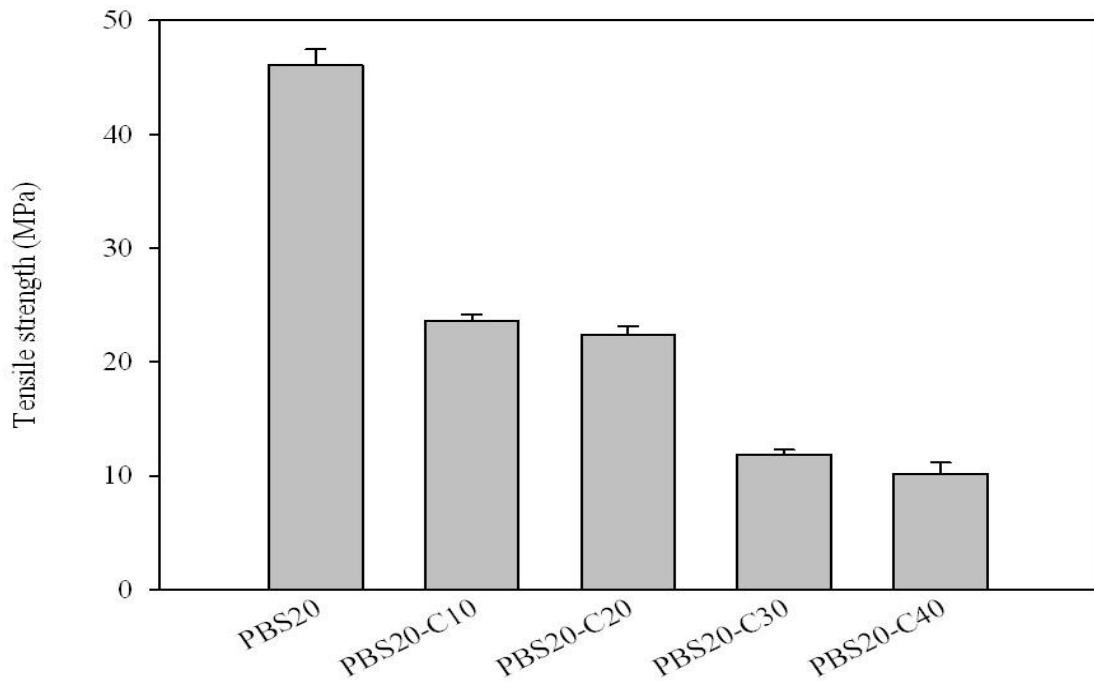


Figure 4.33 Tensile strength of CP/PLA/PBS composites with various CP contents.

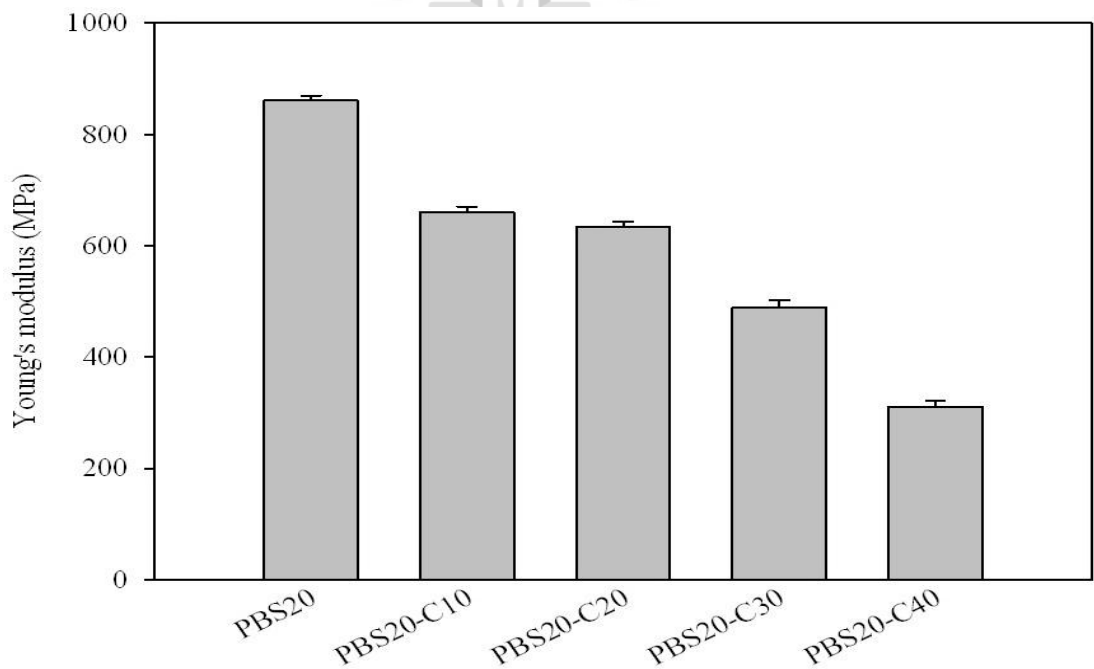


Figure 4.34 Young's modulus of CP/PLA/PBS composites with various CP contents.

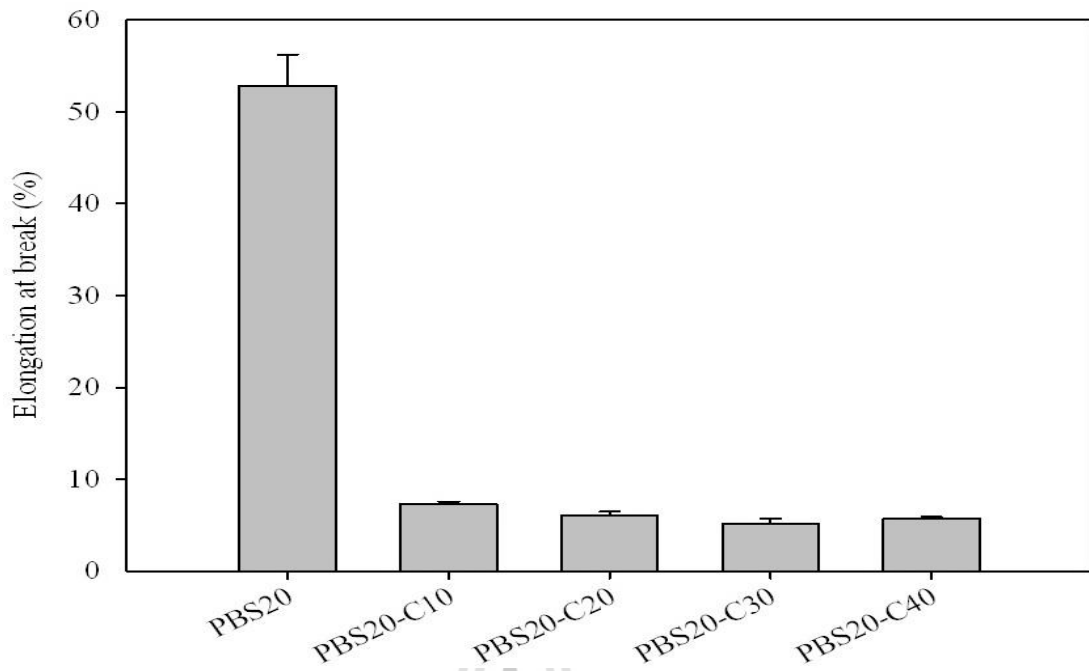


Figure 4.35 Elongation at break of CP/PLA/PBS composites with various CP contents.

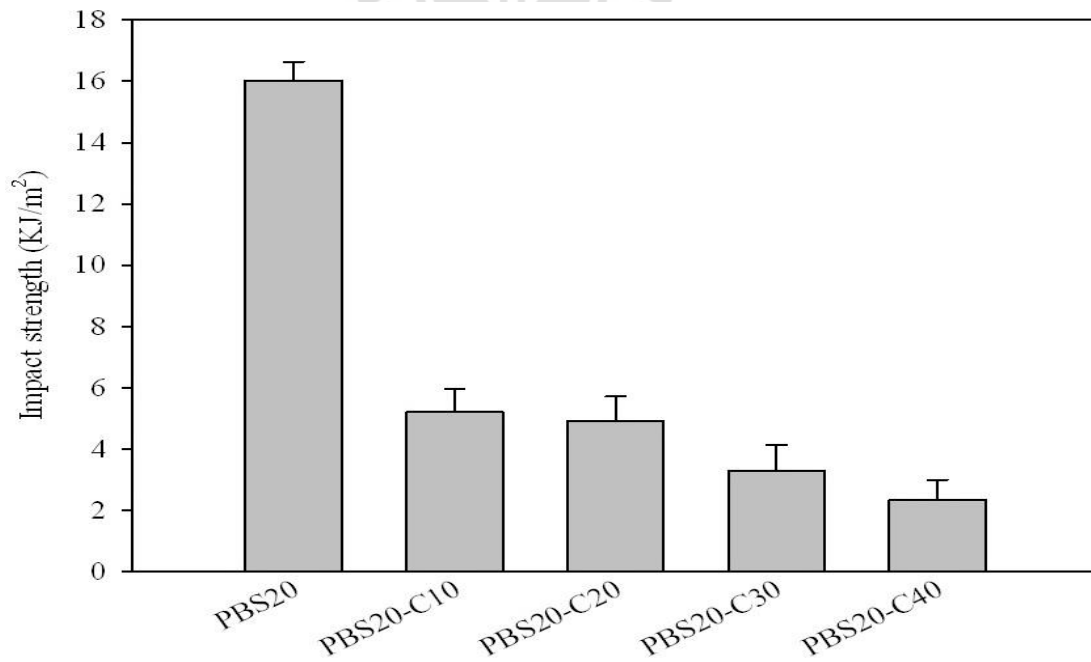


Figure 4.36 Impact strength of CP/PLA/PBS composites with various CP contents.

4.5.2 Morphological properties of CP/PLA/PBS composites

Figure 4.37 shows scanning electron micrographs of CP/PLA/PBS composites with various CP contents. Surface roughness and non-uniform droplet of CP were found in CP/PLA/PBS composites (Figure 4.37 (b-e)). This may be due to poor compatibility between CP and PLA/PBS blends. A clear edge and gap between the CP and matrix were observed. With increasing CP contents, coalescence of CP was increased and the hydrophilic nature of CP that led to poor adhesion (miscibility) with PLA and PBS.



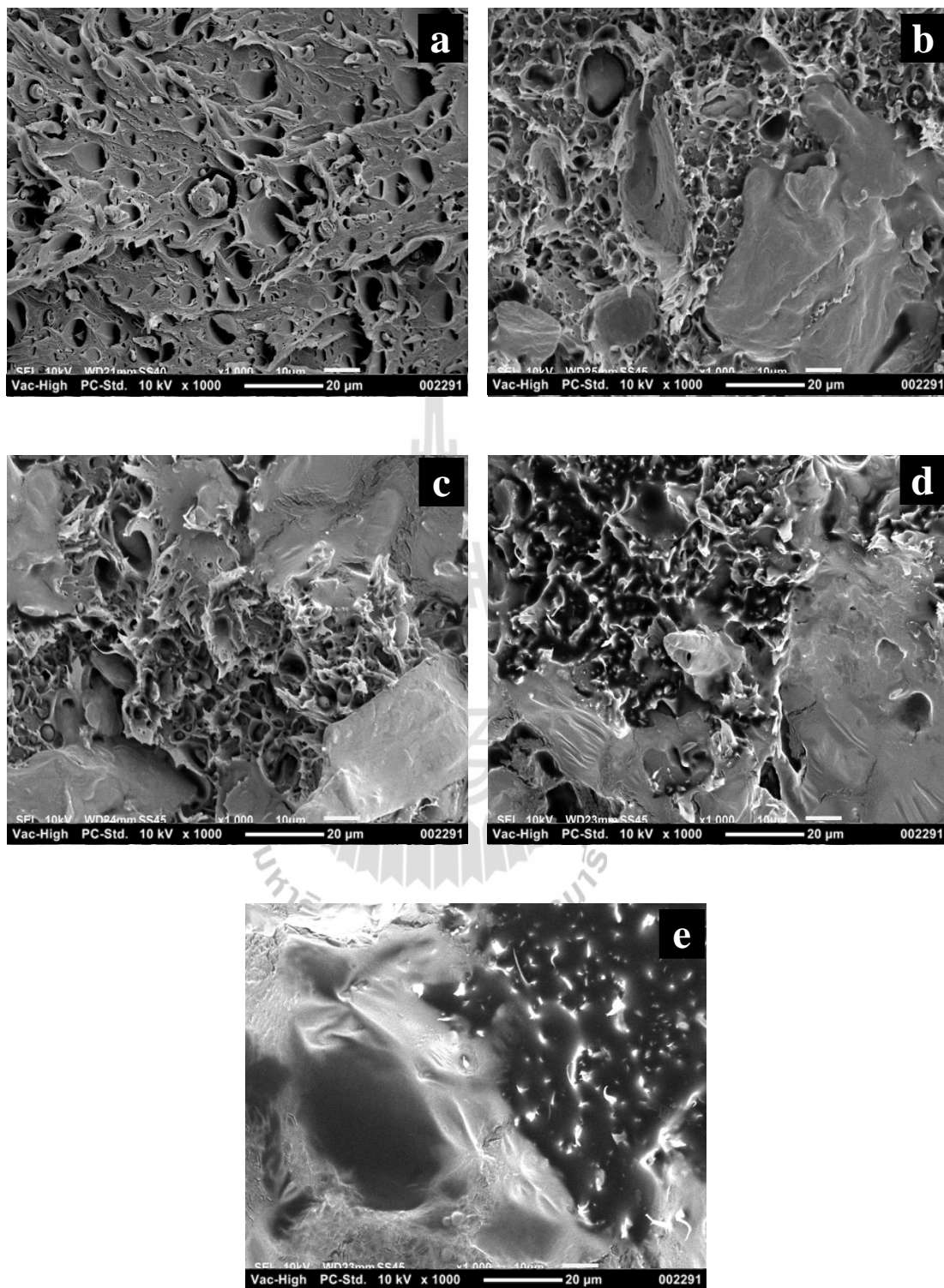


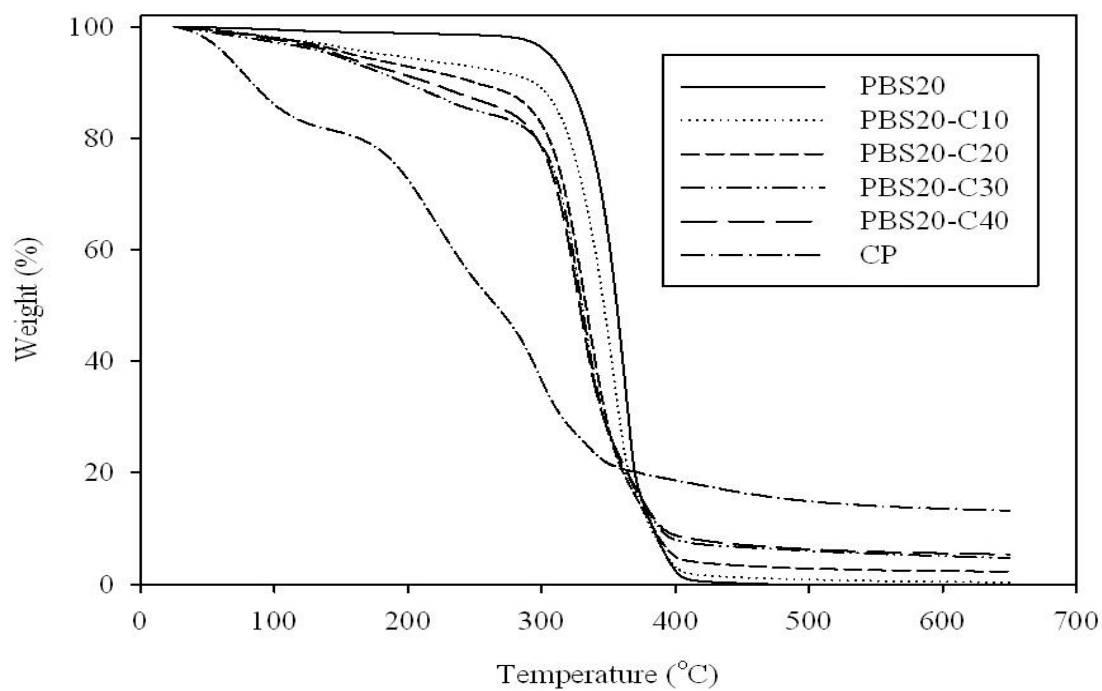
Figure 4.37 SEM micrographs (1000x) of tensile fractured surface of PBS20 (a), PBS20-C10 (b), PBS20-C20 (c), PBS20-C30 (d) and PBS20-C40 (e).

4.5.3 Thermal properties of CP/PLA/PBS composites

Thermogravimetric analysis (TGA) and derivative thermogravimetry (DTG) curves of CP/PLA/PBS composites were shown in Figure 4.38 and 4.39, respectively. The degradation temperature of CP/PLA/PBS composites, degradation temperature of CP and residue at 650°C were listed in Table 4.15. First point degradation (T_{d1}) around 80 - 160°C was the mass loss of moisture and highly volatile materials. Second point degradation (T_{d2}) around 200 °C - 290 °C was glycerol. Third point degradation (T_{d3}) around 300 °C was starch and fourth point degradation (T_{d4}) at 360°C was the decomposition of the cellulose. T_{d5} of PLA and T_{d6} of PBS in PBS20-C10, PBS20-C20, PBS20-C30 and PBS20-C40 were lower than PBS20. This suggested that degradation temperature of composites was decreased with increasing CP content. Thermal stability of CP/PLA/PBS composites was decreased with increasing CP content due to the lower thermal stability of CP (Azwa, Z.N. and Yousif, B.F., 2013). Moreover, CP/PLA/PBS composites showed a three-step decomposition process due to the different thermal resistance of PLA, PBS and CP. First decomposition step (25°C-300°C) corresponded to the decomposition of CP, while second decomposition step (300°C-370°C) corresponded to the decomposition of PLA. The final decomposition step (370°C-410°C) corresponded to the decomposition of PBS. This indicates that the compatibility between PLA, PBS and CP was poor. Residue of CP in CP/PLA/PBS composites was increased with increasing CP content. This result confirmed that CP was added into the composites. T_{d3} and T_{d4} overlap with T_{d5} of PLA.

Table 4.15 TGA analysis of CP/PLA/PBS composites.

Name	T _{d1} (°C)	T _{d2} (°C)	T _{d3} (°C)	T _{d4} (°C)	T _{d5} (°C)	T _{d6} (°C)	Residue at 650°C (%)
PBS20	-	-	N/A*	N/A*	368.32	405.69	0.00
PBS20-C10	150.20	251.22	N/A*	N/A*	357.01	393.05	0.34
PBS20-C20	150.01	250.93	N/A*	N/A*	333.86	392.78	2.27
PBS20-C30	144.70	231.52	N/A*	N/A*	330.29	392.75	4.70
PBS20-C40	143.78	230.15	N/A*	N/A*	328.38	382.88	5.35
CP	88.11	216.93	298.01	338.55	-	-	13.20

*overlap T_{d5}**Figure 4.38** TGA curves of CP and CP/PLA/PBS composites.

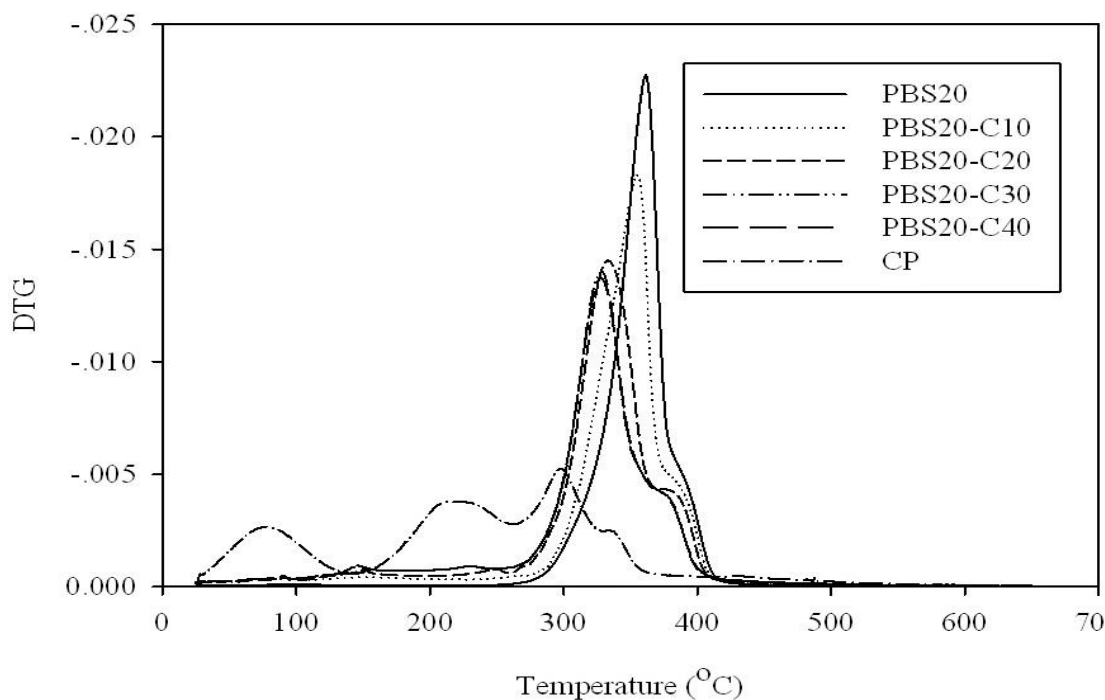


Figure 4.39 DTG curves of CP and CP/PLA/PBS composites.

The DSC thermograms recorded during cooling scan and second heating scan of CP/PLA/PBS composites were reported in Figure 4.40 and Figure 4.41, respectively. The data derived from DSC analyses was reported in Table 4.16 and Table 4.17. Crystallization temperature on cooling scan (T_c) of PBS in PBS20-C10, PBS20-C20 and PBS20-C30 were observed. This may be due to the nucleation effect caused by CP under cooling. At high loading of CP, T_c of PBS in CP/PLA/PBS composites was not found. T_c of PBS in the composites shifted to lower temperature. This indicated that the crystallization of PBS was restricted by high loading of CP. Similar in PLA, T_c of PLA in composites appeared with addition of CP. T_c of PLA in the composites shifted to lower temperature. Glass transition temperature (T_g) of CP/PLA/PBS composites was higher than that of PLA/PBS blends due to the addition of CP reduced chain mobility of the composites. T_g of composites insignificantly

changed with increasing CP content. Cold crystallization temperature on heating step (T_{cc}) of composites shifted to low temperature with increasing CP up to 20wt%. This indicated that crystallization ability of composite was enhanced. The melting temperature (T_m) of composites was decreased with addition of CP. This implied that CP hindered the lamella formation and led to less perfect crystals of PLA. This behavior was also observed in PLA/PBS/calcium sulfate whiskers (CSW) composites (Chen et al., 2014). The degree of crystallinity of PLA in CP/PLA/PBS composites ($\%X_{mPLA}$) was improved with addition of CP up to 10 wt%. The degree of crystallinity of PBS in CP/PLA/PBS composites ($\%X_{mPBS}$) was improved with addition of CP up to 20wt%. This result indicated that high loading of CP inhibited $\%X_m$ of PLA and PBS.

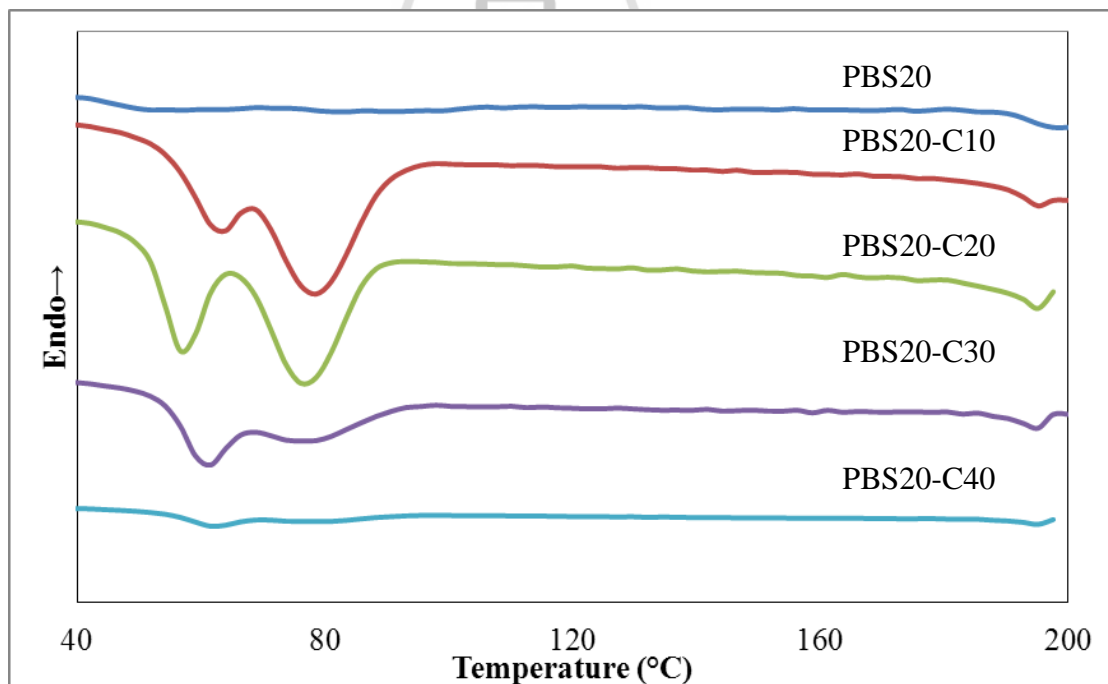


Figure 4.40 DSC curves from the cooling scan of CP/PLA/PBS composites.

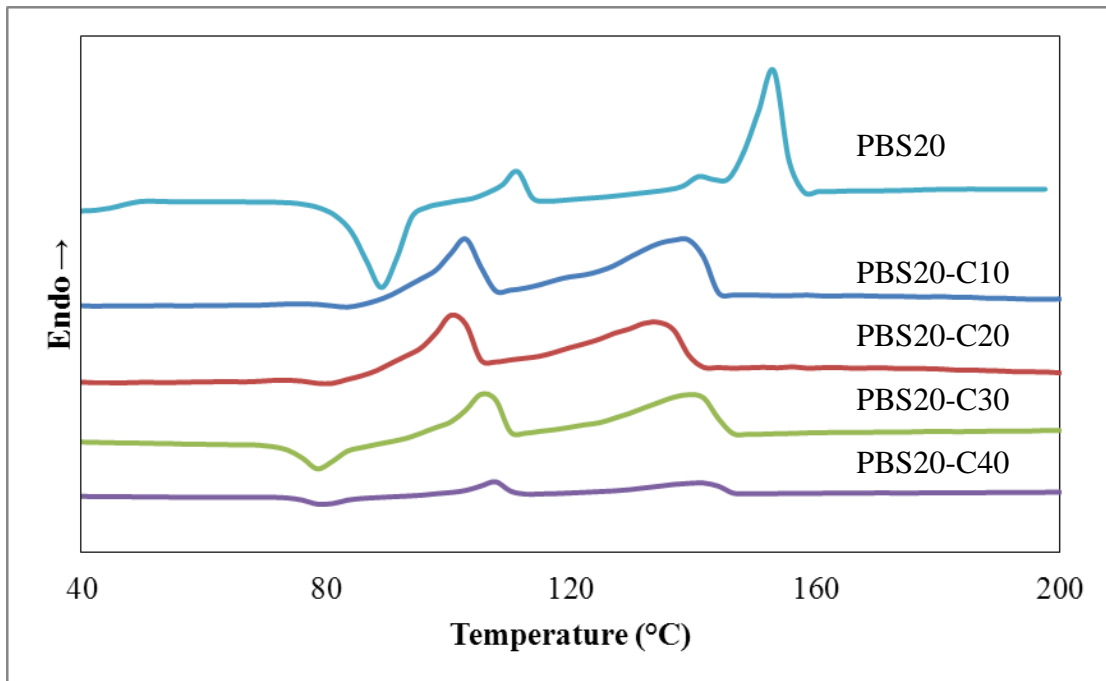


Figure 4.41 DSC curves from the second heating scan of CP/PLA/PBS composites.

Table 4.16 Thermal properties of CP/PLA/PBS composites.

Name	T_g (°C)	T_{m1PLA} (°C)	T_{m2PLA} (°C)	T_{m1PBS} (°C)	T_{m2PBS} (°C)	T_{cc} (°C)	T_c (°C)
PLA	52.5	146.6	155.0	-	-	108.8	-
PBS20	46.4	142.1	153.6	-	111.9	89.3	-
PBS20-C10	54.0	138.5	-	102.9	-	83.2	63.2/78.6
PBS20-C20	54.8	133.7	-	101.6	-	79.4	57.1/76.8
PBS20-C30	54.8	139.7	-	106.5	-	79.0	61.1/75.8
PBS20-C40	54.5	140.6	-	107.9	-	79.7	-
PBS	-22.0	-	-	106.0	113.5	97.8	79.6

Table 4.17 ΔH_m , ΔH_{cc} , ΔH_c and $\%X_m$ of CP/PLA/PBS composites.

Name	ΔH_{mPLA} (J/g)	ΔH_{mPBS} (J/g)	ΔH_{cc} (J/g)	ΔH_c (J/g)	$\%X_{mPLA}$ (%)	$\%X_{mPBS}$ (%)
PLA	39.28	-	37.28	-	41.92	-
PBS20	34.19	5.48	26.55	-	45.61	27.06
PBS20-C10	34.70	16.00	2.05	43.08	51.82	80.58
PBS20-C20	26.36	14.68	4.55	41.61	44.29	83.18
PBS20-C30	21.73	11.13	9.32	20.59	41.72	72.08
PBS20-C40	5.82	3.17	2.66	-	13.04	23.95
PBS	-	84.07	9.55	86.20	-	76.22

4.6 Effect of compatibilizer on physical properties of CP/PLA/PBS composites

4.6.1 Mechanical properties of CP/PLA/PBS composites with and without compatibilizer

Tensile strength, elongation at break, Young's modulus and impact strength of CP/PLA/PBS composites with compatibilizer are shown in Figure 4.42-4.45. Tensile strength, elongation at break, Young's modulus and impact strength of CP/PLA/PBS composites (PBS20-G10-C20) are improved by the addition of PLA-g-GMA. Especially, impact strength of composite was distinctively increased with addition of PLA-g-GMA as a compatibilizer. Tensile strength, elongation at break, Young's modulus and impact strength of CP/PLA/PBS composites (PBS20-M10-

C20) was also improved by addition of PLA-g-MA. It was explained the reaction between the hydroxyl group of CP and anhydride group of MA on PLA-g-MA. This indicated that compatibility between CP and PLA/PBS blends was improved by using PLA-g-GMA and PLA-g-MA. Young's modulus of PBS20-M10-C20 was slightly higher than that of PBS20-G10-C20. PLA-g-MA improved stiffness property of CP/PLA/PBS composites. Impact strength and elongation at break of composite with PLA-g-GMA were higher than those of PBS20-M10-C20. Toughness property was improved by addition of PLA-g-GMA. Tensile strength, elongation at break, Young's modulus and impact strength of CP/PLA/PBS composites are summarized in Table 4.18.

Table 4.18 Tensile strength, elongation at break, Young's modulus and impact strength of CP/PLA/PBS composites with and without compatibilizer.

Name	Tensile strength (MPa)	Young's modulus (MPa)	Elongation at break (%)	Impact strength (kJ/m ²)
PBS20-C20	22.34±0.81	633.71±9.53	6.03±0.42	4.91±0.80
PBS20-G10-C20	33.24±2.10	703.21±13.99	11.07±1.24	12.76±0.50
PBS20-M10-C20	26.85±1.02	750.46±38.51	9.88±1.17	6.74±0.24

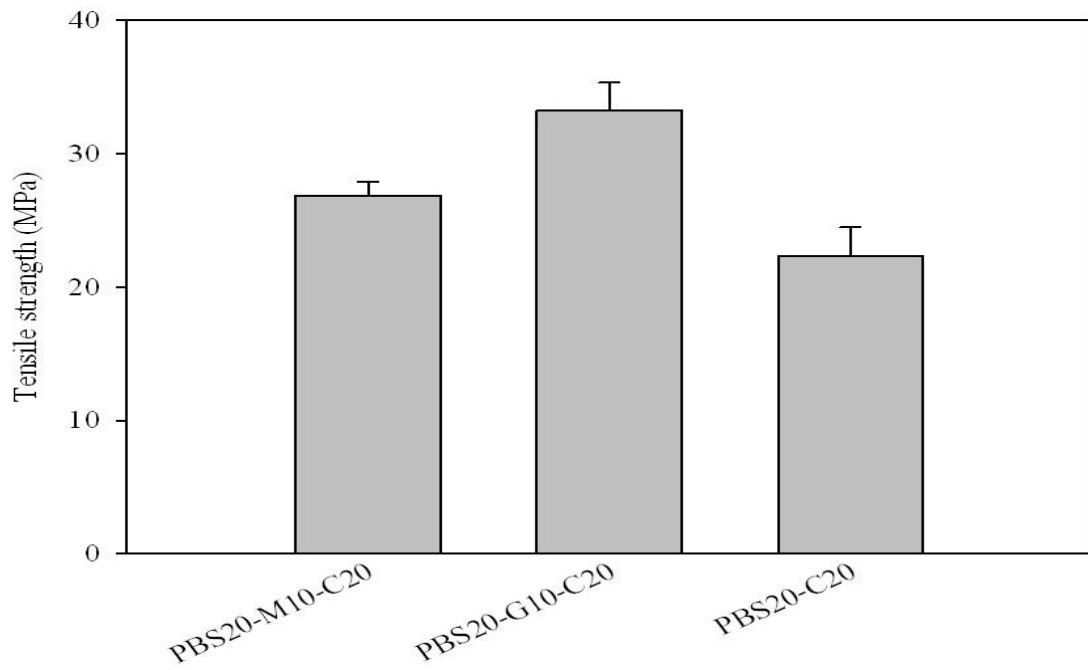


Figure 4.42 Tensile strength of CP/PLA/PBS composites with and without compatibilizer.

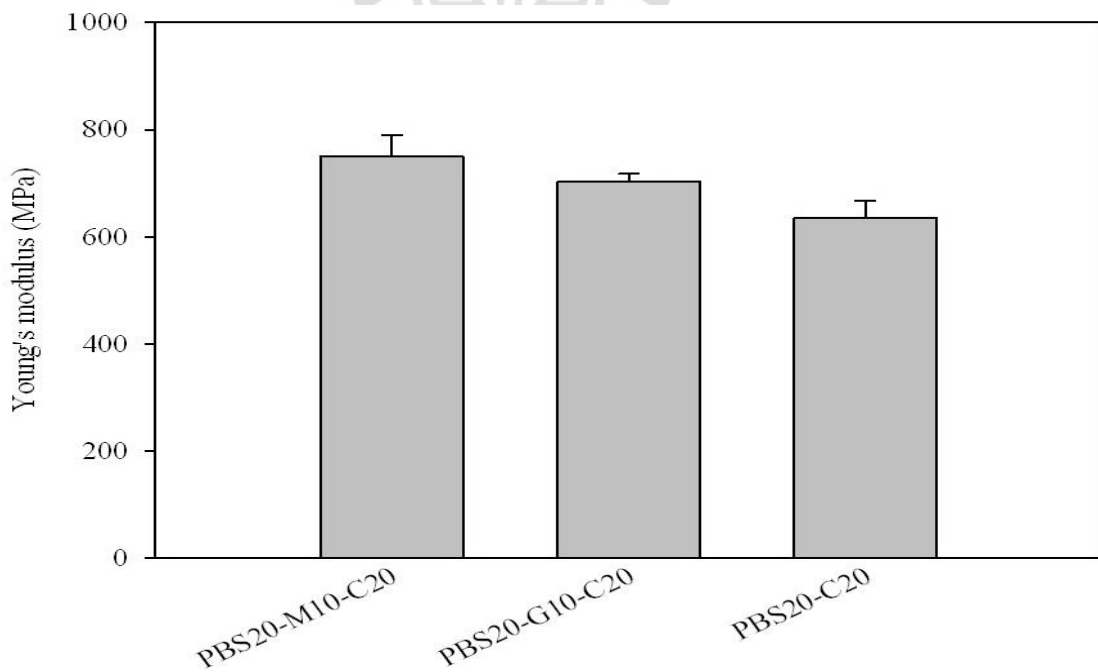


Figure 4.43 Young's modulus of CP/PLA/PBS composites with and without compatibilizer.

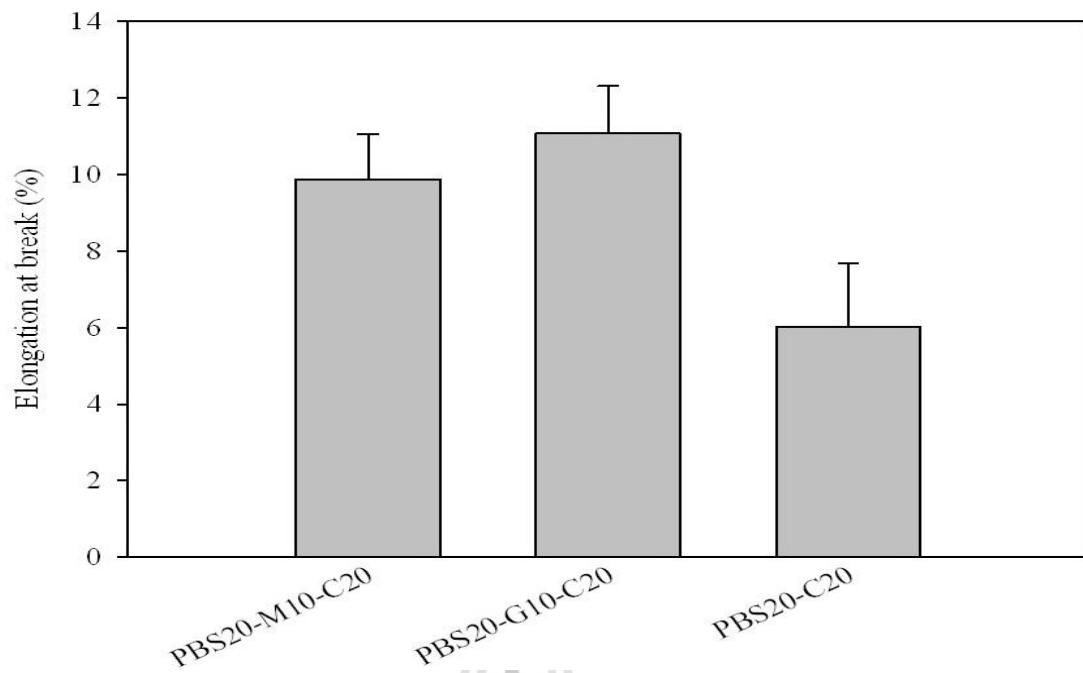


Figure 4.44 Elongation at break of CP/PLA/PBS composites with and without compatibilizer.

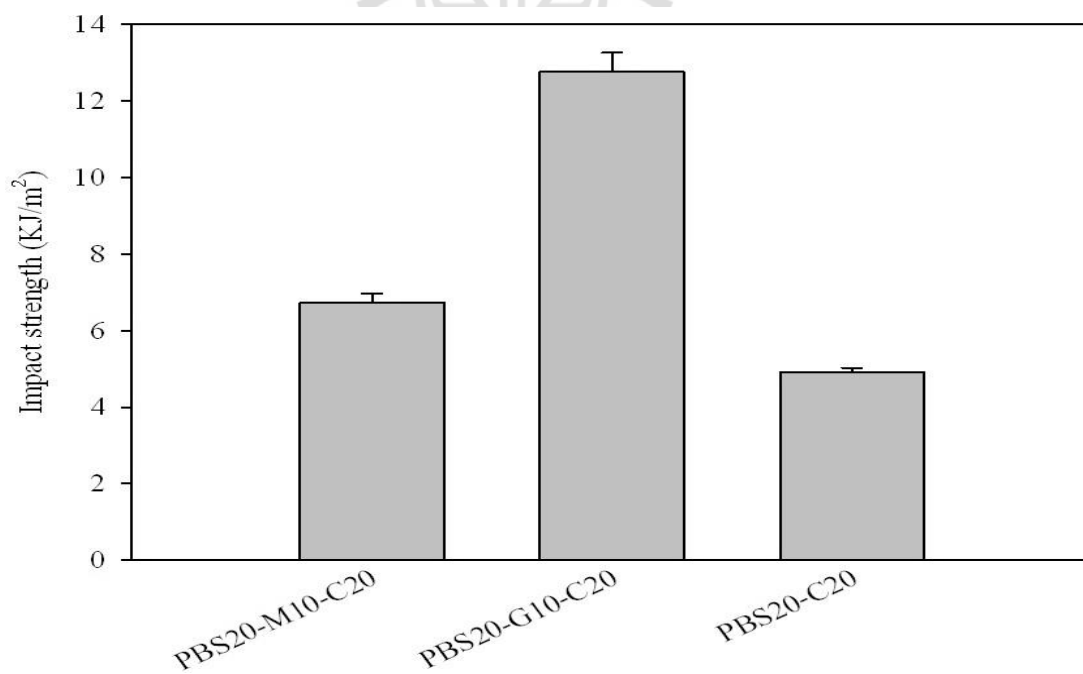


Figure 4.45 Impact strength of CP/PLA/PBS composites with and without compatibilizer.

4.6.2 Morphological properties of CP/PLA/PBS composites with and without compatibilizer

Figure 4.46 (a) - (c) shows SEM micrographs of tensile fractured surface of CP/PLA/PBS composites. Figure 4.46 (a) and Figure 4.46 (b) show SEM images of PBS20-C20 with and without of PLA-g-GMA, respectively. The elongated fibrils in CP/PLA/PBS composites with compatibilizer were observed. This result confirmed that compatibilizer improved compatibility between CP and PLA/PBS blends. The expected mechanism of compatibilization may be that PLA-g-GMA had the glycidyl functional group of the epoxide, which could react with hydroxyl groups of the CP. Moreover, the glycidyl functional group of the epoxide also could react with carboxyl end groups of PLA. As a result, PLA-g-GMA was incorporated into both PLA phase and starch phase as a compatibilizer (Liu, J. et al., 2012). Figure 4.46 (c) shows CP/PLA/PBS composites with PLA-g-MA. Starch in CP could react with MA in PLA-g-MA (Wootthikanokkhan et al., 2012). Some carboxylic acid groups from a ring opening of the MA reacted with starch. PLA-g-MA was improved compatibility of composite. However, PBS20-MA10-C20 showed brittle fracture. The elongated fibril in CP/PLA/PBS composites with PLA-g-MA was found. This result confirmed that compatibilizer improved compatibility between CP and PLA/PBS blends of composites.

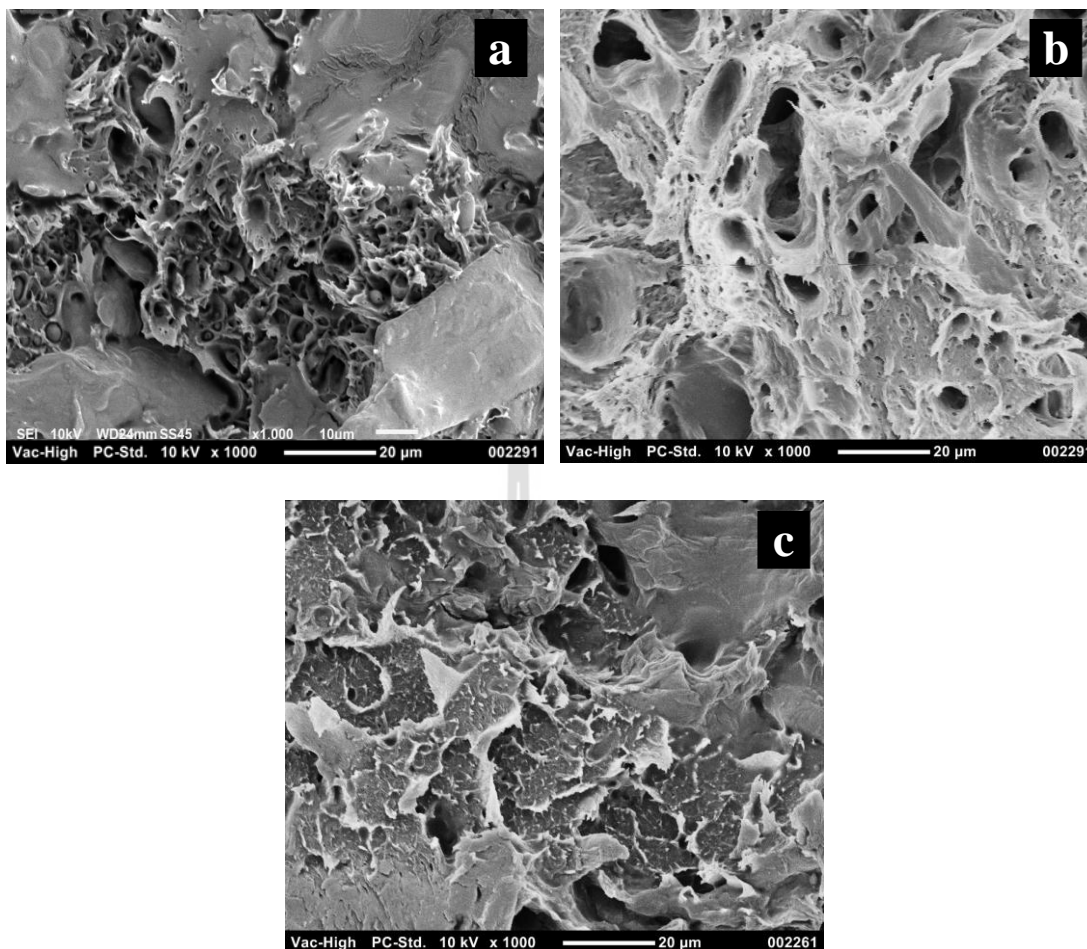


Figure 4.46 SEM micrographs (1000x) of tensile fractured surface of PBS20-C20 (a), PBS20-G10-C20 (b) and PBS20-M10-C20 (c).

4.6.3 Thermal properties of CP/PLA/PBS composites with and without compatibilizer

Thermogravimetric analysis (TGA) and derivative thermogravimetry (DTG) curves of PLA, PLA/PBS blends and PBS were shown in Figure 4.47 and 4.48, respectively. The degradation temperature of CP/PLA/PBS composites was listed in Table 4.19. First point degradation (T_{d1}) around 80 - 160°C was the mass loss of moisture and highly volatile materials. Second point degradation (T_{d2}) around 200 °C – 290 °C was glycerol. T_{d3} of PLA and T_{d4} of PBS in PBS20-G10-C20 were higher

than PBS20-C20. This suggested that degradation temperature of composites was increased with addition of PLA-g-GMA. Thermal stability of CP/PLA/PBS composites was increased with addition of PLA-g-GMA. The compatibility between CP and PLA/PBS blends was improved by using PLA-g-GMA as a compatibilizer. Moreover, CP/PLA/PBS composites showed step decomposition process due to the different thermal resistance of PLA, PBS and CP. The first decomposition step (25°C-300°C) corresponded to the decomposition of CP, while the second decomposition step (300°C-370°C) corresponded to the decomposition of PLA. The final decomposition step (370°C-410°C) corresponded to the decomposition of PBS. This indicated that the compatibility between PLA, PBS and CP was poor. The step decomposition process of PBS20-C20 showed more clearly than that of PBS20-G10-C20. PLA-g-GMA improved compatibility between CP and PLA/PBS blends. T_{d5} at 472.19°C of PBS20-G10-C20 was observed. This result was probably due to reaction of PBS and GMA. glycidyl methacrylate-grafted poly(butylene succinate) (PBS-g-GMA) was studied by Wu et al. (2013).

Table 4.19 TGA analysis of CP/PLA/PBS composites with and without compatibilizer.

Name	T_{d1} (°C)	T_{d2} (°C)	T_{d3} (°C)	T_{d4} (°C)	T_{d5} (°C)	Residue at 650°C (%)
PBS20-C20	150.01	250.93	333.86	392.78	-	2.27
PBS20-G10-C20	155.23	250.55	334.10	392.80	472.19	0.00

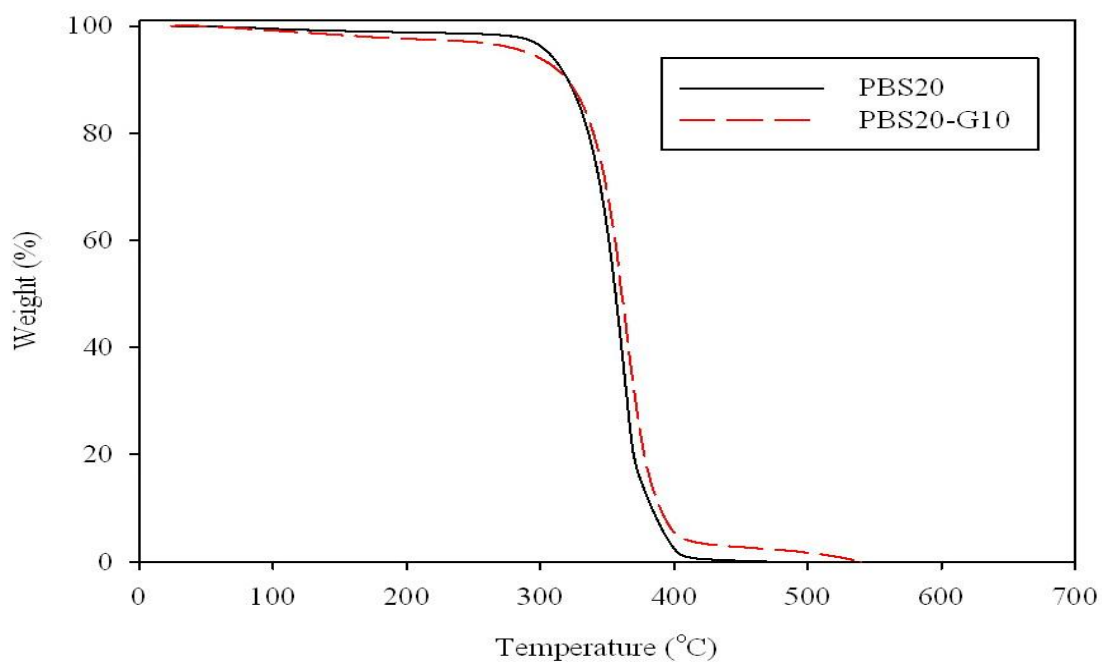


Figure 4.47 TGA curves of CP/PLA/PBS composites with and without compatibilizer.

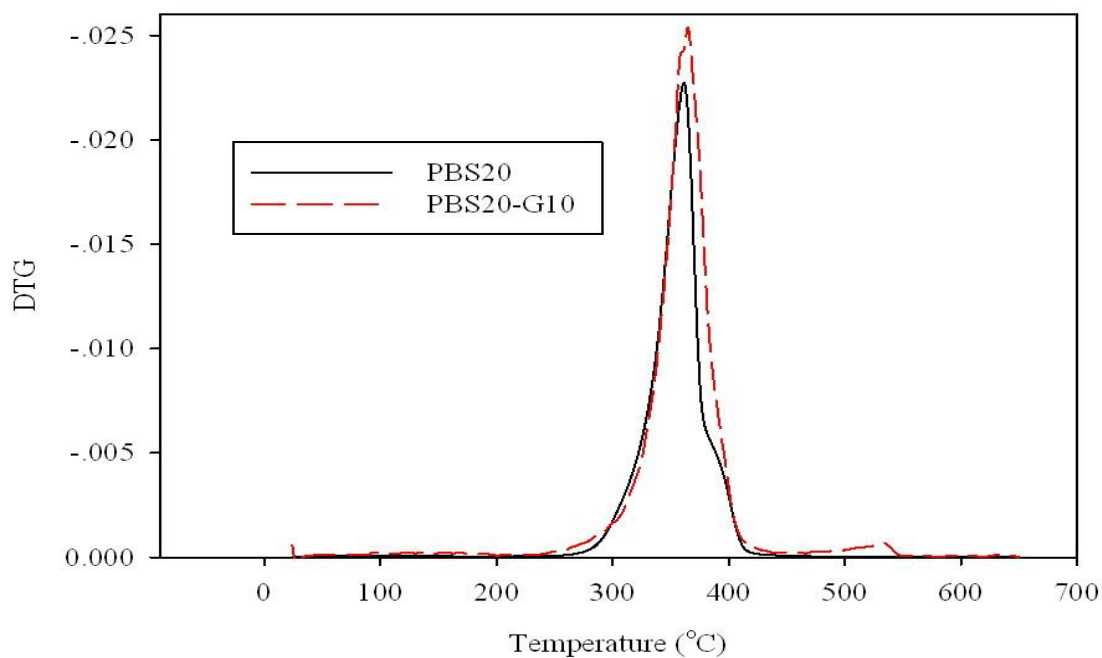


Figure 4.48 DTG curves of CP/PLA/PBS composites with and without compatibilizer.

The DSC thermograms recorded during cooling scan and second heating scan of CP/PLA/PBS composites with and without PLA-g-GMA were reported in Figure 4.49 and Figure 4.50, respectively. The data derived from DSC analysis was reported in Table 4.20 and Table 4.21. Crystallization temperature on cooling scan (T_c) of PLA and PBS in PBS20-C20 was observed. T_c of PBS20-G10-C20 showed one peak. This indicated that compatibility of composites was improved by PLA-g-GMA as compatibilizer. T_c of PBS20-G10-C20 shifted to higher temperature. The crystallization of composites was promoted by addition of compatibilizer. Glass transition temperature (T_g) of PBS20-G10-C20 was lower than that of PBS20-C20. The addition of PLA-g-GMA improved compatibility between CP and PLA/PBS blends. Cold crystallization temperature on heating step (T_{cc}) of PBS20-G10-C20 did not appear. PBS20-G10-C20 completely crystallized on cooling stage. The melting temperature (T_m) of PLA in PBS20-G10-C20 was increased but that of PBS was decreased. This implied that PLA-g-GMA hindered the lamella formation and led to less perfect crystals of PBS but perfect crystal was formed in PLA with PLA-g-GMA. The degree of crystallinity of PLA in PBS20-G10-C20 ($\%X_{mPLA}$) was improved with addition of PLA-g-GMA. The degree of crystallinity of PBS in CP/PLA/PBS composites ($\%X_{mPBS}$) was decreased with addition of PLA-g-GMA. This result indicated that PLA-g-GMA inhibited $\%X_m$ of PBS but $\%X_m$ of PLA was improved by PLA-g-GMA.

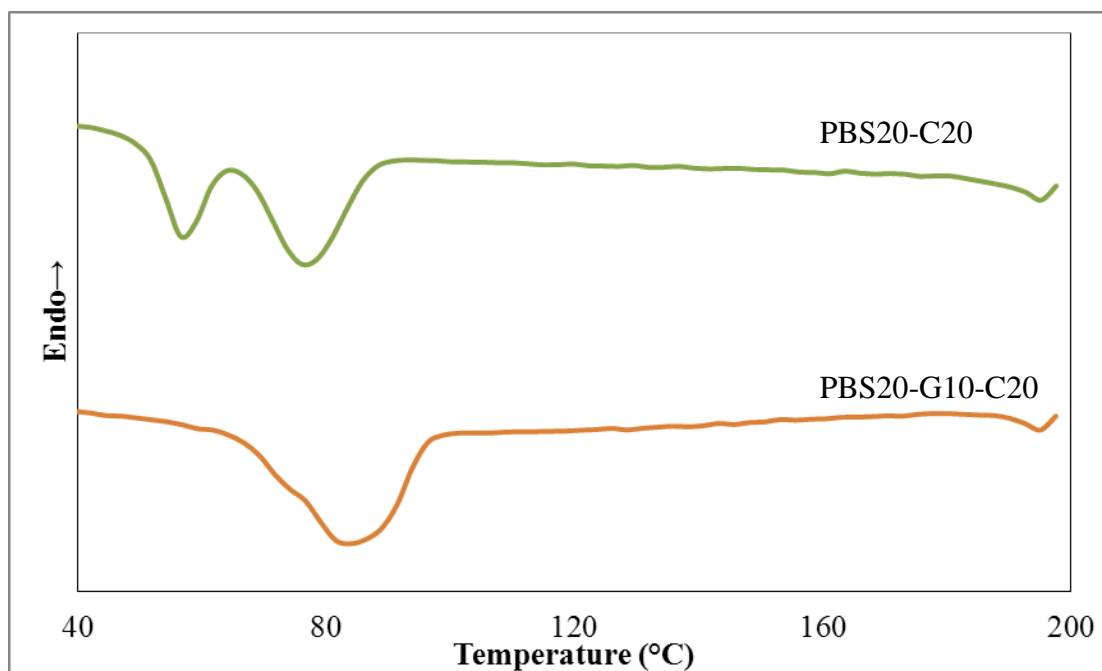


Figure 4.49 DSC curves from the cooling scan of CP/PLA/PBS composites with and without compatibilizer.

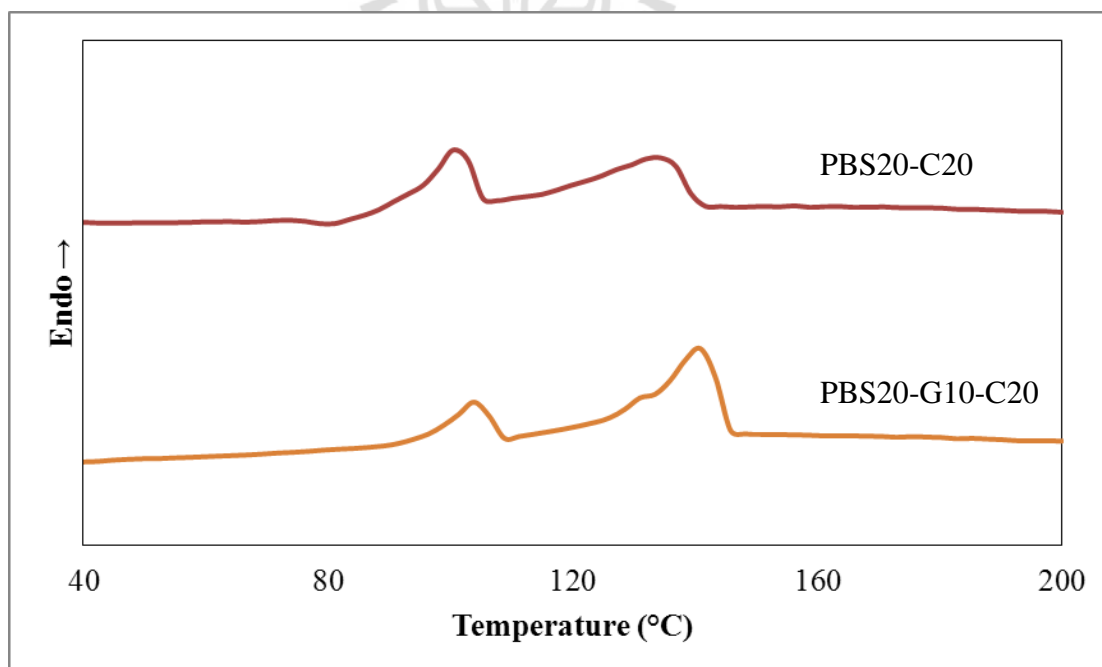


Figure 4.50 DSC curves from the second heating scan of CP/PLA/PBS composites with and without compatibilizer.

Table 4.20 Thermal properties of CP/PLA/PBS composites with and without compatibilizer.

Name	T _g (°C)	T _{m1PLA} (°C)	T _{m2PLA} (°C)	T _{m1PBS} (°C)	T _{m2PBS} (°C)	T _{cc} (°C)	T _c (°C)
PBS20-C20	54.8	133.7	-	101.6	-	79.4	57.1/76.8
PBS20-G10-C20	53.5	140.7	-	105.1	-	-	83.2

Table 4.21 ΔH_m , ΔH_{cc} , ΔH_c and %X of CP/PLA/PBS composites with and without compatibilizer.

Name	ΔH_{mPLA} (J/g)	ΔH_{mPBS} (J/g)	ΔH_{cc} (J/g)	ΔH_c (J/g)	%X _{mPLA} (%)	%X _{mPBS} (%)
PBS20-C20	26.36	14.68	4.55	41.61	44.29	83.18
PBS20-G10-C20	38.02	10.47	-	41.44	63.88	58.76

4.7 References

- Azwa, Z.N. And Yousif, B.F. (2013). Thermal Degradation Study of Kenaf Fibre/Epoxy Composites Using Thermo Gravimetric Analysis. **3rd Malaysian Postgraduate Conference. Australia.** 256-264.
- Bhatia, A., Gupta, R. K., Bhattacharya, S. N. and Choi, H. J. (2007). Compatibility of biodegradable poly (lactic acid) (PLA) and poly (butylene succinate) (PBS) blends for packaging application. **J. Rheol.** 19: 125-131.

- Brito, G. F., Agrawal, P., Araújo, E. M. and Mélo, T. J. A. (2012). Polylactide /Biopolyethylene Bioblends. **Polímeros**. 22: 427-429
- Chen, R.Y., Zou, W., Wu, C. R., Jia, S. K., Huang, Z., Zhang, G. Z., Yang, Z. T. and Qu, J. P. (2014). Poly(lactic acid)/poly(butylene succinate)/calcium sulfate whiskers biodegradable blends prepared by vane extruder: Analysis of mechanical properties, morphology, and crystallization behavior. **Polym. Test**. 34: 1–9.
- Doi, Y. and Fukuda, K. (1994). Biodegradable plastics and polymer. **Studies in Polymer Science** 12. 36: 299.
- Dong, W., Zou, B., Ma, P., Liu, W., Zhou, X., Shi, D., Ni, Z. and Chen, M. (2013). Influence of phthalic anhydride and bioxazoline on the mechanical and morphological properties of biodegradable poly(lactic acid)/poly [(butylene adipate)-co-terephthalate] blends. **Polymer**. 62: 1783-1790.
- Hassan, E., Wei, Y., Jiao H. and Muhuo, Y. (2013). Dynamic Mechanical Properties and Thermal Stability of Poly(lactic acid) and Poly(butylene succinate) Blends Composites. **J. Fiber. Bioeng. Inform.** 6: 85-94.
- Huang, Y., Zhang, C., Pan, Y., Wang, W., Jiang, L. and Dan, Y. (2012). Study on the Effect of Dicumyl Peroxide on Structure and Properties of Poly(Lactic Acid)/Natural Rubber Blend. **J. Polym. Environ.**
- Hvella, M., Errico, M. E., Immirzi, B., Malinconico, M., Martuscelli, E., Poalillo, L. and Falcigno, L. (1997). Radical polymerization of poly(butyl acrylate) in

the presence of poly(L-lactic acid), Synthesis, characterization and properties of blends. **Angew. Makromol. Chem.** 246: 49-63.

Ji, D., Liu, Z., Lan, X., Wu, F., Xie, B. and Yang, M. (2014). Morphology, rheology, crystallization behavior, and mechanical properties of poly(lactic acid)/poly(butylene succinate)/dicumyl peroxide reactive blends. **J. Appl. Polym. Sci.** 131.

John, J., Tang, J., Yang, Z. and Bhattacharya, M. (1997). Synthesis and characterization of anhydride-functional polycaprolactone. **J. Polym. Sci. Part A: Polym. Chem.** 35: 1139-1148.

Juntuek, P. 2011. **Effect of glycidyl methacrylate grafted natural rubber on physical properties of PLA/NR blends and PLA/vetiver/NR composites.** Doctoral Thesis, Suranaree University of Technology. 194.

Kim, H. S., Lee, B. H., Lee, S., Kim, H. J. and Dorgan, J. R. (2010). Enhanced interfacial adhesion, mechanical, and thermal properties of natural flour-filled biodegradable polymer bio-composites. **J. Therm. Anal. Calorim.** 104: 331–338.

Kim, H. S., Yang, H. S. and Kim, H. J. (2005). Biodegradability and Mechanical Properties of Agro-Flour-Filled Polybutylene Succinate Biocomposites. **J. App. Polym. Sci.** 97: 1513–1521.

Kumar, M., Mohanty, S., Nayak, S. K. and Rahail P. M. (2010). Effect of Glycidyl Methacrylate (GMA) on the Thermal, Mechanical and Morphological

Property of Biodegradable PLA/PBAT Blend and Its Nanocomposites.
Biores. Technol. 101: 8406-8415.

Lai, S. M., Hung, K. C., Kao, H. C., Liu, L. C. and Wang, X. F. (2013). Synergistic Effects by Compatibilization and Annealing Treatment of Metallocene Polyethylene/PLA Blends. **J. Appl. Polym. Sci.** 2399-2409.

Liu, J., Jiang, H. and Chen, L. (2012). Grafting of Glycidyl Methacrylate onto Poly(lactide) and Properties of PLA/Starch Blends Compatibilized by the Grafted Copolymer. **J. Polym. Environ.** 20: 810-816.

Ma, P., Wang, X., Liu, B., Li, Y., Chen, S., Zhang, Y. and Xu, G. (2012). Preparation and foaming extrusion behavior of polylactic acid/ polybutylene succinate/ montmorillonoid nanocomposite. **J. Cell. Plast.** 48: 191-205.

Mani, R., Bhattacharya, M., and Tang, J. (1999). Functionalization of polyesters with maleic anhydride by reactive extrusion. **J. Polym. Sci. Pol. Chem.** 37: 1693-1702.

Monshi, A., Foroughi, M. R., Monshi, M.R. (2012). Modified Scherrer Equation to Estimate More Accurately-Nano-Crystallite Size Using XRD. **World Journal of Nano Science and Engineering.** 2: 154-160.

Ojijo, V., Sinha, R. S., and Sadiku, R. (2012). Role of Specific Interfacial Area in Controlling Properties of Immiscible Blends of Biodegradable Polylactide and Poly[(butylene succinate)-co-adipate]. **ACS. Appl. Mater. Interfaces.** 4: 6690–6701.

- Orozco, H. V., Brostow, W., Chonkaew, W. and Lo'pez, B. L. (2009). Preparation and Characterization of Poly(Lactic Acid)-g-Maleic Anhydride/Starch Blends. **Macromol. Symp.** 277: 69–80.
- Oyama, H. T. (2009). Super-tough poly (lactic acid) materials: Reactive blending with ethylene copolymer. **Polymer.** 50: 747–75.
- Park, J. W. and Im, S. S. (2002). Phase Behavior and Morphology in Blends of Poly(L-lactic acid) and Poly(butylene succinate). **J. Appl. Polym. Sci.** 86: 647–655.
- Peltzer, M., Pei, A., Zhou, Q., Berglund, L. and Jim'enez, A. (2014). Surface modification of cellulose nanocrystals by grafting with poly(lactic acid). **Polym. Int.** 63: 1056–1062.
- Shibata, M., Inoue, Y., and Miyoshi, M. (2006). Mechanical properties, morphology, and crystallization behavior of blends of poly (L-lactide) with poly (butylene succinate-co-L-lactate) and poly (butylene succinate). **Polymer.** 47: 3557–3564.
- Sis, A. L. M. and Yunus, W. M. Z. W. (2013). Effect of (3-aminopropyl) trimethoxysilane on mechanical properties of PLA/PBAT blend reinforced kenaf fiber. **Iran. Polym. J.** 22: 101-108.
- Song, L. and Qiu, Z. (2009). Crystallization behavior and thermal property of biodegradable poly(butylene succinate)/functional multi-walled carbon nanotubes nanocomposite. **Polym. Deg. Stab.** 94: 632–637.

- Su, Z., Li, Q., Liu, Y., Hu, G. H. and Wu, C. (2009). Compatibility and phase structure of binary blend of pol (lactic acid) and glycidyl methacrylare grafted poly (ethylene octane). **Eur. Polym. J.** 45: 2428-2433.
- Tábi, T., Sajó, I. E., Szabó, F., Luyt, A. S. and Kovács, J. G. (2010). Crystalline structure of annealed polylactic acid and its relation to processing. *eXPRESS Polymer Letters*. 4: 659–668.
- Todo, M., Park, S.-D., Takayama, T. and Arakawa K. (2007). Fracture micromechanisms of bioabsorbable PLLA/PCL polymer blends. **Eng. Fract. Mech.** 74: 1872–1883.
- Tokiwa, Y., Calabia, B. P., Ugwu, C. U. and Aiba, S. (2009). Biodegradability of Plastics. **Int. J. Mol. Sci.** 10: 3722-3742.
- Wang, R., Wang, S., Zhang, Y., Wan, C. and Ma, P. (2009). Toughening Modification of PLLA/PBS Blends via In Situ Compatibilization. **Polym. Eng. Sci.** 49: 26-33.
- Wootthikanokkhan, J., Kasemwananimit, P., Sombatsompop, N., Kositchaiyong, A. Ayutthaya, S. I. N. and Kaabbuathong, N. (2012). Preparation of Modified Starch-Grafted Poly(lactic acid) and a Study on Compatibilizing Efficacy of the Copolymers in Poly(lactic acid)/Thermoplastic Starch Blends. **J. Appl. Polym. Sci.** 126: E388–E395.

- Wu, C. S., Liao, H. T. and Jhang, J. J. (2013). Palm fibre-reinforced hybrid composites of poly(butylene succinate): characterization and assessment of mechanical and thermal properties. **Polym. Bull.** 70: 3443–3462.
- Wu, C.-S. (2003). Physical properties and biodegradability of maleated-polycaprolactone/starch composite. **Polym. Degrad. Stab.** 80: 127-134.
- Xu, T., Tang, Z. and Zhu, J. (2012). Synthesis of Polylactide-graft-Glycidyl Methacrylate Graft Copolymer and its Application as a Coupling Agent in Polylactide/Bamboo Flour Biocomposites. **Inc. J. Appl. Polym. Sci.** 125: 622-627.
- Yokohara, T. and Yamaguchi M. (2008). Structure and properties for biomass-based polyester blends of PLA and PBS. **Eur. Polym. J.** 44: 677–685.
- Zhang, C., Wang, W., Huang, Y., Pan, Y., Jiang, L., D, Y., Luo, Y. and Peng, Z. (2013). Thermal, mechanical and rheological properties of polylactide toughened by epoxidized natural rubber. **Mater. Des.** 45: 198–205.
- Zhang, F., Endo, T., Kitagawa, R., Kabeya, H. and Hirotsu, T. (2000). Synthesis and characterization of a novel blend of polypropylene with Chlorella. **J. Mater. Chem.** 10: 2666-2672.
- Zhang, K., Mohanty, A. K. and Misra, M. (2012). Fully Biodegradable and Biorenewable Ternary Blends from Polylactide, Poly(3-hydroxybutyrate-co-hydroxyvalerate) and Poly(butylene succinate) with Balanced Properties. **ACS Appl. Mater. Interfaces.** 4: 3091–3101.

CHAPTER V

CONCLUSIONS

PLA-g-GMA was used as compatibilizer for PLA/PBS blends and CP/PLA/PBS composites. The graft content of GMA grafted onto PLA molecule determined from the titration method was 2.277%. PLA-g-MA was also used as compatibilizer CP/PLA/PBS composites. The graft content of MA grafted onto PLA molecule determined from the titration method was 1.814%.

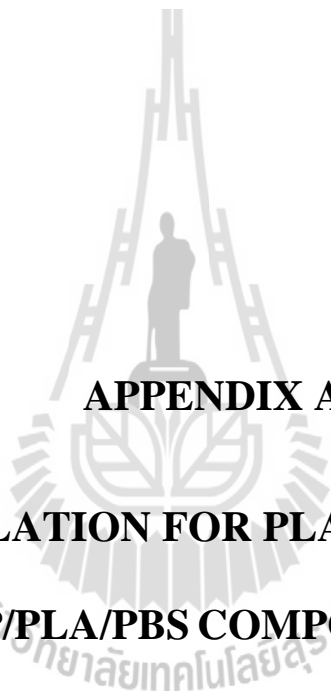
Tensile strength and Young's modulus of PLA/PBS blends was decreased with increasing PBS contents. Elongation at break of blends was increased with increasing PBS content up to 20 wt%. Elongation at break was increased from 5.20% for neat PLA to 52.82% for PBS20. Impact strength of PLA/PBS blends increased with increasing PBS content. At PBS 40 wt%, impact strength of PLA/PBS blend was about 2 times higher than that of neat PLA. From SEM result, the particles represent the PBS phases distributed in the PLA matrix. The particle size of PBS was increased with increasing PBS content. T_c of PLA/PBS blends shifted to higher temperature. PLA/PBS blends with PBS up to 20 wt%, T_{cc} of the blends was decreased. This indicates that the addition of PBS up to 20 wt% enhanced the crystallization of PLA. T_g of blends was decreased with addition of PBS. T_m of PLA in PLA/PBS blends was decreased with increasing PBS contents but T_m of PBS was increased. The degree of crystallinity of PLA ($\%X_{PLA}$) in PLA/PBS blends was increased with increasing PBS contents.

From the stress-strain curves, PLA exhibited brittle fracture. PLA/PBS blends showed higher toughness compared to that of neat PLA. PLA-g-GMA showed ductile fracture. Necking and cold drawing of PLA-g-GMA was observed. The elongation at break of PLA/PBS blends was dramatically increased up to 308.87% with adding 10 phr of PLA-g-GMA.

Tensile strength, elongation at break and impact strength of PLA/PBS blends with addition of PLA-g-GMA were increased. PLA-g-GMA improved the mechanical properties of PLA/PBS blends due to enhanced interfacial adhesion between PLA and PBS. The domain sizes of PBS of blend with PLA-g-GMA were much smaller than that of PBS20. Moreover, thermal stability of PLA/PBS blends was improved with addition of PLA-g-GMA. T_c of PLA-g-GMA was observed. T_{cc} of PBS20-G10 was high than that of PBS20. T_g of PLA/PBS blends was decreased with adding PLA-g-GMA. T_m of PBS20-G10 decreased approximately 1–2°C with the addition of PLA-g-GMA. The degree of crystallinity of PLA in PBS20-G10 was decreased with addition of PLA-g-GMA.

Tensile strength, Young's modulus, elongation at break and impact strength of CP/PLA/PBS composites were decreased with increasing CP contents. Thermal stability of composites was decreased with increasing CP contents. T_c of composites shifted to low temperature. T_g of composites insignificant changed with increasing CP contents. T_{cc} of composites shifted to low temperature with increasing CP up to 20wt%. T_m of composites was decreased with addition of CP. The degree of crystallinity of PLA in CP/PLA/PBS composites was improved with addition of CP up to 10 wt%.

PLA-g-GMA and PLA-g-MA were used as compatibilizer of CP/PLA/PBS composites. Tensile strength, Young's modulus, elongation at break and impact strength of CP/PLA/PBS composites was improved by using compatibilizer. Young's modulus was improved with addition of PLA-g-MA more than that of PLA-g-GMA. PLA-g-GMA was shown to be an effective for tensile strength, elongation at break and impact strength of composites than that of PLA-g-MA. Thermal stability of CP/PLA/PBS composites was increased addition of PLA-g-GMA. The compatibility between CP and PLA/PBS blends was improved by using PLA-g-GMA as compatibilizer. Two peak of T_c in PBS20-C20 were observed. T_c of PBS20-G10-C20 showed one peak. This indicated that compatibility of composites was improved by PLA-g-GMA as compatibilizer. T_c of PBS20-G10-C20 shifted to high temperature. T_g of PBS20-G10-C20 was lower than that of PBS20-C20. T_{cc} of PBS20-G10-C20 did not appear. T_m of PLA in PBS20-G10-C20 was increased but that of PBS was decreased. The degree of crystallinity of PLA in PBS20-G10-C20 was increased with addition of PLA-g-GMA.



APPENDIX A

**COST CALCULATION FOR PLA/PBS BLENDS AND
CP/PLA/PBS COMPOSITES**

Cost analysis of PLA/PBS blends and CP/PLA/PBS composites

1. Cost of materials for preparing PLA/PBS blends

Total cost of materials for preparing PLA/PBS blends based on 1 kg of the blends are shown in Table A.1

Table A.1 Cost of materials for preparing PLA/PBAT blends based on 1 kg of the blends.

Sample	Component	Content (kg)	Price/Unit (bath/kg)	Total Price (bath/kg)
PLA	PLA	1.00	100.00	100.00
PBS10	PLA	0.90	100.00	120.00
	PBS	0.10	300.00	
PBS20	PLA	0.80	100.00	140.00
	PBS	0.20	300.00	
PBS30	PLA	0.70	100.00	160.00
	PBS	0.30	300.00	
PBS40	PLA	0.60	100.00	180.00
	PBS	0.40	300.00	
PBS	PBS	1.00	300.00	300.00

2. Cost of materials for preparing CP

CP was used as a filler for CP/PLA/PBS composites. Total cost of materials for preparing CP based on 1 kg is shown in Table A.2.

Table A.2 Cost of materials for preparing CP based on 1 kg

Sample	Component	Content (kg)	Price/Unit (bath/kg)	Total Price (bath/kg)
CP	RCP _t	0.70	3.00	11.70
	Glycerol	0.30	32.00	



3. Cost of materials for preparing CP/PLA/PBS composites

CP was used as a filler for CP/PLA/PBS composites. Total cost of materials for preparing CP/PLA/PBS composites based on 1 kg of the composites are shown in Table A.3.

Table A.3 Cost of materials for preparing CP/PLA/PBS composites based on 1 kg of the blends.

Sample	Component	Content (kg)	Price/Unit (bath/kg)	Total Price (bath/kg)
PBS20	PLA	0.80	100.00	140.00
	PBS	0.20	300.00	
PBS20-C10	PLA	0.72	100.00	127.17
	PBS	0.18	300.00	
	CP	0.10	11.70	
PBS20-C20	PLA	0.64	100.00	114.34
	PBS	0.16	300.00	
	CP	0.20	11.70	
PBS20-C30	PLA	0.56	100.00	101.51
	PBS	0.14	300.00	
	CP	0.30	11.70	
PBS20-C40	PLA	0.48	100.00	88.68
	PBS	0.12	300.00	
	CP	0.40	11.70	

4. Cost of materials for preparing PLA-g-GMA and PLA-g-MA

PLA-g-GMA and PLA-g-MA were used as a compatibilizer. Total cost of materials for preparing PLA-g-GMA and PLA-g-MA based on 1 kg of the compatibilizer are shown in Table A.4.

Table A.4 Cost of materials for preparing PLA-g-GMA and PLA-g-MA based on 1 kg of the compatibilizer.

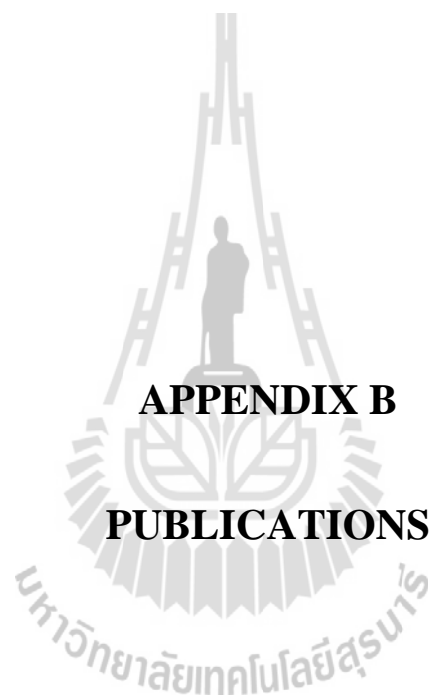
Sample	Component	Content (kg)	Price/Unit (bath/kg)	Total Price (bath/kg)
PLA-g-GMA	PLA	0.9074	100.00	120.36
	GMA	0.0907	320.00	
	DCP	0.00181	320.00	
PLA-g-MA	PLA	0.9074	100.00	120.36
	MA	0.0907	320.00	
	DCP	0.00181	320.00	

5. Cost of materials for preparing compatibilized PLA/PBS blends and compatibilized CP/PLA/PBS composites

Total cost of materials for preparing compatibilized PLA/PBS blends and compatibilized CP/PLA/PBS composites based on 1 kg of the blends and composites are shown in Table A.5.

Table A.5 Cost of materials for preparing compatibilized PLA/PBS blends and compatibilized CP/PLA/PBS composites based on 1 kg of the blends and composites.

Sample	Component	Content (kg)	Price/Unit (bath/kg)	Total Price (bath/kg)
PBS20-G10	PLA	0.80	100.00	138.21
	PBS	0.20	300.00	
	PLA-g-GMA	0.10	120.36	
PBS20-G10-C20	PLA	0.64	100.00	114.89
	PBS	0.16	300.00	
	CP	0.20	11.70	
	PLA-g-GMA	0.10	120.36	
PBS20-M10-C20	PLA	0.64	100.00	114.89
	PBS	0.16	300.00	
	CP	0.20	11.70	
	PLA-g-GMA	0.10	120.36	



APPENDIX B
PUBLICATIONS

List of publications

Kangwanwatthanasiri, P., Suppakarn, N. and Ruksakulpiwat, Y. (2012). Effect of cassava pulp on physical properties of polylactic acid and polybutylene succinate blends. **In Proceedings of Pure and Applied Chemistry International Conference 2012**. Chiang Mai, Thailand., PP 89-92.

Kangwanwatthanasiri, P., Suppakarn, N., Ruksakulpiwat, C. and Ruksakulpiwat, Y. (2013). Biocomposites from cassava pulp /polylactic acid/poly (butylenes succinate). **Adv. Mater. Res.** 747: 367-370.

Patent 1301003316, Assoc. Prof. Dr. Yupaporn Ruksakulpiwat, Asst. Prof. Dr. Nitinat Suppakarn, Asst.Prof.Dr. Chaiwat Ruksakulpiwat, Parina Kangwanwatthanasiri

Patent 1301003317, Assoc. Prof. Dr. Yupaporn Ruksakulpiwat, Asst. Prof. Dr. Nitinat Suppakarn, Asst.Prof.Dr. Chaiwat Ruksakulpiwat, Parina Kangwanwatthanasiri

EFFECT OF CASSAVA PULP ON PHYSICAL PROPERTIES OF POLYLACTIC ACID AND POLYBUTYLENE SUCCINATE BLENDS

Parina Kangwanwatthanasiri^{1,2}, Nitinat Suppakarn^{1,2} and Yupaporn Ruksakulpiwat^{1,2,*}

¹School of Polymer Engineering, Institute of Engineering, Suranaree University of Technology, Nakorn Ratchasima 30000, Thailand

²National Center of Excellence for Petroleum, Petrochemicals and Advanced Materials, Chulalongkorn University, Bangkok 10330, Thailand

* Author for correspondence; E-Mail: yupa@sut.ac.th

Abstract: In this study, effect of content of cassava pulp (CP) on physical properties of polylactic acid (PLA) and polybutylene succinate (PBS) blends was studied. The ratio of PLA to PBS were 80 to 20 wt% and content of CP was varied from 0 to 40 phr. It was shown that young's modulus of PLA/PBS blend was increased with increasing content of CP in the blend. But tensile strength, elongation at break and impact strength of the blend were decreased. This result was due to an incompatibility between CP and PLA/PBS blends. The compatibilizer, Dicumyl peroxide (DCP) and Maleic anhydride (MA), were used in this study. DCP and MA were expected to improve interfacial adhesion between CP and PLA/PBS blends. Effect of DCP and MA as the compatibilizer on the physical properties of PLA/PBS/CP blends was studied. The blends were pre-mixed using high-speed mixer and prepared using a one-step extrusion process. The physical properties of blends were examined. Addition of a small amount of compatibilizer increased the physical properties of blends compared to the non-compatibilized blends. Tensile strength, impact strength and young's modulus of the blends were increased with the addition of compatibilizer.

1. Introduction

In recent years, poly (lactic acid) (PLA) have been gathering much attention because it has less harmful effect on environment compared to fossil fuel based plastics. However, its inherent brittleness, and low-heat distortion temperature of PLA have restricted its applications [1]. In order to improve mechanical properties of PLA, several polymers were blended with PLA. Generally, these blends showed considerably higher toughness than pure PLA. Poly (butylene succinate) (PBS) was used to improve toughness of PLA [2]. PBS has high flexibility, excellent impact strength, and thermal and chemical resistance. It can be processed easily and was one of the best choice to blend with PLA. Impact strength and elongation at break of PLA was increased when adding PBS. Adding fillers into plastics was usually implemented to improve their mechanical properties. In this study, cassava pulp (CP) was used as filler of PLA/PBS blend. CP was a by-product of cassava starch factory [3]. CP was obtained from natural renewable resource, contains a large quantity of starch and fiber. Starch in CP can be acted as a plasticizer in the blend when prepared as the thermoplastic starch

(TPS). Common plasticizers used for TPS preparation are water, glycerol, sorbitol, and other low-molecular weight-polyhydroxy - compounds [4].

Starch can improve the biodegradability and lower cost of the blend. The starch can be added as granule form or gelatinized. To improve the interfacial adhesion, the reactive compatibilization with reactant such as maleic anhydride (MA), dioctyl maleate and methylene diphenyl diisocyanate were used [5]. They were intended to introduce chemical bonds between PLA and starch molecules. Narayan et al. achieved very good interfacial adhesion PLA/starch blend by using maleic anhydride grafted PLA [6]. The reactive compatibilization with reactant was chose to use as a compatibilizer between PLA/PBS blend and CP.

The fiber of CP was used as reinforcement in polymer blend. CP was expected to improve mechanical properties of PLA/PBS blend. The mechanical properties and morphology of PLA, PBS, PLA/PBS blends and PLA/PBS/CP blends with and without MA were also studied.

2. Materials and Methods

2.1 Materials

A commercial grade of PLA (PLA FZ71PD) and a commercial grade of PBS (PBS FZ91PD) was purchased from Mitsubishi Chemical Co., Ltd. Diameter of CP were less than 1 mm., was purchased from Ratchasima Boonpa Co., Ltd. Maleic anhydride(MA) and dicumyl peroxide(DCP) was purchased from Italmar (Thailand) Co., Ltd.

2.2 Internal mixers

The compositions of PLA/PBS blends are shown in Table 1. A ratio of PLA and PBS was 80:20 [2]. Before mixing, PLA was dried in an oven at 70 °C for 4 hours to eliminate moisture. All compositions of each PLA blends were mixed using an internal mixer (Hakke Rheomix, 3000p) at temperature of 170 °C with a rotor speed of 60 rpm for 10 min. (G is Glycerol and W is water)

2.3 Injection molding

Injection molding (Chuan Lih Fa Machinery Works co., Ltd., CLF-80T) were used to prepare the specimens. The melting temperature of 170 °C and mold temperature of 25 °C were used.

2.4 Impact testing

Impact test was performed according to ASTM D256 in Izod mode using an Atlas testing machine (model BPI). Unnotched impact strength was conducted at room temperature using the impact pendulum with impact energy of 2.7 Joule.

2.5 Tensile properties

Tensile properties were obtained according to ASTM D638 using an Instron universal testing machine (UTM, model 5565) with a load cell of 5 kN.

2.6 Morphological investigation

Morphology of the fractured surface of PLA/PBS/CP blend was examined using scanning electron microscope (SEM). The broken piece of notched specimen from impact test was cut in to small piece of sample. It was then attached onto the sample holder. The samples were coated with layers of gold for 8 min by ionization before analysis. SEM photograph was taken using JOEL machine model JSM6400 at the accelerating voltage of 10 keV.

Table 1: Blends composition

Name	PLA wt.%	PBS wt.%	CP phr	G phr	W phr	MA phr	DCP phr
PLA	100	-	-	-	-	-	-
A	80	20	-	-	-	-	-
B	80	20	10	2	1	-	-
C	80	20	20	4	2	-	-
D	80	20	30	6	3	-	-
E	80	20	40	8	4	-	-
F	80	20	-	-	-	0.5	0.05
G	80	20	10	2	1	0.5	0.05
H	80	20	20	4	2	0.5	0.05
I	80	20	30	6	3	0.5	0.05
J	80	20	40	8	4	0.5	0.05
PBS	-	100	-	-	-	-	-

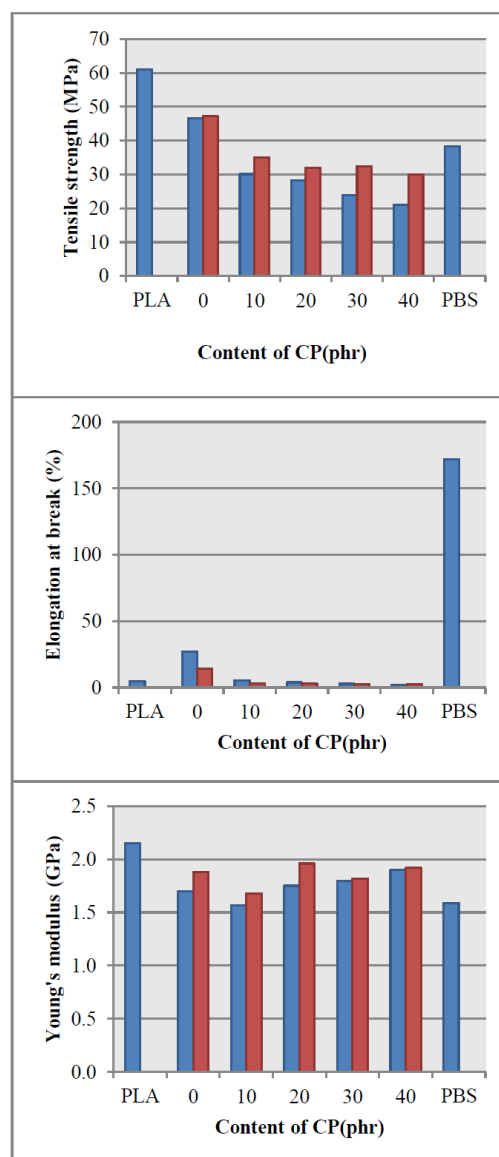
3. Results and Discussion

3.1 Mechanical property

Tensile strength, elongation at break, modulus and impact strength of PLA, PBS and PLA/PBS blends were shown on Figure 1. It was shown that when adding PBS into PLA impact strength and elongation at break of PLA were increased. However, tensile strength and modulus of PLA were decreased with addition of PBS. Moreover, impact strength, tensile strength, elongation at break and modulus of PLA/PBS blend with CP was greatly decreased with the addition of CP. This may be due to the poor compatibility between PLA/PBS and CP. With increasing amount of CP in PLA/PBS blend with CP from 10-40wt. % impact strength, tensile strength and elongation at break were decreased. This behavior can

be related to the probable tendency to form CP agglomerates, resulting in a poor dispersion of CP on the PLA/PBS blend.

Nevertheless, mechanical properties of blend were improved with the addition of compatibilizer as shown in Figure 1. Mechanical properties were increased with addition of MA in PLA/PBS blends and PLA/PBS/CP blends.



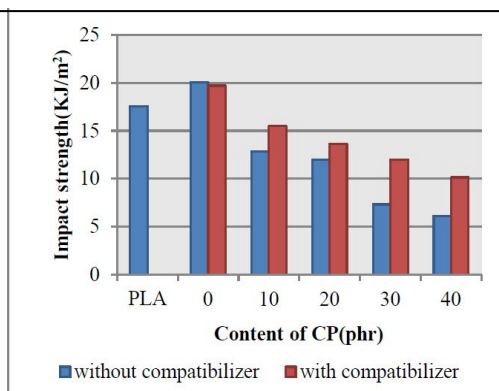


Figure 1. Tensile strength, Young's modulus, elongation at break, and impact strength of PLA, PBS, PLA/PBS blends and PLA/PBS/CP blends.

3.2 Morphological investigation

Morphology of PLA, PBS, PLA/PBS blends and PLA/PBS/CP blends with and without compatibilizer were shown in Figure 2. CP was distributed in the PLA/PBS matrix. Large phase domains could be found for the non-compatible blends. The CP phase that formed from agglomerated CP, was partially plasticized, and could not totally flow as a thermoplastic. While after compatibilized, CP was formed a continuous phase with matrix. Therefore, the non-compatible blends showed poor mechanical properties compared to those of compatibilized ones as described earlier. These results confirm that the anhydride functionalized polymer acted as compatibilizer and increases the interfacial adhesion between the blend components and thereby produces a finer and more uniform morphology, hence, resulting in significantly improvement of mechanical properties.

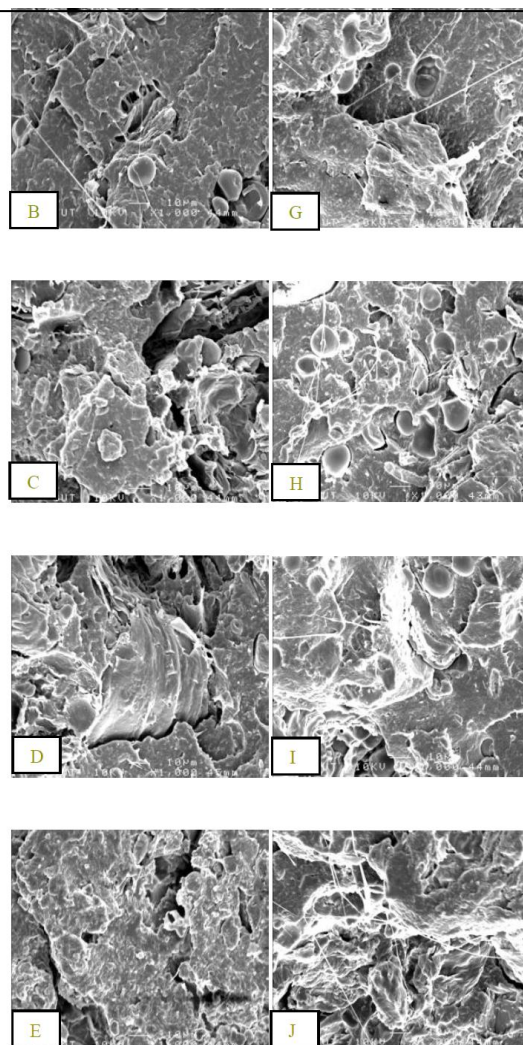
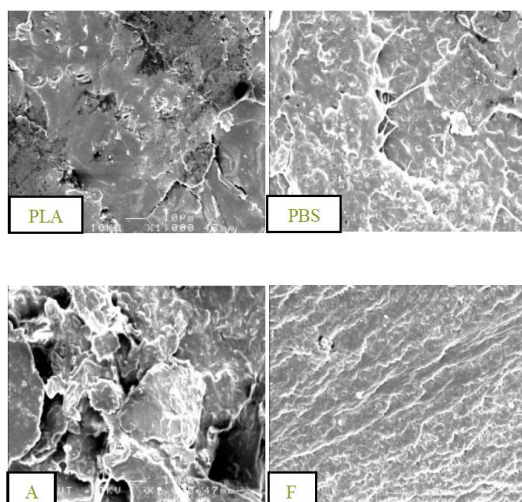


Figure 2. SEM micrographs of fracture surfaces of PLA, PBS, PLA/PBS blends and PLA/PBS/CP blends at various CP contents without compatibilizer (A) 0 phr, (B) 10 phr, (C) 20 phr, (D) 30 phr and (E) 40 phr and PLA/PBS blends and PLA/PBS/CP blends at various CP contents with compatibilizer (F) 0 phr, (G) 10 phr, (H) 20 phr, (I) 30 phr and (J) 40 phr.

4. Conclusions

Dicumyl peroxide (DCP) and maleic anhydride (MA), were used as a compatibilizer in PLA/PBS/CP blends. DCP and MA were shown to improve interfacial adhesion between CP and PLA/PBS blends. Thus, the mechanical properties of PLA/PBS/CP with compatibilizer were higher than those of uncompatibilized blends.

Acknowledgements

The authors wish to thank Suranaree University of Technology and National Innovation Agency, Thailand for financial support.

References

- [1] J. Lunt, *Polym. Degrad. Stab.* **59** (1998) 145
- [2] A. Bhatia, R. K. Gupta, S. N. Bhattacharya and H. J. Choi, *J. Rheo.* **19** (2007) 126
- [3] S. Khempaka, W. Molee, and M. Guillaume, *Poul. Sci. Ass.* (2009) 487
- [4] C. Bangyekan, D. Aht-Ong and K. Srikulkit, *Carbohyd. Polym.* **63** (2006) 61
- [5] B. Y. Shin, G. S. Jo, B. S. Kim, K. H. Hong, S. H. Jang and B. H. Cho, *Applied Chem.* **10** (2006) 77-80
- [6] W. Y. Jang, B. Y. Shin, T. J. LEE and R. Narayan, *J. Ind. Eng. Chem.* **3** (2007) 457-464

Biocomposites From Cassava Pulp/Poly(lactic acid)/Poly (butylene succinate)

Parina Kangwanwatthanasiri¹, Nitinat Suppakarn¹, Chaiwat Ruksakulpiwat²
 and Yupaporn Ruksakulpiwat^{1, a}

¹School of Polymer Engineering, Institute of Engineering, Suranaree University of Technology,
 Nakorn Ratchasima 30000, Thailand

²Department of Chemistry, Faculty of Science, Khon Kaen University, Khon Kaen 40002, Thailand

^ayupa@sut.ac.th

Keywords: Cassava pulp; PLA; PBS; Compatibilizer

Abstract. In this study, effect of PBS content on physical properties of polylactic acid (PLA) and polybutylene succinate (PBS) blends was studied. The content of PBS was varied from 0 – 30 %wt. The blends were mixed using an internal mixer. The samples were prepared using a compression molding. It was shown that tensile strength and Young's modulus of PLA/PBS blends were decreased with increasing PBS content from 0 – 30 %wt. Nevertheless, elongation at break and impact strength of the blend were increased with increasing the amount of PBS up to 20 %wt. Poly(lactic acid) grafted glycidyl methacrylate (PLA-g-GMA) was used as the compatibilizer in PLA/PBS/PLA-g-GMA blends. PLA-g-GMA was shown to improve interfacial adhesion between PLA and PBS. With the addition of PLA-g-GMA, mechanical properties of PLA/PBS blend were improved. The preparation of cassava pulp (CP) to be used as filler in PLA/PBS blends and PLA/PBS/PLA-g-GMA blends was studied. Effect of CP content on mechanical properties CP/PLA/PBS composites was studied. PLA-g-GMA was also used as compatibilizer in CP/PLA/PBS composites. The mechanical properties of CP/PLA/PBS composites were improved with the addition of PLA-g-GMA as well.

Introduction

In recent years, the environmental pollution caused by the plastic waste is an emerging problem. To overcome this, biopolymer such as poly (lactic acid) (PLA) has been developed. PLA has good physical properties including high strength, thermoplasticity, processability and excellent biodegradability. However, its inherent brittleness, and low-heat distortion temperature of PLA have restricted its applications [1]. In order to improve mechanical properties of PLA, several polymers were blended with PLA [2]. Generally, these blends showed considerably higher toughness than pure PLA. Poly (butylene succinate) (PBS) is a biodegradable aliphatic polyester [3, 4]. It has high flexibility, excellent impact strength, and thermal and chemical resistance [5]. It can be processed easily and is one of the best choices to blend with PLA. However, PLA/PBS blends usually exhibit poor impact strength, mainly due to the poor miscibility between PLA and PBS. Moreover, PLA/PBS blends still suffer from poor tensile strength [6]. Adding fillers into plastics was usually implemented to improve their mechanical properties. In this study, cassava pulp (CP) was used as a filler in PLA/PBS blend. CP was a by-product of cassava starch processing from factories. CP was natural renewable resource containing a large quantity of starch and fiber. Starch in CP can be used to prepare thermoplastic starch (TPS) by adding plasticizers. Common plasticizers used for starch preparation are water, glycerol, sorbitol, and other low-molecular weight-polyhydroxy-compounds [7]. Moreover, the fiber in CP can be used as reinforcing filler in polymer composite. CP was expected to improve mechanical properties of PLA/PBS blend. PLA-g-GMA was use as a compatibilizer between PLA/PBS blend and CP. CP was expected to improve mechanical properties of PLA/PBS blend. The mechanical properties and morphology of PLA, PBS, PLA/PBS blends and CP/PLA/PBS composites with and without PLA-g-GMA were also studied.

Materials and Methods

Materials. A commercial grade of PLA (PLA 4043D) was purchased from BC Polymers Marketing Co., Ltd. A commercial grade of PBS (PBS FZ91PD) was purchased from Mitsubishi Chemical Co., Ltd. CP was purchased from Ratchasima Boonpa Co., Ltd. The mesh size of CP was in the range of 150-250 μm .

Experimental. The compositions of CP/PLA/PBS composites are shown in Table 1., Before mixing, PLA was dried in an oven at 70 °C for 4 hours to eliminate moisture. All compositions of each PLA blends were mixed using an internal mixer (Hakke Rheomix, 3000p) at temperature of 170 °C with a rotor speed of 60 rpm for 10 min. Samples were forming by compression molding at 170 °C.

Impact testing. Impact test was performed according to ASTM D256 in Izod mode using an Atlas testing machine (model BPI). Unnotched impact strength was conducted at room temperature using the impact pendulum with impact energy of 2.7 Joule.

Tensile properties. Tensile properties were obtained according to ASTM D638 using an Instron universal testing machine (UTM, model 5565) with a load cell of 5 kN.

Morphological investigation. Morphology of the fractured surface of PLA/PBS/CP blend was examined using scanning electron microscope (SEM). The broken piece of specimen from tensile test was cut into small piece of sample. It was then attached onto the sample holder. SEM photograph was taken using JOEL machine model JSM6400 at the accelerating voltage of 10 keV.

Table 1 Blends and composites composition

Name	PLA wt.%	PBS wt.%	CP wt.%	PLA-g-GMA phr
PLA	100	-	-	-
PBS10	90	10	-	-
PBS20	80	20	-	-
PBS30	70	30	-	-
PBS20-G10	80	20	-	10
PBS20-G10-C5	76	19	5	10
PBS20-G10-C10	72	18	10	10
PBS20-G10-C20	64	16	20	10
PBS20-C20	64	16	20	-
PBS	-	100	-	-

Results and Discussion

Mechanical properties

Table 1. shows the mechanical properties of PLA, PBS, PLA/PBS blends and CP/PLA/PBS composites. PLA is high modulus and brittle material while PBS is flexible polymer. The addition of PBS leads to a reduction in the brittleness of PLA. Tensile strength and Young's modulus of PLA/PBS blends were decreased with the addition of PBS. The elongation at break and impact strength of PLA/PBS blends were increased with increasing PBS content up to 20 wt%. However, at 30 wt% PBS content, the elongation at break and impact strength of blends were decreased. It was likely attributed to the coagulation of PBS at high loading. The effect of PLA-g-GMA on physical properties of PLA/PBS blends was studied. Results from the work show that all mechanical properties especially elongation at break of the blend were improved with the addition of PLA-g-GMA. This indicated that the compatibility between PLA and PBS was improved when

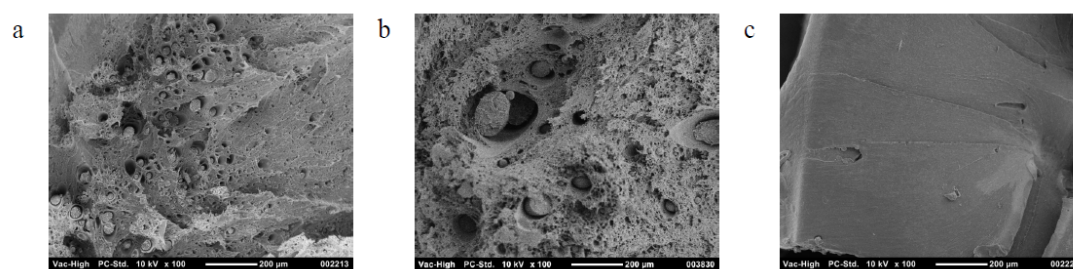
PLA-g-GMA was used as a compatibilizer. When CP was added in PLA/PBS blends with PLA-g-GMA, a decrease in mechanical properties (tensile strength, elongation at break and impact strength) of the composites was observed. This behavior may be related to the probable tendency to form CP agglomerates, resulting in a poor dispersion of CP on the CP/PLA/PBS composites. However, Young's modulus of CP/PLA/PBS composites was slightly increased with increasing CP content. This may be due to the fact that the cassava fiber in CP possibly increased the modulus in CP/PLA/PBS composites. The effect of PLA-g-GMA on tensile strength, Young's modulus, elongation at break and impact strength of CP/PLA/PBS composite was also studied. The mechanical properties of CP/PLA/PBS composites without PLA-g-GMA were decreased compared to that of the blends without CP. This indicated that the compatibility between PLA/PBS and CP was poor. PLA-g-GMA was used as compatibilizer in CP/PLA/PBS composites. Tensile strength, Young's modulus, elongation at break and impact strength of composites were improved by using PLA-g-GMA.

Table 2 Mechanical properties of blends and composites

Name	Tensile strength (MPa)	Elongation at Break (%)	Young's modulus (MPa)	Impact strength (KJ/m ²)
PLA	61.44±2.29	5.20±0.39	890.20±12.64	12.61±0.75
PBS10	50.66±4.70	40.07±2.59	749.42±17.59	13.88±0.99
PBS20	46.10±1.37	52.82±3.43	657.04±37.55	16.03±0.61
PBS30	40.67±1.96	11.76±0.86	652.43±17.59	15.60±0.85
PBS20-G10	55.15±1.09	308.87±12.45	676.33±21.71	22.57±0.23
PBS20-G10-C5	40.57±0.72	56.78±3.17	682.27±39.32	22.43±1.72
PBS20-G10-C10	36.71±3.82	11.97±1.22	698.28±33.03	15.65±0.28
PBS20-G10-C20	19.47±2.10	11.07±1.24	703.21±13.99	12.76±0.50
PBS20-C20	8.590±2.13	7.280±1.65	635.00±32.09	4.910±0.12
PBS	27.53±1.90	82.28±2.82	571.96±27.72	29.26±1.22

Morphological properties

Fig. 1(a-f) show SEM micrographs of PLA/PBS blends and CP/PLA/PBS composites. The droplet sizes of PBS in PBS30 sample [Fig. 1(b)] were much bigger than that of PBS20 [Fig. 1(a)]. The enlargement of the dispersed PBS caused by the coagulation of PBS phase at higher PBS content. This led to the poor mechanical properties of the blends. Fig. 1(c) and (a) show the tensile fractured surface of PLA/PBS blends with and without PLA-g-GMA. PBS20-G10 showed smaller droplet size on the fractured surface than that of PBS20. This indicated that the compatibility between PLA and PBS was improved when PLA-g-GMA was used as compatibilizer. Surface roughness and non-uniform droplet of CP were found in PBS20-G10-C5 and PBS20-G10-C20 [Fig. 1(d) and 1(e)]. This may be due to poor compatibility between CP and PLA/PBS blends. The surface of PBS20-G10-C20 was much rougher than PBS20-G10-C5. With to increasing CP contents, agglomeration of CP was observed. Fig. 1(e) and 1(f) show SEM images of CP/PLA/PBS composites with and without of PLA-g-GMA, respectively. It was observed the elongated fibrils in CP/PLA/PBS blend with PLA-g-GMA. This result confirmed that compatibilizer improved compatibility between CP and PLA/PBS blends of composites.



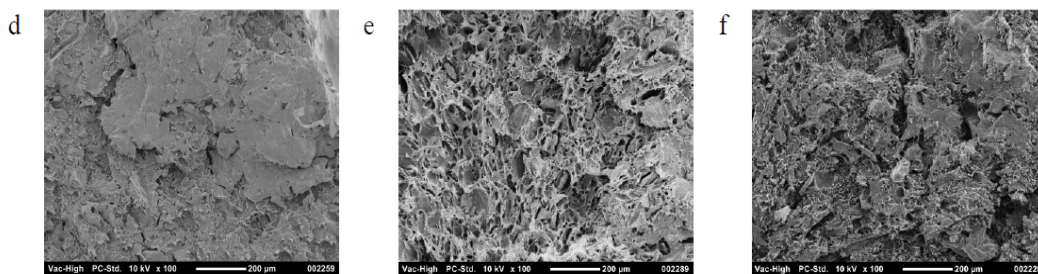


Fig. 1 SEM micrographs of tensile-fractured surfaces of: (a) PBS20, (b) PBS30, (c) PBS20-G10, (d) PBS20-G10-C5, (e) PBS20-G10-C20 and (f) PBS20-C20. Symbols are named according to Table 1.

Summary

From the results, it can be concluded that elongation at break and impact strength of PLA/PBS blends without PLA-g-GMA were increased with increasing PBS content up to 20 wt%. However, tensile strength and Young's modulus of PLA/PBS blends significantly decreased with increasing PBS contents. With the addition of PLA-g-GMA into PLA/PBS blend, tensile strength, Young's modulus, elongation at break and impact strength of PLA/PBS blends were increased. This shows that PLA-g-GMA can improve compatibility between PLA and PBS. Compatibility between CP and PLA/PBS blends was improved by using PLA-g-GMA as a compatibilizer as well. Young's modulus of CP/PLA/PBS composites with PLA-g-GMA was increased with increasing of CP contents.

Acknowledgements

The authors wish to thank Suranaree University of Technology and National Center of Excellence for Petroleum, Petrochemicals and Advanced Materials for financial support.

References

- [1] J. Lunt, *Polym. Degrad. Stab.* 59 (1998) 145-152.
- [2] W. Pivsa-Art, S. Pavasupree, N. O-Charoen, U. Insuan, P. Jailak and S. Pivsa-Art, *Energy Procedia*. 9 (2011) 581 – 588.
- [3] K. Bhari, H. Mitomo, T. Enjoji, F. Yoshii and K. Makuuchi, *Polym. Degrad. Stab.* 62 (1998) 551-557.
- [4] Y. Doi, K. Kasuya, H. Abe, N. Koyama, S. Ishiwatara, K. Takagi and Y. Yoshida, *Polym. Degrad. Stab.* 51(1996) 281-286.
- [5] Y. Doi and K. Kasuya, *Studies in Polymer Science 12*. Elsevier Science, Amsterdam, 1994, pp. xvii+627.
- [6] A. Bhatia, R. K. Gupta, S. N. Bhattacharya and H. J. Choi, *J. Rheol.* 19 (2007) 125-131.
- [7] C. Bangyekan, D. Aht-Ong and K. Srikulkit, *Carbohydr.Polym.* 63 (2006) 61-71.

BIOGRAPHY

Miss Parina Kangwanwatthanasiri was born June 2, 1987 in Phitsanulok, Thailand. She graduated her Bachelor's Degree in Polymer Engineering from Suranaree University of Technology (SUT) in 2009. She then continued her Master's degree in Polymer Engineering at School of Polymer Engineering, Institute of Engineering at Suranaree University of Technology. During her study, she presented two papers, "*Effect of Cassava Pulp on Physical Properties of Polylactic Acid and Polybutylene Succinate Blends*" in Pure and Applied Chemistry International Conference 2012 (PACCON2012) in Chiang Mai, Thailand and "*Biocomposites from Cassava Pulp/Poly lactic Acid/Poly (Butylene Succinate)*" in the 4th International Conference on Multi-Functional Materials and Structures (MFMS 2013), Bangkok Thailand.

